https://doi.org/10.15388/vu.thesis.907
https://orcid.org/0009-0003-6847-8270

VILNIUS UNIVERSITY
CENTER FOR PHYSICAL SCIENCES AND TECHNOLOGY

Barkha Bale

Abundances of Chemical Elements in Magnetically Active Stars

DOCTORAL DISSERTATION

Natural Sciences,
Physics (N 002)

VILNIUS 2026

This dissertation was prepared between 2021 and 2025 at Vilnius University (VU), Institute of Theoretical Physics and Astronomy (ITPA).

Academic Supervisor: Prof. Habil. Dr. Gražina Tautvaišienė (Vilnius University, Natural Sciences, Physics, N 002)

Dissertation Defence Panel:

Chairman – Prof. Habil. Dr. Gediminas Gaigalas (Vilnius University, Natural Sciences, Physics, N 002)

Members:

Dr. Svetlana Berdyugina (University of Italian Switzerland, Natural Sciences, Physics, N 002)

Dr. Vidas Dobrovolskas (Vilnius University, Natural Sciences, Physics, N 002)

Dr. Habil. Tamara Mishenina (Odesa National University, Natural Sciences, Physics, N 002)

Assoc. Prof. Dr. Donatas Narbutis (Vilnius University, Natural Sciences, Physics, N 002)

The dissertation shall be defended at a public meeting of the Dissertation Defence Panel at 14 hour on May 5, 2026 in the National Center for Physical Sciences and Technology, Room A101. Address: Saulėtekio al. 3, LT–10257, Vilnius, Lithuania Tel. +370 5 2234637; email tfai@tfai.vu.lt

The text of this dissertation can be accessed at the libraries of Vilnius University and Center for Physical Sciences and Technology, as well as on the website of Vilnius University: www.vu.lt/lt/naujienos/ivykiu-kalendorius

https://doi.org/10.15388/vu.thesis.907
https://orcid.org/0009-0003-6847-8270

VILNIAUS UNIVERSITETAS
FIZINIŲ IR TECHNOLOGIJOS MOKSLŲ CENTRAS

Barkha Bale

Cheminių elementų gausa magnetiškai aktyviose žvaigždėse

DAKTARO DISERTACIJA

Gamtos mokslai,
Fizika (N 002)

VILNIUS 2026

Disertacija rengta 2021 – 2025 metais Vilniaus universiteto Teorinės fizikos ir astronomijos institute (TFAI).

Mokslinis vadovas: prof. habil. dr. Gražina Tautvaišienė (Vilniaus universitetas, gamtos mokslai, fizika, N 002)

Gynimo taryba:

Pirmininkas – prof. habil. dr. Gediminas Gaigalas (Vilniaus universitetas, gamtos mokslai, fizika, N 002)

Nariai:

Dr. Svetlana Berdyugina (Italijos Šveicarijos universitetas, gamtos mokslai, fizika, N 002)
Dr. Vidas Dobrovolskas (Vilniaus universitetas, gamtos mokslai, fizika, N 002)
Habil. Dr. Tamara Mishenina (Odesos nacionalinis universitetas, gamtos mokslai, fizika, N 002)
Doc. dr. Donatas Narbutis (Vilniaus universitetas, gamtos mokslai, fizika, N 002)

Disertacija ginama viešame Gynimo tarybos posėdyje 2026 m. gegužės mėn. 5 d. 14 val. Nacionalinio fizininų ir technologijos mokslų centro posėdžių salėje A101. Adresas: Saulėtekio al. 3, LT–10257, Vilnius, Lietuva Tel. +370 5 2234637; el. paštas tfai@tfai.vu.lt

Disertaciją galima peržiūrėti Vilniaus universiteto ir Fizinių ir technologijos mokslų centro bibliotekose ir Vilniaus universiteto interneto svetainėje adresu: https://www.vu.lt/naujienos/ivykiu-kalendorius

Contents

Acronyms and Abbreviations

Term	Abbreviation
RS Canum Venaticorum	RS CVn
First dredge-up	1DUP
Red Giant Branch	RGB
Local thermodynamic equilibrium	LTE
Non-local thermodynamic equilibrium	NLTE
Data release 3	DR3
Gaia-ESO survey	GES
Model Atmospheres with Radiative and Convective Scheme	MARCS
Radial velocity	RV
Signal-to-noise ratio	S/N
Vilnius University Echelle Spectrograph	VUES
Vienna Atomic Line Database	VALD
Fibre-fed Echelle Spectrograph	FIES
Below bump	BB
Above bump	AB
Red Clump	RC
Subgiant	SG
Subgiant of Thick disc	SGTH
Equivalent width	EW

Problem statement and relevance of the research topic

RS Canum Venaticorum (RS CVn) stars are close binary systems characterized by strong chromospheric activity, tidal locking, and rapid rotation. These conditions causes extensive starspots, flaring, and enhanced Ca II H & K emission, marking them as excellent laboratories for studying the interplay of magnetism, rotation, and internal mixing.

Stellar evolution theory predicts well-defined changes in surface chemical composition as stars evolve up the red giant branch (RGB). During the first dredge-up (1DUP), the convective envelope transports processed material to the surface, lowering the $^{12}C/^{13}C$ and C/N ratios, while lithium, a fragile element destroyed at relatively low temperatures, is significantly depleted. Later, additional extra-mixing processes (e.g., thermohaline or rotation-induced mixing) further alter surface abundances. In standard models, these extra-mixing events become effective only at or above the RGB luminosity bump.

However, observations of RS CVn stars frequently reveal departures from these classical expectations. Some RS CVn giants show anomalously high lithium abundances compared with inactive field stars of similar type, while others display early reductions in carbon isotope ratios below the RGB bump. Such evidence suggests that magnetic activity may either suppress depletion (by inhibiting convection) or accelerate mixing (via magnetically or rotationally driven processes). Yet, earlier studies were often based on small samples or limited chemical diagnostics, lacking simultaneous determinations of lithium, CNO abundances, and isotope ratios. This has left the role of magnetic activity in governing stellar mixing processes uncertain and unanswered.

The combined investigations of more than 50 RS CVn stars across different evolutionary stages including detailed measurements of Li, C, N, O abundances, and isotopic ratios directly address this gap. It provides one of the most comprehensive datasets for testing whether magnetic activity fundamentally alters chemical evolution in RS CVn stars.

This research holds broad significance for stellar and galactic astrophysics, demonstrating that extra mixing can commence earlier than predicted in magnetically active stars. The results challenge the canonical framework of stellar evolution and impose important constraints on models that incorporate thermohaline and rotation-induced mixing processes.

Lithium abundances offer one of the most sensitive diagnostics of internal mixing in stars. The detection of RS CVn systems with either suppressed depletion or anomalous enrichment provides key evidence for assessing whether Li survival originates from inhibited mixing, fresh production through the Cameron–Fowler mechanism, or external accretion events such as planet engulfment.

A critical aspect of this investigation is to determine whether RS CVn stars diverge from the chemical trends of typical red giants and to identify any peculiar abundance patterns. Establishing a connection between magnetic activity and abundance variations underscores the role of magnetism in altering evolutionary routes. The insights derived have broader implications for magnetically active stars across different evolutionary phases, from young open-cluster giants to helium-burning red clump stars.

Alongside RS CVn stars, the dataset further includes a subset of twelve eruptive stars, characterised by violent atmospheric activity such as flares and mass outflows. Their presence in the sample provides an opportunity to examine whether episodic variability in giants is associated with any departure from the predicted CNO abundance and $^{12}C/^{13}C$ patterns expected in He–burning stars.

In summary, this research tackles the unresolved question of how magnetic activity influences internal mixing and chemical evolution in stars. The findings offer new observational constraints that illuminate the processes through which evolved stars deplete, retain, or enhance fragile elements such as lithium. Together, these results strengthen the link between theoretical models and observations, enriching our understanding of stellar and Galactic evolution.

Main aims and tasks

The principal goal of this work is to investigate the influence of stellar magnetic activity on internal mixing and surface abundance patterns in chromospherically active RS CVn, and eruptive stars. Using detailed spectroscopic diagnostics and comparison with theoretical models, the study examines the occurrence of mixing signatures in RS CVn stars and evaluates the contribution of magnetic processes to the observed anomalies in lithium, carbon, nitrogen, and other key elements.

In order to address the aims of this thesis, a sequence of well-defined tasks was undertaken, each building upon the previous step to construct a coherent framework for understanding the role of magnetic activity in the chemical evolution of RS CVn, and eruptive stars. The first stage consisted of compiling a representative sample of stars spanning different evolutionary stages. The following tasks were the acquisition of high-quality spectra and the determination of stellar atmospheric parameters (effective temperatures, surface gravities, microturbulent velocities, and metallicities), as well as other fundamental parameters as age, mass, evolutionary stage, attribution to the Galactic thin or thick disc, etc. The final task involved a detailed abundance analysis of up to 13 chemical elements and testing the observational results with theoretical stellar evolution models and the general Galactic chemical evolution trends.

Scientific novelty and statements for defence

The scientific novelty of this research lies in its comprehensive spectroscopic investigation of RS CVn stars, a class of magnetically active binaries whose chemical composition had previously been insufficiently studied. While earlier studies provided partial evidence that activity might influence surface abundances, most of them were restricted to small samples, lacked carbon isotope measurements, or focused on individual elements such as lithium alone. This study, by contrast, combines lithium, carbon, nitrogen, and oxygen abundances together with $^{12}C/^{13}C$ isotope ratios for more than fifty RS CVn stars, covering a wide range of evolutionary stages. By assembling a coherent set of observations for RS CVn stars, the study enables systematic comparisons with normal giants as well as theoretical models of stellar evolution.

A key novel aspect of the research is the demonstration that extra-mixing processes can begin earlier in magnetically active stars than in inactive stars of comparable mass and evolutionary stage. In particular, several RS CVn stars situated below the red giant branch luminosity bump exhibit lowered $^{12}C/^{13}C$ ratios and depleted lithium abundances, patterns that in theoretical models are expected only after the bump. This provides systematic evidence that magnetic activity alters the timing and efficiency of mixing. Equally novel is the identification and characterisation of lithium-rich RS CVn giant, which challenges existing models of lithium depletion and enrichment, and raises questions about the role of planet engulfment, binary interactions, or internal nucleosynthesis in producing their anomalous chemical signatures.

Statements for Defence

The following hypotheses and statements will be defended in the course of this thesis:

- In chromospherically active RS CVn giants, extra-mixing processes may begin earlier than in normal, inactive giants. This is expected to be observable through systematically lowered $^{12}C/^{13}C$ ratios in stars which are still below the RGB luminosity bump.
- The existence of Li-rich RS CVn stars, such as V* OP And, indicates that mechanisms beyond the standard first dredge-up and thermohaline mixing are responsible for lithium enrichment in magnetically active stars.

- The behaviour of lithium abundances in RS CVn stars depends on stellar mass: in low-mass stars, thermohaline-induced mixing acts in addition to the first dredge-up, whereas in intermediate-mass stars lithium depletion is predominantly driven by rotation-induced mixing.

- RS CVn stars follow the overall evolutionary trend of lithium decline as in normal giants, but their deviations at earlier evolutionary stages confirm that magnetic activity significantly alters the canonical pathways of stellar chemical evolution.

- In eruptive core He-burning stars, despite the occurrence of violent flares, shell events, and episodic mass outflows, the CNO abundances and ratios of $^{12}C/^{13}C$ remain indistinguishable from those of ordinary core He-burning stars, demonstrating that such activity does not significantly alter their surface chemical composition.

Publications related to this thesis

1. Lagarde N., Minkevičiūtė R., Drazdauskas A., Tautvaišienė G., Charbonnel C., Reylé C., Miglio A., Kushwahaa T., **Bale B.**, *$^{12}C/^{13}C$ of Kepler giant stars: The missing piece of the mixing puzzle*, Astronomy & Astrophysics, Vol. 684, A70, 2024.
2. **Bale B.**, Tautvaišienė G., Minkevičiūtė R., Drazdauskas A., Mikolaitis Š., Stonkutė E., Ambrosch M., *Chromospherically active stars: Chemical composition of photospheres in 20 RS CVn stars*, Astronomy & Astrophysics, Vol. 696, A23, 2025.
3. **Bale B.**, Tautvaišienė G., Minkevičiūtė R., Drazdauskas A., Mikolaitis Š., Stonkutė E., Ambrosch M., *Chromospherically active stars: Lithium and CNO abundances in northern RS CVn stars*, Astronomy & Astrophysics, Vol. 703, A128, 2025.

Presentations at international conferences

1. Cambridge Workshops of Cool Stars, Stellar Systems and the Sun, 4-9 July 2022, Toulouse, France, Remote participation: Presented a poster "CNO abundances in magnetically active RS CVn giants".

2. European Astronomical Society Annual meeting, 10-14 July 2023, Krakow Poland, Poster presentation, "Mixing process in the atmospheres of RS CVn giants".

3. Open readings, 23-26 April 2024, Vilnius, Lithuania, Oral presentation: "Mixing process in the atmosphere of magnetically active RS CVn giants".

4. European Astronomical Society Annual meeting, 23-27 June 2025, Cork, Ireland, Poster presentation,"Chemical composition of photospheres in 20 RS CVn stars".

Presentations at national conferences

1. 45th Lithuanian National Physics Conference (LNFK'45), 25-27 October 2023, Vilnius, Lithuania, Poster presentation: "Mixing process in the atmosphere of RS CVn giants".

2. 46th Lithuanian National Physics Conference (LNFK'46), 8-10 October 2025, Vilnius, Lithuania, Oral presentation: "Lithium and CNO Abundances in chromospherically active RS CVn stars".

Contributions by the author

The main part of this thesis, based on data obtained at the Vilnius University Molėtai Astronomical Observatory, was carried out through the collaborative efforts of the Astrospectroscopy and Exoplanets Team. The author's personal contributions include selection of targets, observation of the selected targets, measurements of Equivalent Width (EW) of spectral lines, determination of the main atmospheric parameters of stars, determination of abundances of different chemical elements, determination of ages, masses, orbits, and kinematics. In addition, the author was fully responsible for data processing, statistical analysis, investigation, conceptualisation, critical scientific assessment, visualisation of results, preparation of scientific papers and the thesis work, and a subsequent review and editing, under the supervision of the thesis director.

Structure of dissertation

The structure of this work is as follows. Introduction outlines the scientific context and motivation of the study.

Chapter 1 presents the introduction of RS CVn stars and their characteristic properties, mixing process in stellar atmospheres, the role of lithium as a tracer of stellar evolution, and characteristic properties of eruptive stars.

Chapter 2 presents the research methodology, including target selection, differential analysis by the EW method, observations, determination of atmospheric parameters, elemental abundances and carbon isotope ratios, consideration of non–local thermodynamic equilibrium (NLTE) effects, stellar mass estimates, kinematic properties, and the evaluation of uncertainties.

Chapter 3 presents the results and discussion of the analysis of RS CVn stars, covering stellar parameters, CNO abundances, the carbon isotopic ratios, elemental abundances, lithium abundances and mixing processes of elements.

Chapter 4 presents the results and discussion of the analysis of eruptive stars, covering the CNO abundances, the carbon isotopic ratios, and mixing processes of elements.

Chapter 5 provides a summary of the results and main conclusions.

The thesis concludes with a summary of the thesis in lithuanian, a list of references, acknowledgment, and appendix tables.

1 Introduction

1.1 Overview of RS CVn stars

The earliest discussions of RS Canum Venaticorum (RS CVn) stars can be traced back to the pioneering work of Keller & Limber (1951), who first highlighted the unusual variability and strong activity of certain binary systems. A more systematic classification was later established by Hall (1976), who defined the class of RS CVn binaries through a set of observational criteria: (i) an orbital period ranging from 1 to 14 days, (ii) emission in the Ca II H & K lines, and (iii) the presence of at least one hot component of spectral type F or G, typically with luminosity class IV or V. This systematic classification provided the basis for identifying RS CVn stars and spurred extensive research into their nature. An overview of their properties and evolutionary significance was presented by Montesinos et al. (1988), further consolidating the understanding of RS CVn stars as a distinct and astrophysically important group.

RS CVn stars are widely recognised today as chromospherically active stars, characterised by vigorous magnetic activity that manifests in numerous observational signatures. Their surfaces are often covered by extensive dark starspots, bright chromospheric plages, and active regions that are many times larger and more long-lived than sunspots. These features contribute to complex patterns of photometric and spectroscopic variability. The activity of RS CVn systems is frequently detected across the electromagnetic spectrum, with intense flares observed in optical, ultraviolet, X-ray, and radio bands (Zhilyaev et al. 2024; Buccino & Mauas 2009). Their active regions are generally distributed across large fractions of the stellar surface (Sciortino et al. 1994; Schmitt & Stern 1994), although in some cases correlations between spots and emission regions, analogous to those observed on the Sun, have also been reported (Baliunas & Dupree 1982).

The variability of RS CVn stars can be understood in part through the finite lifetimes and differential rotation of their numerous starspots. As spots form, evolve, and dissipate, the resulting changes in stellar brightness give rise to rotational modulation and long-term cycles of variability. Eaton et al. (1996) showed that the evolution and redistribution of starspots can explain most of the observed photometric variations, while in eclipsing RS CVn systems cool spots contribute to prominent distortions of light curves even outside of eclipse events (Berdyugina 2005). Spectroscopic indicators of activity are equally striking: emission cores in chromospheric lines such as Ca II H & K and H_α are much stronger than those observed in the Sun, reflecting the intense non-radiative heating of their outer atmospheres (Strassmeier et al. 2000).

A refined classification was proposed by Fekel et al. (1986), who emphasised that RS CVn stars typically contain at least one cool component often a subgiant or giant with strong chromospheric emission and large spotted regions. The companion is usually a less evolved main-sequence star. The combination of tidal synchronisation and rapid rotation sustains powerful magnetic dynamos, driving levels of stellar activity that far exceed those of single stars of similar mass and evolutionary stage (Walter et al. 1980; Cao & Gu 2025). As a result, RS CVn stars have become astrophysical laboratories for studying the interplay between stellar magnetism, binarity, and evolution. They display intense multiwavelength behaviour, including coherent radio emission, frequent X-ray flares, ultraviolet excesses, and dramatic optical variability (Rucinski et al. 1993; White et al. 1978; Toet et al. 2021; Cao et al. 2023).

The study of RS CVn stars extends beyond their variability and magnetism; their chemical composition is also of fundamental interest. Surface abundances provide direct information on both the evolutionary state of the star and the internal physical processes shaping its structure. In particular, photospheric abundances of light elements such as lithium, carbon, nitrogen, and oxygen serve as sensitive tracers of mixing processes. Since RS CVn stars are magnetically active, any deviation of their chemical signatures from canonical stellar evolution predictions may reflect the influence of rotation, tidal forces, and magnetic fields. Interpreting the observed coronal abundance anomalies also requires a detailed comparison with the underlying photospheric composition (Tautvaišienė et al. 2010a).

Numerous studies have reported that RS CVn stars display distinctive photospheric abundance patterns that differ from those of inactive giants, supporting the idea that activity and binarity modify surface compositions. Early work by Pallavicini et al. (1992) and Tautvaisiene et al. (1992) suggested systematic differences in CNO abundances, while subsequent detailed spectroscopic analyses by Randich et al. (1993, 1994), Savanov & Berdyugina (1994), and Berdyugina et al. (1998, 1999) confirmed peculiarities in both elemental abundances and isotopic ratios. Later investigations expanded the scope to include heavier elements and refined isotopic measurements, revealing a consistent picture of altered surface chemistry in active binaries (Katz et al. 2003; Morel et al. 2003, 2004; Barisevičius et al. 2010, 2011; Tautvaišienė et al. 2010b, 2011; Pakhomov et al. 2015; Xing et al. 2021).

A crucial aspect of this field lies in understanding how RS CVn stars differ from single stars of comparable spectral type and age. While normal giants evolve along well-predicted tracks of chemical evolution undergoing first dredge-up dilution of lithium, reductions in carbon abundances, and increases in nitrogen, the RS CVn stars often deviate from these expectations. The enhanced activity in these systems may suppress or delay deep convective mixing, preserving higher lithium abundances than expected, or conversely may accelerate extra-mixing processes, producing prematurely lowered $^{12}C/^{13}C$ ratios. Both scenarios have been observed, indicating that magnetic fields and tidal effects play a decisive role in modifying stellar interiors. In Fig. 1, the elements studied in this thesis work are presented.

RS CVn stars constitute an important class of magnetically active stars whose rapid rotation, variability, pronounced chromospheric emission, and frequent multiwavelength flaring events indicate that magnetic activity plays a central role in shaping both their atmospheres and internal structure. Chemical abundance studies of RS CVn stars show that magnetic activity can modify the timing and efficiency of internal mixing. In particular, some objects exhibit signatures of extra mixing below the red giant branch luminosity bump, contrary to theoretical stellar evolution predictions. Lithium abundances in these stars also depart from expectations, with cases of apparent preservation or enrichment as well as severe depletion, indicating that activity-related processes strongly influence lithium evolution. Detailed spectroscopy of key elements and isotopic ratios in RS CVn stars therefore provides a direct probe of the interaction between magnetic fields and mixing in evolved stars, and serves as a critical test of how stellar magnetism alters otherwise standard evolutionary pathways.

1.2 Mixing process in the stars

Carbon, nitrogen, and oxygen (CNO) occupy a niche role in astrophysics because they both trace the chemical enrichment of stellar populations and regulate the lifetimes, energy production, and evolutionary paths of stars. Their abundances determine the efficiency of the CNO cycle in hydrogen burning, directly influencing stellar luminosities and lifespans, while at the same time providing valuable insight into Galactic chemical evolution (Tautvaišienė et al. 2015). Among these elements, oxygen is of particular importance: as the third most abundant element in the Universe, it acts as a cornerstone tracer of the formation and evolution of stars, planets, and galaxies. Unlike carbon and nitrogen, the oxygen abundance in stellar photospheres remains comparatively

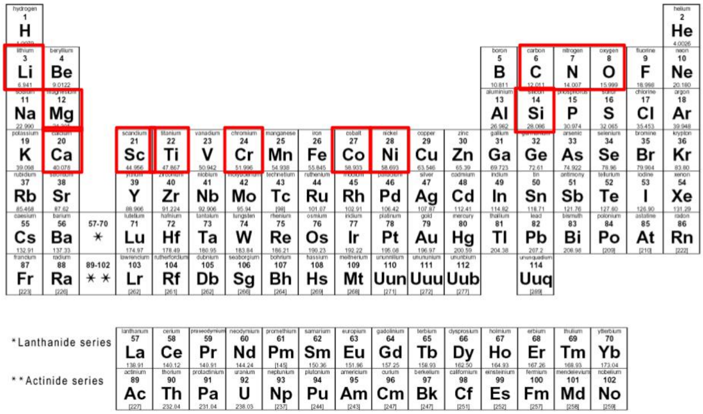

Figure 1: Elements studied and analysed in the thesis work are marked in red.

stable over much of a star's lifetime, making it a robust reference point for chemical evolution studies (e.g. Stonkutė et al. 2020).

By contrast, carbon and nitrogen abundances are strongly modified during stellar evolution by internal transport processes. The classical picture is that of the first dredge-up (1DUP), a convective event that occurs when low- and intermediate-mass stars ascend the red giant branch (RGB). During this stage, the convective envelope deepens and engulfs layers previously affected by partial hydrogen burning, thereby bringing nuclear-processed material to the surface. The immediate consequence is a decline in the photospheric abundance of ^{12}C and a corresponding increase in ^{13}C and ^{14}N (Iben 1965). The extent of these abundance alterations provides a direct diagnostic of stellar mixing efficiency, mass, and evolutionary status.

While the 1DUP is well described by stellar evolution models, subsequent observations revealed discrepancies that required the introduction of additional, non-canonical mixing processes. As early as the 1970s, spectroscopic analyses reported further depletion of carbon and enhancement of nitrogen in red giants beyond the predictions of standard models (Day et al. 1973; Pagel 1974; Tomkin et al. 1976; Lambert & Ries 1981). Systematic studies confirmed that ^{12}C/^{13}C ratios decline further than expected, in some cases reaching values as low as 10, compared to canonical predictions of 20–30 after the first dredge-up (Gilroy 1989; Gilroy & Brown 1991). Later studies, including those by Gratton et al. (2000); Tautvaišienė et al. (2001, 2005), and more recently by Smiljanic et al. (2009); Mikolaitis et al. (2011a,b, 2012); Lagarde et al. (2012, 2019), firmly established that an additional mechanism, often termed "extra mixing" must be operating during the RGB phase.

The onset of this extra mixing appears to be associated with the RGB luminosity bump. At this stage, the advancing hydrogen-burning shell crosses the molecular weight discontinuity left by the deepest penetration of the convective envelope during the dredge-up. The removal of this barrier allows further transport between the convective envelope and deeper regions, enabling chemical anomalies to develop (Charbonnel 1994; Charbonnel et al. 1998). The amplitude of these anomalies depends strongly on stellar mass, metallicity, and evolutionary state (Lambert & Ries 1977; Boothroyd & Sackmann 1999; Charbonnel & Zahn 2007).

A variety of physical mechanisms have been proposed to explain this additional transport. One long-standing idea is rotation-induced mixing, in which differential rotation and shear instabilities drive slow circulation currents that connect surface and interior layers. Models by Palacios et al. (2003), Chanamé et al. (2005), and Denissenkov et al. (2006) explored the extent to which rotation can explain the observed chemical patterns. Another set of hypotheses involves magnetic processes: magnetic buoyancy, magneto-rotational instabilities, or magnetically induced turbulence may transport material in ways not captured by purely hydrodynamical models (Busso et al. 2007; Nordhaus et al. 2008; Palmerini et al. 2009). Some studies have considered the combined effects of rotation and magnetic fields, showing that together they can enhance mixing efficiency beyond either process alone (Eggenberger et al. 2005; Denissenkov et al. 2009).

Internal gravity waves represent another proposed driver. These waves, generated at the convective–radiative boundary, can propagate into stellar interiors and redistribute angular momentum and chemical elements (Zahn et al. 1997; Denissenkov & Tout 2000). More recently, thermohaline instability has emerged as a leading candidate for the main non-standard mixing mechanism. This process arises when the burning of ^{3}He produces a local inversion in the mean molecular weight, creating conditions analogous to “salt-finger” instabilities in terrestrial fluids. As shown in pioneering work by Eggleton et al. (2006, 2008) and later modeled by Charbonnel & Zahn (2007) and Cantiello & Langer (2010), thermohaline convection can efficiently transport material on the RGB, lowering carbon abundances, raising nitrogen, and reducing ^{12}C/^{13}C ratios.

The interplay of multiple mechanisms is almost certainly required to fully reproduce the observed abundance patterns. Charbonnel & Lagarde (2010) and Lagarde et al. (2012) developed detailed models combining both rotation-induced transport and thermohaline mixing, demonstrating that their simultaneous action provides a much better match to observations across a wide mass range than either mechanism alone. These models predict distinctive evolutionary trends in lithium, C/N, and $^{12}C/^{13}C$ ratios, which can be tested with high-resolution observations.

Among the available abundance diagnostics (Charbonnel & Lagarde 2010; Lagarde et al. 2012, 2017), the $^{12}C/^{13}C$ ratio stands out as one of the most sensitive probes of internal mixing. Unlike absolute abundances, it depends only weakly on metallicity, initial composition, or atmospheric modeling uncertainties. Instead, it directly reflects the depth to which CN-cycled material has been transported. Ratios close to the solar value of 90 are typical for unevolved stars, while post-dredge-up giants exhibit values of 20–30; lower values signal the operation of extra mixing. Complementary indicators include the C/N ratio and lithium abundances, both of which respond sensitively to the internal transport but are somewhat more dependent on initial conditions.

The study of mixing processes is especially significant in magnetically active stars such as RS CVn stars (Tautvaisiene et al. 1992; Tautvaišienė et al. 2010a, 2011; Barisevičius et al. 2010, 2011). Observations have already indicated that RS CVn stars can display unusually low $^{12}C/^{13}C$ ratios even below the RGB bump, suggesting that magnetic activity triggers extra mixing earlier than in inactive stars. Similarly, lithium abundances in RS CVn stars often depart from the standard trends, with some objects retaining higher Li than expected, while others show extreme depletion or enrichment. Understanding these anomalies requires disentangling the effects of standard dredge-up, thermohaline transport, rotation, and magnetism.

A comprehensive study of CNO abundances and isotopic ratios in chromospherically active stars offers powerful constraints on internal mixing processes. Such measurements clarify how magnetic activity alters stellar interiors while simultaneously informing broader astrophysical contexts. On the one hand, they help to improve theoretical models of stellar structure and evolution; on the other, they sharpen our interpretation of chemical abundance surveys of Galactic stellar populations. Given the widespread use of red giants as indicators of Galactic chemical evolution, it is imperative to characterise the chemical peculiarities of the RS CVn stars with precision to reduce the potential systematic uncertainties in tracing the evolution of the Milky Way.

In conclusion, mixing processes in evolved stars remain one of the most active areas of stellar astrophysics. Standard models reproduce the first dredge-up, but they fall short of explaining the abundance anomalies observed in giants, necessitating the inclusion of additional physical mechanisms. By combining detailed models of rotation, magnetism, thermohaline convection, and gravity waves with precise spectroscopic data, significant progress has been made. However, RS CVn stars highlight the complexity of the problem: their enhanced activity reveal that the onset and efficiency of mixing can be profoundly altered by magnetic and tidal effects. For this reason, the systematic study of CNO abundances and isotope ratios in RS CVn stars, such as the one undertaken in this thesis, provides a unique and powerful window into the fundamental physics of mixing in stellar atmospheres.

1.3 Lithium in Stellar Evolution and RS CVn Stars

Lithium occupies a special place in astrophysics because of its unique nucleosynthetic origin, its extreme fragility in stellar interiors, and its diagnostic value for understanding material mixing and transport processes in stars. As one of the few light elements produced in measurable quantities during Big Bang nucleosynthesis (BBN), lithium provides a direct link between cosmology and stellar evolution. The primordial abundance predicted by standard BBN, combined with the baryon density inferred from cosmic microwave background observations, yields $A(\mathrm{Li}) \simeq 2.72$ dex (Cyburt et al. 2008), later revised to $\simeq 2.75$ dex (Pitrou et al. 2018). This value, however, is systematically higher than what is observed in the atmospheres of old, metal-poor halo dwarfs, which show a nearly constant lithium abundance $A(\mathrm{Li}) \simeq 2.05$ dex for $-2.4 < [\mathrm{Fe/H}] < -1.5$ and $5500 < T_{\mathrm{eff}} < 6250$ K – a feature known as the *Spite plateau* (Spite & Spite 1982). The discrepancy between BBN predictions and stellar measurements, often called the "cosmological lithium problem", remains unsolved. At the lowest metallicities, the plateau appears to break down, producing a "meltdown" with a wide spread of lithium abundances (Norris et al. 2023). Among lower RGB stars of very low metallicity, a thin lithium plateau has recently been identified at $A(\mathrm{Li}) \simeq 1.09 \pm 0.01$ dex, accompanied by a tail of Li-poor stars with $A(\mathrm{Li}) \lesssim 0.7$ dex (Mucciarelli et al. 2022).

Today's Galactic lithium budget reflects a balance of production and destruction channels. In Population I stars, the meteoritic abundance $A(\mathrm{Li}) = 3.26$ dex (Asplund et al. 2009) serves as the reference for the initial lithium content of the interstellar medium from which young stars form. However, stellar evolution theory predicts that red giants should exhibit photospheric abundances of only $A(\mathrm{Li}) \lesssim 1.5$ dex due to dilution and destruction. Lithium is destroyed at relatively low temperatures, $T \gtrsim 2.5 \times 10^6$ K, making it extremely sensitive to internal transport of material. The pre-main sequence already initiates lithium depletion as deep convection mixes surface material into hot stellar interiors. On the main sequence, gradual depletion continues through slow mixing below the convection zone. A dramatic reduction occurs during the first dredge-up (FDU) as the convective envelope deepens, carrying lithium-depleted material to the surface and diluting the atmospheric abundance (Iben 1968). Another phase of depletion follows at the RGB luminosity bump, when the hydrogen-burning shell erases the molecular weight discontinuity left by the FDU, allowing non-canonical extra mixing to operate (e.g. Pinsonneault 1997; Lyubimkov 2016; Randich & Magrini 2021).

Beyond standard predictions, a variety of processes have been invoked to explain anomalous lithium behaviour in evolved stars. Rotation-induced mixing can enhance internal transport, gradually depleting surface lithium (Palacios et al. 2003; Chanamé et al. 2005). Magnetic fields may also play a role, either by suppressing or enhancing mixing process, depending on field geometry and strength (Busso et al. 2007; Nordhaus et al. 2008). Thermohaline convection, triggered by local molecular weight inversions created by ^{3}He burning, has been proposed as a key non-canonical mixing mechanism (Eggleton et al. 2006, 2008; Charbonnel & Zahn 2007; Cantiello & Langer 2010). Models combining rotation and thermohaline processes provide the best agreement with observational data across different stellar populations (Charbonnel & Lagarde 2010; Charbonnel et al. 2017).

At the same time, lithium can also be created or acquired externally. Possible enrichment channels include internal nucleosynthesis via the Cameron–Fow ler mechanism operating in AGB stars (Cameron & Fowler 1971; Sackmann & Boothroyd 1992), production in novae (Starrfield et al. 1978; Vigroux & Arnould 1979; Izzo et al. 2015; Molaro et al. 2016; Rukeya et al. 2017), and cosmic-ray spallation (Reeves et al. 1970; Olive & Schramm 1992). External processes such as planet engulfment (Villaver & Livio 2009; Adamów et al. 2012), interaction with substellar companions (King et al. 1997; Israelian et al. 2004), or accretion from circumstellar material may also contribute. The growing number of Li-rich red giants about 1.2–2.2% of the total population (Gao et al. 2019; Casey et al. 2019; Charbonnel et al. 2020) demonstrates that additional enrichment processes must be at work. However, no single mechanism fully accounts for the observed diversity of Li-rich stars.

The problem of lithium-rich giants remains one of the most enduring puzzles in stellar astrophysics. Some stars show Li abundances approaching or even exceeding the meteoritic value, despite being in evolutionary stages where canonical theory predicts near to complete depletion. Explanations range from internal production via non-standard mixing to external replenishment from engulfed planets, brown dwarfs, or binary companions. Others invoke episodic or phase-dependent enrichment, such as sudden Li production during the helium flash (Kumar et al. 2020; Mallick et al. 2023). Rotation-driven instabilities, magnetic buoyancy, or mass transfer in interacting binaries may also provide viable channels (Denissenkov & Herwig 2004; Guandalini et al. 2009). The variety of proposed scenarios underscores the complexity of lithium evolution and the importance of studying it in different stellar environments.

In this context, RS CVn binaries offer an exceptional case to investigate lithium. As post main sequence systems (Popper & Ulrich 1977), their primaries should, in principle, display strongly diluted lithium abundances. However, the Li I 6707 Å doublet is frequently detected even in late-type RS CVn stars (later than about G8–K0), suggesting that either mixing is inhibited by rapid rotation and strong magnetic fields, or that lithium has been recently replenished (Herbig 1965; Soderblom 1984; Randich et al. 1992).

Observational efforts have long pointed to an anomalous lithium behaviour in RS CVn stars. Pallavicini et al. (1992), analysing southern active stars, found lithium abundances well above those of inactive field giants of similar type. High-resolution synthesis studies by Randich et al. (1993) confirmed systematic Li overabundances, a strong dependence on effective temperature, weak correlations with $v \sin i$ and activity indicators, and no evidence for flare-induced spallation. A subsequent northern survey by Randich et al. (1994) also reported no flare-induced Li production but argued that tidal locking and magnetic activity may inhibit deep convective mixing, thereby preserving higher Li. They further proposed that lithium abundances, combined with $^{12}C/^{13}C$ isotopic ratios, provide a powerful diagnostic of mixing in evolved binaries.

Despite these advances, many earlier studies of RS CVn stars suffered from limitations: small sample sizes, lack of homogeneous abundance determinations, incomplete coverage of CNO abundances and isotope ratios, and uncertainties in stellar masses and evolutionary status. This gap has motivated more recent work, including the present study, which systematically derives atmospheric parameters, lithium abundances, CNO abundances, and $^{12}C/^{13}C$ ratios for a large sample of RS CVn stars. By providing a coherent dataset, we are able to investigate whether lithium anomalies in RS CVn binaries arise primarily from inhibited depletion due to magnetic activity, premature extra mixing, or episodic enrichment processes.

In summary, lithium is both a cosmological relic and a fragile stellar diagnostic. Its abundance evolution is shaped by a delicate interplay of nuclear destruction, convective dilution, non-canonical mixing, and possible enrichment events. The anomalies observed in RS CVn stars challenge standard expectations and suggest that rotation, tidal interactions, and magnetic fields fundamentally alter lithium behaviour. Understanding lithium in RS CVn stars is therefore crucial not only for clarifying the physics of stellar mixing but also for addressing the broader astrophysical questions of lithium enrichment and depletion in the Galaxy.

1.4 Eruptive stars

Eruptive variables are broadly defined as stars whose irregular or impulsive brightness changes are driven by violent processes in their outer atmospheres most commonly chromospheric and coronal flares, and whose photometric and spectroscopic signatures are often accompanied by shell ejections, episodic mass outflows and variable emission-line strengths (Good 2003). Stellar flares are multi-wavelength, magnetically driven bursts of electromagnetic radiation (from X-rays to radio) that occur preferentially on stars with outer convective envelopes and can produce shocks, particle acceleration and, in some cases, coronal mass-ejection–like phenomena (Kowalski 2024; Veronig et al. 2021). Episodic shell ejections and strong wind signatures (e.g. P Cygni profiles) have long been documented in luminous eruptive stars and are a hallmark of mass-loss episodes in such objects (Lamers et al. 1985). Theoretical work has suggested that sufficiently energetic flashes or prolonged high-energy activity may, in principle, alter surface abundances by exposing or redistributing nucleosynthetically processed material (Sackmann et al. 1974); however, the observational evidence for flare- or eruption-driven, long-lived changes to photospheric CNO abundances remains limited and is an open question for further monitoring and detailed abundance studies (Testa et al. 2015).

2 Research methodology

2.1 Target selection and data reduction

The first step of this study involved the careful selection of a representative sample of chromospherically active RS CVn stars. Our goal was to assemble a dataset sufficiently large to probe systematic abundance patterns, while at the same time ensuring that the stars were bright enough and well placed in the sky for high-resolution spectroscopic observations. In total, 52 RS CVn stars were selected. The 52 RS CVn stars are divided into first subsample and second subsample as displayed in Table B1 and Table B2, respectively. The subsample was deliberately restricted to low and intermediate mass stars in order to focus on evolutionary phases where the effects of dredge-up and extra mixing are most apparent, and where comparison with models is meaningful.

The majority of our objects were drawn from the catalogue of Strassmeier (1994), which has long served as a fundamental reference for RS CVn stars. This source provided a well-documented list of chromospherically active stars with confirmed binary nature and detailed photometric and spectroscopic information. From this work we included, *iot Gem, *bet Gem, *g Gem, HD 71028, V* FI Cnc, *10 LMi, V* FG UMa, *tau Leo, *93 Leo, *c Vir, V* IT Com, *7 Boo, *eta Boo, V* FR Boo, HD 141690, HD 161832, HD 179094, *f Aql, V* V1971 Cyg, *alf Sge, *eps Leo, V* V403 Aur, V* V834 Her, *62 Ser, *ksi Leo, HD 200740, *mu. Leo, and *b01 Cyg. These stars have been extensively studied in terms of their activity signatures and variability, making them ideal candidates for chemical abundance analysis.

A second major source was the catalogue of Eker et al. (2008), which provided a compilation of chromospherically active systems, paying special attention to the diagnostic emission features in Ca II H & K and H_α. From this list we selected *33 Psc, V* V1149 Ori, *sig Gem, V* BM CVn, V* HK Boo, V* V835 Her, V* V2075 Cyg, V* IM Peg, *lam And, *eps Umi, HD 191588, V* KX Peg, V* BF Psc, *3 Cam, V* CL Cam, *29 Dra, and *39 Cet. The inclusion of these stars was motivated by the detailed documentation of their emission signatures, which confirm strong chromospheric activity typical of RS CVn systems.

The stars HD 145742, BD+15 3367, and HD 221639 were included based on references cited by Pace (2013), while the RS CVn star V* OP And was taken from the early work of Strassmeier et al. (1990). The magnetically active star *37 Com, for which Aurière et al. (2015) reported direct magnetic field measurements, was included to extend the subsample to objects with well-constrained field strengths. Finally, HD 6497 was incorporated following the classification and analysis by Massarotti et al. (2008).

In assembling the final subsample, practical considerations were also applied. The brightness of the targets was an important factor, as sufficiently high signal-to-noise ratios (S/N) were required to derive reliable abundances of weak spectral features such as the Li I 6707 Å line or molecular bands of CN and C_2. Positional constraints were equally relevant, since the observations were carried out using the 1.65 m telescope of the Vilnius University Moletai Astronomical Observatory in Lithuania and with Vilnius University Echelle Spectrograph (VUES; Jurgenson et al. 2016). Stars had to be observable with adequate elevation during scheduled observing runs. The spectra were obtained with resolving powers of $R \sim 36\,000$ and $R \sim 68\,000$, with the choice of resolution depending on the observing nights, observing time available. In the case of binaries, only single-lined stars were selected.

The resulting list of 52 RS CVn stars constitutes one of the most extensive spectroscopic subsamples of its kind. It combines well-known bright stars, frequently studied for their activity, with less common but highly active systems. By including stars from different catalogues and references, we ensured diversity in terms of mass, spectral type, orbital properties, and chromospheric activity levels. This breadth of selection allows for a systematic investigation of how lithium, carbon, nitrogen, and oxygen abundances, along with carbon isotopic ratios, vary across the RS CVn class.

For eruptive stars, the target list was constructed from giant stars in the *Kepler* field and to cover a range in stellar mass and metallicity. High-resolution spectra were obtained with the FIES spectrograph on the Nordic Optical Telescope, and seismic parameters from *Kepler* together with astrometry from *Gaia* provided accurate stellar properties and evolutionary classification. The list included: KIC2696955, KIC3730953, KIC3854605, KIC4571402, KIC4575645, KIC11188067, KIC6838707, KIC7374855, KIC7820638, KIC9652494, KIC4755467, KIC11819760. All these stars belong to the core He-burning stage of evolution.

2.2 Method of analysis

In this study, a traditional differential analysis approach was employed to investigate the abundances of chemical elements in magnetically active RS CVn stars. The differential method, in which stellar abundances are derived relative to the

Sun or another well-studied reference star, reduces the impact of uncertainties in atomic data and model atmospheres, thereby improving the precision of the results. This strategy is especially useful for active stars, whose spectra are often more complex because of line broadening, surface inhomogeneities, and chromospheric emission.

Two complementary approaches were adopted to determine elemental abundances: the *EW* method and *spectral synthesis*. The EW method was applied to elements for which numerous isolated, unblended absorption lines are present in the stellar spectra. Measurement of the integrated area of such lines allows for straightforward abundance determination once the atmospheric parameters are established. This technique is efficient for elements such as Fe, Si, Ca, Ti, and Ni, which provide many measurable lines throughout the observed spectral range.

In contrast, spectral synthesis was used for elements that are poorly represented by isolated lines or for cases where only a few weak features exist. Oxygen provides a typical example, as its reliable diagnostics are limited to the forbidden [O I] lines or blended molecular bands. Similarly, carbon and nitrogen abundances were derived using synthesis of C_2 and CN molecular features, which are not suitable to the EW measurement. Spectral synthesis also proved essential for determining isotopic ratios such as $^{12}C/^{13}C$, where blended features must be modelled in detail. By combining both methods, the analysis framework ensured comprehensive coverage of elements with widely differing spectral behaviour.

For the measurement of EW, two specialised software tools were employed. The first was `DAOSPEC`, an automated program maintained by Peter B. Stetson at the Dominion Astrophysical Observatory (Stetson & Pancino 2008). DAOSPEC is designed to automatically identify and fit absorption lines across high-resolution spectra, delivering consistent EW measurements while minimising human bias. The second tool was Spectral Analysis Tool – Virtual Observatory `SPLAT-VO`, a package developed by the German Astrophysical Virtual Observatory in collaboration with the Astronomical Institute of the Academy of Sciences of the Czech Republic (Škoda et al. 2014). SPLAT-VO is a versatile spectroscopic analysis tool that allows for both automated and interactive EW measurements, providing flexibility when dealing with complex or blended lines.

In both cases, the selection of spectral lines was carried out with great care. Only features that were free of significant blending, telluric contamination, or other distortions were retained in the final analysis. This selection process was based on the line lists from the Vienna Atomic Line Database (VALD) and by previous abundance studies of late-type stars. Special attention was also paid to the continuum placement, since inaccurate continuum normalisation can introduce systematic errors into EW measurements. Whenever possible, lines were cross-checked by comparing their behaviour in spectra of reference stars to verify their suitability.

The spectral synthesis calculations were performed using one-dimensional LTE model atmospheres, in conjunction with radiative transfer codes capable of handling line blending and molecular equilibria. For each target star, synthetic spectra were generated over the relevant wavelength ranges and compared directly with the observed spectra. Abundances were then adjusted iteratively until the best match between the synthetic and observed profiles was achieved. This procedure was particularly crucial for molecular bands, where overlapping features require simultaneous fitting of multiple species, and for lithium, where the Li I 6707 Å resonance doublet must be disentangled from nearby blends and corrected for NLTE effects.

The combined use of the EW method and spectral synthesis provided a reliable and flexible framework for abundance determination. The EW approach offered speed and precision for elements with rich line spectra, while spectral synthesis extended the analysis to elements and isotopic ratios inaccessible through EW measurements. By employing both techniques and cross-validating the results, systematic uncertainties were minimised, ensuring that the derived abundances reflect the intrinsic properties of the stars rather than methodological biases.

2.3 Observations

We conducted a comprehensive spectroscopic survey of 52 RS CVn type stars between 2021 and 2024 using the 1.65 m Ritchey–Chrétien telescope at the Vilnius University's Moletai Astronomical Observatory (MAO). Over the course of the observing program, we secured a total of 72 high-resolution echelle exposures with the VUES. VUES provides continuous wavelength coverage from 4000 Å to 8800 Å, which fully encompasses the diagnostic features required for chemical abundance studies, including the Li I 6707 Å doublet, molecular CN and C_2 bands, and the forbidden [O I] lines at 6300 Å.

The VUES spectrograph offers three selectable resolution settings; for our programme, we used two modes. The lower resolution was adopted for relatively faint targets or for exploratory observations, while the higher resolution was employed for brighter systems and for stars where detailed isotopic or molecular synthesis was required. For the first subsample, 20 stars were observed at $R = 36\,000$ and 10 of the stars were observed at $R = 68\,000$ later. For the second subsample, 32 objects were observed in two spectroscopic modes: 17 stars were observed at $R = 36\,000$, whereas 6 were observed at $R = 68\,000$ and 9 were observed in both resolutions. A total of 41 observations were made for the second subsample.

Exposure times were tailored to the apparent brightness of each target, ranging from 1200 s for the brightest RS CVn stars to 3600 s for the faintest. This level of quality ensured that even weak or blended lines could be measured with confidence. Observation runs were distributed across different seasons to optimise target visibility. All raw frames were reduced using the dedicated VUES pipeline described by Jurgenson et al. (2016). The final step of continuum normalisation was carried out interactively for abundance-critical regions such as the Li I 6707 Å doublet and CN molecular bands. Special care was taken to avoid over-normalisation in heavily line-blanketed spectral regions typical of late-type stars.

For observations of eruptive stars, we carried out two observing runs with the high-resolution Fibre-fed Echelle Spectrograph (FIES; Telting et al. 2014) mounted on the Nordic Optical Telescope (NOT). Observations were obtained in the medium-resolution configuration ($R \sim 46\,000$), which provides a broad and continuous wavelength coverage from ∼4100 to 8500 Å. This range includes several key spectral features such as the forbidden [O I] line, C_2 molecular bands, strong $^{12}C^{14}N$ features, and the $^{13}C^{14}N$ line at 8004 Å, all of which are suitable for constraining the C/N and $^{12}C/^{13}C$ ratios. The first observing run was conducted from 27 June to 2 July 2018 (programme P57-105) and was dedicated to 41 stars with masses below $1.5 M_{\odot}$. The second run, carried out between 25 and 28 July 2019 (programme P59-103), targeted stars of higher mass ($1.5 - 2.2 M_{\odot}$) as well as subsolar objects with $[Fe/H] < -0.2$. Exposure times were selected to ensure a minimum signal-to-noise ratio of 80. Data reduction was performed with the dedicated FIESTOOL pipeline, available at the telescope. The pipeline produces fully reduced spectra by applying the nightly calibration frames.

2.4 Atmospheric parameters

The determination of reliable stellar atmospheric parameters is a fundamental prerequisite for any abundance analysis, since the effective temperature ($T_{\rm eff}$), surface gravity ($\log g$), microturbulent velocity ($v_{\rm t}$), and metallicity ([Fe/H]) strongly influence the behaviour of absorption lines in stellar spectra. In this study, we derived these parameters for each of the 52 RS CVn stars in our subsample using the classical EW method, which exploits the sensitivity of neutral and ionised iron lines to different atmospheric conditions. Iron was chosen as the diagnostic element because of its high cosmic abundance, the large number of well-studied transitions throughout the optical range, and the fact that its neutral (Fe I) and singly ionised (Fe II) species provide complementary constraints on temperature and gravity. EW for Fe I and Fe II lines were measured independently with the software packages `DAOSPEC` (Stetson & Pancino 2008) and `SPLAT-VO` (Škoda et al. 2014). Both tools were used to ensure consistency and to minimise systematic biases related to line fitting and continuum placement. The atomic line list was adopted from the critically evaluated Gaia-ESO compilation (Heiter et al. 2015), which provides accurate oscillator strengths and damping parameters. To minimise the risk of systematic errors, only lines deemed unblended and of sufficient quality in our spectra were included, resulting in the use of approximately for the subsample: 70 Fe I lines, 7 Fe II lines per star and in the second subsample: 58 Fe I lines, 6 Fe II lines per star on average.

The parameter determination was performed iteratively with the LTE spectral analysis code `MOOG` (Sneden 1973), following a standard excitation and ionisation equilibrium procedure. The effective temperature was adjusted until no correlation remained between the abundances derived from Fe I lines and their excitation potential, thereby ensuring excitation balance. The microturbulent velocity was determined by removing any trend between Fe I abundances and reduced EW, a correction required because unresolved velocity fields in the stellar atmosphere affect stronger lines more than weaker ones. The surface gravity was obtained by enforcing ionisation equilibrium, requiring that the mean abundance derived from Fe I lines matched that from the Fe II lines. Once these three equilibria were satisfied, the metallicity was adopted as the mean iron abundance. This iterative process was repeated until all conditions were fulfilled simultaneously, yielding a self-consistent set of atmospheric parameters for each star.

The model atmospheres used in this work were taken from the MARCS model (Gustafsson et al. 2008), which provides one-dimensional, plane-parallel models calculated under the assumptions of hydrostatic equilibrium, flux conservation, and local thermodynamic equilibrium (LTE). While these assumptions do not capture the full complexity of stellar atmospheres (particularly in active stars with magnetic fields and surface inhomogeneities) they remain standard in abundance work and provide consistency with large spectroscopic surveys such as Gaia-ESO. Solar abundances were adopted from Grevesse et al. (2007), enabling a strictly differential analysis relative to the Sun. This approach reduces systematic uncertainties associated with oscillator strengths, line broadening parameters, and allows a direct comparison between RS CVn stars and inactive field giants.

Atmospheric parameters for all 52 RS CVn stars were derived through a rigorous spectroscopic procedure that combines high-quality EW measurements of iron lines, iterative adjustments using `MOOG`, MARCS model atmospheres, and a differential approach relative to the Sun. This framework ensures that the $T_{\rm eff}$, $\log g$, $v_{\rm t}$, and [Fe/H] values obtained are precise, internally consistent, and directly comparable across the entire subsample. These parameters provide the essential foundation for the subsequent determination of lithium, carbon, nitrogen, oxygen, and isotopic abundances, as well as for the broader investigation of how magnetic activity influences chemical evolution in RS CVn type stars.

For determining atmospheric parameters of eruptive stars, we applied a two-step approach. EW of Fe I and Fe II lines were measured with DAOSPEC (Stetson & Pancino 2008) and abundances computed using MOOG (Sneden 1973). Since surface gravities are more reliably obtained from asteroseismic constraints (Morel & Miglio 2012; Creevey et al. 2013), we adopted a second step in which stellar $\log g$ values were derived from *Kepler* asteroseismic data (Mosser et al. 2012) combined with the spectroscopic effective temperatures obtained in the first step. We then fixed the asteroseismic $\log g$ and recalculated the other atmospheric parameters, ensuring consistency between Fe I abundances, excitation potential, and the EW. This approach minimise the main weakness of purely spectroscopic analyses, namely the uncertain determination of $\log g$.

2.5 Elemental abundances and carbon isotope ratios

To derive the abundances of carbon, nitrogen, oxygen, magnesium, and lithium, we primarily employed the spectral synthesis method using the `TURBOSPECTRUM` code (Plez 2012), which is well suited for handling molecular equilibria and blended features in late-type stellar spectra. For carbon, we relied on the C_2

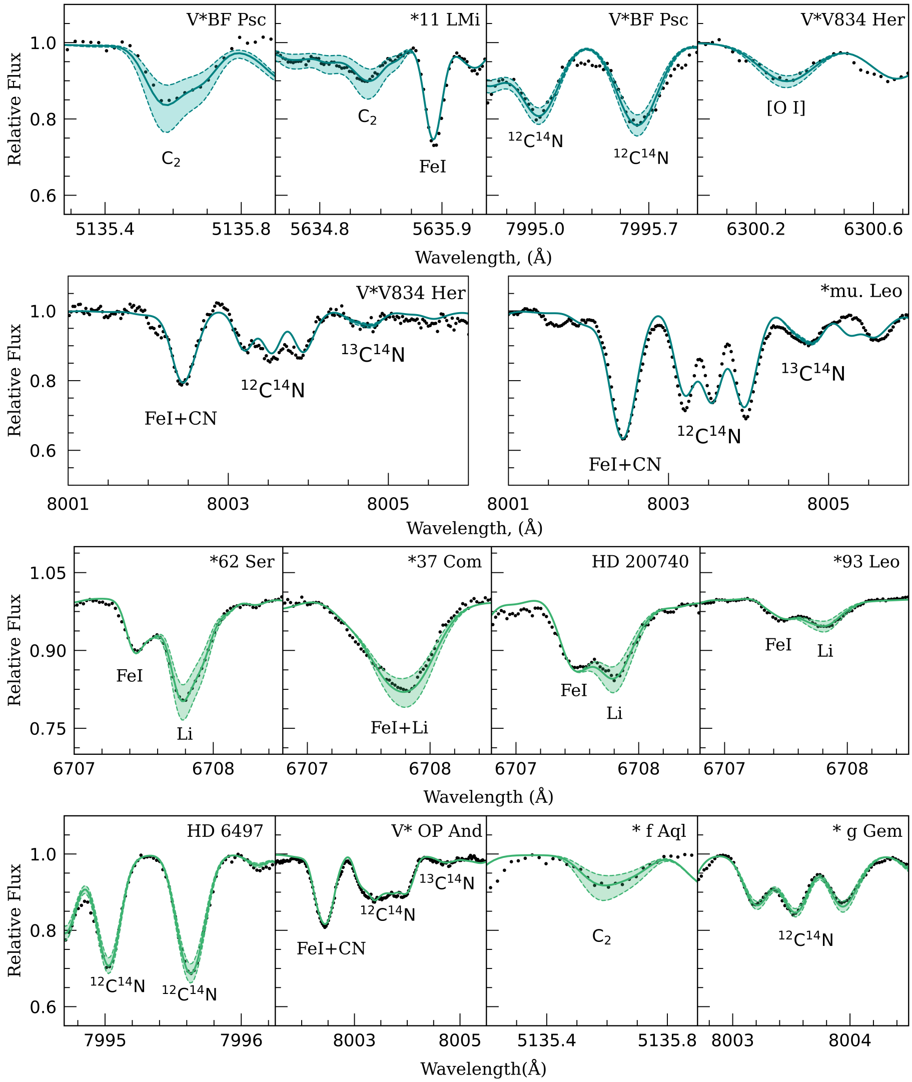

Figure 2: Examples of stellar spectra and spectral syntheses. The observed spectra are displayed using the black dots, while the solid green lines represent the optimal fit of synthetic spectra to the observed data, accounting for variations of ±0.10 dex in abundance marked by the filled region around the optimal fit.

Swan bands at 5135 Å and 5635 Å, which are strong molecular indicators in G–K type stars and provide sensitive diagnostics of carbon abundance once the continuum is carefully normalised. The oxygen abundances were determined from the forbidden [O I] line at 6300.3 Å, a well-established tracer of oxygen in cool stars, given its relative insensitivity to NLTE effects and its straightforward atomic physics. Nitrogen abundances were measured from $^{12}C^{14}N$ molecular features in the regions 6470–6490 Å and 7980–8005 Å, which are rich in CN lines suitable for spectral synthesis, while the $^{13}C^{14}N$ molecular band at 7990–8010 Å was used to determine the isotopic ratio $^{12}C/^{13}C$. The isotope ratio is particularly valuable as it provides a sensitive diagnostic of internal mixing processes that complements the absolute carbon and nitrogen abundances.

The determination of carbon and oxygen abundances was performed iteratively, since the two elements are linked through molecular equilibrium: the formation of CO locks up whichever of C or O is less abundant, influencing the molecular balance of the atmosphere. As a result, oxygen must be known to constrain carbon and vise versa. Our procedure began with an initial estimate of oxygen from the [O I] line, which was then used to derive carbon from the C_2 bands. The updated carbon value was fed back into the synthesis of the oxygen line, and the cycle was repeated until convergence was achieved. Once consistent C and O abundances were established, nitrogen was determined from the CN molecular lines, using the adopted C and O values as fixed inputs. Finally, the $^{12}C/^{13}C$ ratio was derived by fitting the ^{13}CN features, which are weak and blended but measurable in our high-resolution spectra.

For lithium, abundances were derived from the Li I 6707.8 Å resonance doublet, which remains the only viable diagnostic in cool stars. This line, however, is blended with nearby Fe I and CN features, making spectral synthesis essential for a reliable measurement. Synthetic spectra were computed using the line lists from VALD, and the lithium abundance was adjusted until the observed and synthetic spectra matched closely. NLTE corrections were applied to all LTE abundances using the INSPECT database (Lind et al. 2009)[1], ensuring that systematic biases from LTE assumptions were minimised. These corrections were positive for Li-poor stars, raising the abundance slightly, and negative for Li-rich objects, lowering the LTE-derived value. The potential impact of NLTE effects on the C_2 Swan bands is believed to be negligible, since comparisons with results from the forbidden [C I] line yield consistent abundances (Gustafsson et al. 1999). Similarly, the [O I] 6300.3 Å line is generally robust under LTE

[1] https://www.inspect-stars.com/

assumptions, with little evidence for strong NLTE departures (Asplund 2005).

Magnesium abundances were determined using several Mg I lines at 5528.4 1 Å, 5711.07 Å, 6318.71 Å, and 6319.24 Å. These lines are moderately strong, well characterised, and relatively unaffected by blending in most of our stars. Magnesium was also used as a proxy for oxygen in cases where the [O I] line at 6300.3 Å was severely affected by telluric absorption. Specifically, for V* HK Boo, HD 141690, V* V835 Her, V* V1971 Cyg, *eps UMi, *3 Cam, and V* CL Cam, telluric contamination prevented a reliable oxygen measurement, and the magnesium abundance was used in its place following the models presented in Pagel & Tautvaisiene (1995). The comparison between magnesium and oxygen is justified because both elements are α-process products, and their Galactic evolution is closely linked, making Mg a reasonable surrogate when direct O measurements are unavailable.

For the remaining set of chemical elements, including silicon, calcium, scandium (both neutral and singly ionised), titanium (both neutral and singly ionised), chromium, cobalt, and nickel, we employed the EW method. EW were measured using `DAOSPEC` (Stetson & Pancino 2008), and abundances were calculated with `MOOG` (Sneden 1973), adopting the same MARCS model atmospheres used for Fe-line analysis. The number of lines used for each element varied according to spectral quality but was generally sufficient to reduce statistical uncertainties. Methodological details for the treatment of atomic data, damping constants, and continuum placement followed the procedures established in the Gaia-ESO Survey (Tautvaišienė et al. 2015), ensuring homogeneity with large-scale stellar abundance studies.

Figure 2 presents examples of spectral synthesis fits in representative regions, illustrating the quality of the observed spectra and the reliability of synthetic modeling. The ability to reproduce weak features such as the Li I 6707.8 Å doublet and the ^{13}CN bands around 8000 Å demonstrates the robustness of our approach and the suitability of the data for detailed abundance determinations.

2.6 Non-local thermodynamic equilibrium effects

The determination of chemical abundances in RS CVn stars requires consideration of possible deviations from local thermodynamic equilibrium (LTE). In our studies, NLTE effects were evaluated where relevant, in particular for lithium. Lithium abundances were derived from the 6708 Å line using spectral synthesis, and NLTE corrections were applied following the INSPECT database (Lind

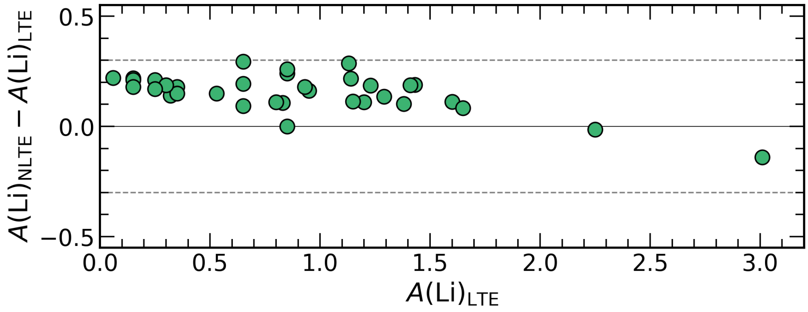

Figure 3: NLTE vs. LTE lithium abundances.

et al. 2009). For stars with $A(\mathrm{Li}) < 2.0$ dex, the NLTE corrections were positive and reached up to ~ 0.3 dex, while for stars with larger Li abundances the corrections became slightly negative. This ensured a more reliable determination of Li abundances in magnetically active stars, where LTE assumptions would otherwise underestimate or overestimate the photospheric lithium content.

For carbon and oxygen abundances, the molecular equilibrium of C, N, and O was taken into account in an iterative manner. The C abundances were derived from C_2 Swan bands, and although NLTE effects on these bands remain poorly characterised, previous studies have shown them to be negligible, as the abundances from C_2 features agree with those derived from the forbidden [C I] line (Gustafsson et al. 1999). Similarly, the [O I] 6300.3 Å line is well modelled under LTE conditions, and no significant NLTE corrections are required (Asplund 2005).

Nitrogen abundances and the $^{12}C/^{13}C$ ratios were derived from CN molecular features, where NLTE effects are less significant compared to atomic lines. Thus, the main focus of NLTE corrections in these studies was on lithium, which is the most sensitive element to such effects in cool chromospherically active stars.

2.7 Stellar mass

To determine both the ages and masses of the stars in the sample of RS CVn stars, we employed the UniDAM tool (Mints & Hekker 2017, 2018), which applies a Bayesian framework to combine spectroscopic and photometric constraints with theoretical stellar isochrones. UniDAM is particularly suitable for large stellar samples, as it self-consistently integrates observational uncertainties with model-based constraints, providing probability distribution functions for all stellar parameters rather than single estimates. For theoretical models, UniDAM makes use of the PAdova and TRieste Stellar Evolution Code (PARSEC) isochrones (Bressan et al. 2012), which represent one of the most widely used and thoroughly calibrated grids of stellar evolution tracks, covering a broad range in metallicity, mass, and evolutionary stage. By mapping observed properties onto these theoretical tracks, the tool delivers estimates of stellar age, mass, and radius, as well as the probability that the star belongs to different evolutionary phases.

The observational input consisted of the spectroscopic atmospheric parameters derived in thesis: effective temperature, surface gravity, and metallicity supplemented with near-infrared photometry to constrain luminosities. Specifically, we adopted the J, H, and K magnitudes from the Two Micron All-Sky Survey (2MASS; Skrutskie et al. 2006), which are well calibrated and provide fluxes for cool stars. These were complemented with mid-infrared magnitudes from the AllWISE survey (Cutri et al. 2021), namely $W1$ and $W2$, which probe longer wavelengths and help mitigate degeneracies in stellar evolutionary model fitting. For each target, we carried out a positional cross-match with the WISE catalog using a five-arcsecond search radius, which ensured reliable associations even in crowded fields. Photometric measurements were screened for quality using the survey flags, and only entries with the highest photometric reliability were retained.

With these inputs, UniDAM constructs likelihood functions for each star by comparing its measured properties to the PARSEC isochrones, simultaneously accounting for observational uncertainties and priors on stellar distributions. The Bayesian approach allows for the full exploration of degeneracies inherent in stellar evolution, particularly the overlap between subgiant and low-luminosity red giant phases or between red giant branch and core-helium burning stars. For each star, UniDAM outputs posterior probability distributions of stellar mass and age, from which we adopted the median as the representative value. In addition, UniDAM classifies stars into three broad evolutionary stages: the red giant branch (pre-core-helium burning; stage I), the core-helium burning phase (stage II), and the asymptotic giant branch (post-core-helium burning; stage III). This classification provides additional context for interpreting chemical abundances, since mixing and surface composition changes are strongly dependent on evolutionary state.

In estimating stellar masses, we followed the criteria outlined in Sect. 6.1 of Mints & Hekker (2017, 2018), which involve discarding solutions with poorly constrained likelihoods and adopting only those with high posterior probability. Stars with the most probable evolutionary stage were selected based on consistency with spectroscopic parameters and abundances. This procedure ensured that our final mass estimates were robust against artifacts of the Bayesian inference. The typical uncertainties in mass were 0.1–0.2 $M_{\odot}$ for well-constrained stars, while ages were naturally less precise, often spanning several Gyr owing to the intrinsic degeneracy of isochrone fitting for giants.

The combination of precise spectroscopic parameters with multi-band infrared photometry allowed us to exploit the full potential of the UniDAM Bayesian framework, yielding homogeneous mass and age estimates for all 52 RS CVn stars in the sample. These values not only provide fundamental constraints on the evolutionary status of the stars but also form an essential ingredient in interpreting the observed abundance patterns, especially in the context of mixing processes, lithium evolution, and chromospheric activity.

For the evaluation of stellar mass and age of eruptive stars, an independent determination was done using the `SPInS` (Stellar Parameters INferred Systematically) tool (Lebreton & Reese 2020). This code employs a Markov Chain Monte Carlo approach to match observed stellar properties with evolutionary tracks computed using the `STAREVOL` code (Lagarde et al. 2017, 2019). Two sets of input parameters were tested: (i) spectroscopic constraints only ($T_{\rm eff}$, $\log g$, [Fe/H]) and (ii) a combination of spectroscopy and asteroseismic quantities ($\Delta\nu$, $\nu_{\rm max}$, and $\Delta\Pi_1$). A Kroupa initial mass function and a truncated uniform star formation prior from 0–13.8 Gyr were adopted in both cases. We found that using only spectroscopy can lead to mass deviations of up to $\sim 50\%$ when compared with PARAM seismic masses. However, when asteroseismic information is included, the agreement improves to within $\sim 20\%$, as $\Delta\Pi_1$ efficiently distinguishes between RGB and core He-burning stars. Therefore, seismic masses from PARAM are used throughout this work, while SPInS was employed to derive consistent masses and ages for stars from the literature sample that lack asteroseismic constraints.

2.8 Kinematics properties

We computed the Galactic space velocities (U, V, W) and mean galactocentric distances for our subsample using the Python package `galpy`[2] (Bovy 2015). The necessary observational inputs like stellar distances from Bailer-Jones et al.

[2] http://github.com/jobovy/galpy

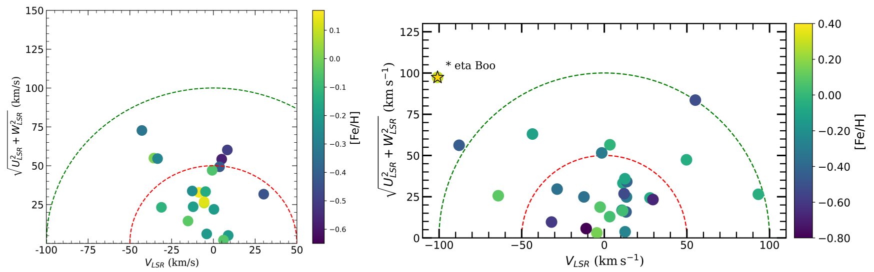

Figure 4: Toomre diagram for the stars in the first (left) and the second (right) subsamples of stars. The dashed lines represent the constant total space velocity. The symbols have been colour-coded according to the stellar metallicity [Fe/H].

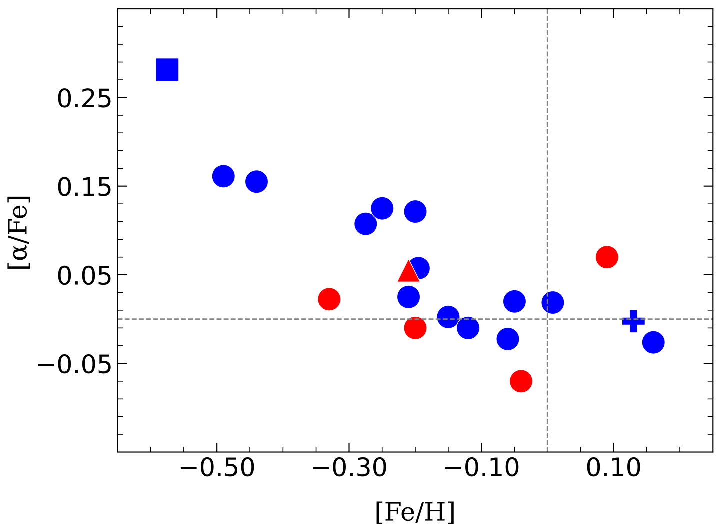

Figure 5: Observed α-to-iron element abundance ratios as a function of [Fe/H]. The value of $[\alpha/\mathrm{Fe\,I}]$ is computed as an average of the following elements: Mg I, Si I, Ca I, and Ti I. The meaning of symbols: the square is for the thick disc star, the circles are for the red giant branch stars, the plus sign marks a subgiant star, and the triangle is for the red clump star. The blue symbols mean that a star is at the evolutionary stage below the red giant luminosity bump, and the red is for stars at the evolutionary stage above the RGB luminosity bump.

(2021), proper motions and coordinates from *Gaia* Data Release 3 (Gaia Collaboration et al. 2021), and radial velocities derived from our own measurements were incorporated for each star. The resulting kinematic properties are displayed in a Toomre diagram Fig. 4. We adopted the classical thin/thick disc separation at $|V_{\rm tot}| = 50\,{\rm km, s^{-1}}$, as established by Yoshii (1982), Gilmore & Reid (1983), and Recio-Blanco et al. (2014); stars lying outside this velocity boundary were classified as thick disc members, while those within were attributed to the thin disc. To refine the classification, we also considered atmospheric parameters and the [α/Fe] versus [Fe/H] trends (see Figure 5). Based on these combined kinematic and chemical abundance criteria, HD 191588, the most metal-poor star in the first subsample of RS CVn stars with a notably elevated [α/Fe] ratio, was assigned to the thick disc, while all remaining targets were classified as thin disc stars. In the second subsample, *eta Boo was also assigned to the thick disc according to its kinematic parameters and chemical abundance analysis.

2.9 Estimation of uncertainties

In this study, we systematically identified and quantified uncertainties at every stage of the analysis, distinguishing between systematic and random sources. Systematic errors primarily arise from uncertainties in atomic data, but these were significantly mitigated by employing a differential analysis relative to the Sun. Random uncertainties result mainly from continuum placement and spectral line fitting. To ensure robust atmospheric parameter determination, we carefully selected Fe I and Fe II lines, avoiding blends and telluric contamination.

Uncertainties in the parameters were estimated by evaluating the sensitivity of the equilibrium conditions to perturbations in $T_{\rm eff}$, $\log g$, and $v_{\rm t}$. For typical stars in our subsample, internal uncertainties were on the order of $\pm$50–80 K in $T_{\rm eff}$, $\pm$0.1–0.2 dex in $\log g$, and $\pm 0.1\,{\rm km\,s^{-1}}$ in $v_{\rm t}$, while the uncertainty in [Fe/H] was generally below $\pm$0.05 dex for high-quality spectra. For fainter stars or those with broader lines due to high rotational velocities, uncertainties were somewhat larger, but remained within acceptable limits for reliable abundance determinations. For stars observed multiple times, parameters were determined independently for each spectrum and then averaged, further reducing the impact of random noise.

The mean values of uncertainties in the first stellar subsample are $\sigma_{T_{\rm eff}} = 50\,{\rm K}$, $\sigma_{\log g} = 0.18\,{\rm dex}$, $\sigma_{\rm [Fe/H]} = 0.08\,{\rm dex}$, and $\sigma_{v_t} = 0.22\,{\rm km\,s^{-1}}$. The mean values of uncertainties in the second subsample are $\sigma_{T_{\rm eff}} = 55\,{\rm K}$, $\sigma_{\log g} = 0.16\,{\rm dex}$,

Table 1: Effect of uncertainties in atmospheric parameters on the derived chemical abundances for the stars *29 Dra and HD 179094, representing the first and second subsamples of RS CVn stars, respectively.

*29 Dra	El.	$\Delta T_{\rm eff}$ $\pm$50 K	$\Delta\log g$ $\pm$0.18 dex	Δ[Fe/H] $\pm$0.08 dex	$\Delta v_{\rm t}$ $\pm$0.22 km s^{-1}
	C(C_2)	$\pm$0.01	$\pm$0.01	$\mp$0.02	$\mp$0.02
	N(CN)	$\pm$0.03	$\pm$0.04	$\pm$0.04	$\mp$0.00
	O([O I])	$\pm$0.01	$\pm$0.08	$\mp$0.01	$\pm$0.00
	Mg I	$\pm$0.03	$\mp$0.02	$\mp$0.02	$\mp$0.08
	Si I	$\pm$0.02	$\pm$0.04	$\pm$0.01	$\pm$0.03
	Ca I	$\pm$0.05	$\mp$0.03	$\pm$0.01	$\mp$0.09
	Sc I	$\pm$0.07	$\pm$0.00	$\pm$0.00	$\mp$0.03
	Sc II	$\mp$0.00	$\pm$0.08	$\pm$0.02	$\mp$0.08
	Ti I	$\pm$0.07	$\pm$0.00	$\mp$0.00	$\mp$0.07
	Ti II	$\mp$0.01	$\pm$0.08	$\pm$0.02	$\mp$0.07
	Cr I	$\pm$0.05	$\mp$0.01	$\pm$0.00	$\mp$0.06
	Cr II	$\mp$0.04	$\pm$0.08	$\pm$0.01	$\mp$0.04
	Co I	$\pm$0.03	$\pm$0.04	$\pm$0.01	$\mp$0.04
	Ni I	$\mp$0.02	$\pm$0.04	$\pm$0.01	$\mp$0.09
HD 179094	El.	$\Delta T_{\rm eff}$ $\pm$55 K	$\Delta\log g$ $\pm$0.16 dex	Δ[Fe/H] $\pm$0.09dex	$\Delta v_{\rm t}$ $\pm$0.21 km s^{-1}
	Li	$\pm$0.07	$\pm$0.02	$\mp$0.02	$\pm$0.00
	C(C_2)	$\pm$0.01	$\mp$0.02	$\mp$0.02	$\mp$0.01
	N(CN)	$\pm$0.02	$\mp$0.04	$\mp$0.03	$\pm$0.01
	O([O I])	$\pm$0.01	$\pm$0.07	$\mp$0.01	$\pm$0.01
	Mg I	$\pm$0.04	$\mp$0.06	$\mp$0.01	$\mp$0.06
	^{12}C/^{13}C	$\mp$0.30	$\mp$1	$\mp$0.30	$\pm$0.00

$\sigma_{[Fe/H]} = 0.09\,$dex, and $\sigma_{v_t} = 0.21\,$km s^{-1}. The precision of elemental abundances is influenced by uncertainties in atmospheric parameters, which we quantified by varying each parameter individually while keeping others fixed; detailed values for individual stars are provided in Table 1.

Random uncertainties for elements such as nitrogen and magnesium were estimated from line-to-line scatter, while for oxygen and the carbon isotopic ratio (where only one line was used), uncertainties were assessed based on continuum placement and signal-to-noise considerations. For example, the standard deviation in magnesium abundances is typically 0.07 dex.

Our analysis of molecular equilibrium effects on C, N, and O for the first subsample showed that Δ[O/H] $=$ 0.10 drives changes of Δ[C/H] $=$ 0.03 and Δ[N/H] $=$ 0.07; Δ[C/H] $=$ 0.10 induces variations of Δ[N/H] $=$ 0.10 and Δ[O/H] $=$ 0.01; while Δ[N/H] $=$ 0.10 leads to Δ[C/H] $=$ 0.00 and Δ[O/H] $=$ 0.01. For the second subsample, molecular coupling effects yielded Δ[O/H] $=$ 0.10 producing Δ[C/H] $=$ 0.05 and Δ[N/H] $=$ 0.02; Δ[C/H] $=$ 0.10 giving Δ[N/H] $=$ 0.07 and Δ[O/H] $=$ 0.04; and Δ[N/H] $=$ 0.10 leading to Δ[C/H] $=$ 0.03 and Δ[O/H] $=$ 0.01.

The uncertainty in the ^{12}C/^{13}C ratio depends on the strength of the ^{13}CN features, with a mean uncertainty of approximately ± 2. Stellar masses and ages were derived using the UniDAM tool (Mints & Hekker 2017, 2018), from which corresponding uncertainties were also obtained. The individual values are presented alongside the results in the machine-readable tables: https://cdsarc.cds.unistra.fr /vizbin/cat/J/A+A/696/A23 and https://cdsarc.cds.unistra.fr/vizbin/cat/J/A+A/703/A128

3 Results and discussion of analysis of RS CVn stars

3.1 Stellar parameters

Our targets RS CVn stars are spanning multiple post-main-sequence phases. Atmospheric parameters derived from spectra at both resolutions are listed in Table B1. For the first subsample, the effective temperatures cover 4380–5450 K (mean 4855 K), surface gravities span $1.9 \leq \log g \leq 4.35$ dex (mean 2.83 dex), metallicities range from -0.60 to $+0.17$ dex (mean -0.19 dex), and microturbulent velocities lie between 0.72 and 1.83 km s^{-1}. Considering the second subsample, the effective temperature is in the range of 4120–6220 K , while $\log g$ ranges from 1.4–4.3 dex, and [Fe/H] covers a range of -0.85 to $+0.34$ dex. Stellar ages range from 224 Myr to 11.7 Gyr for the first subsample

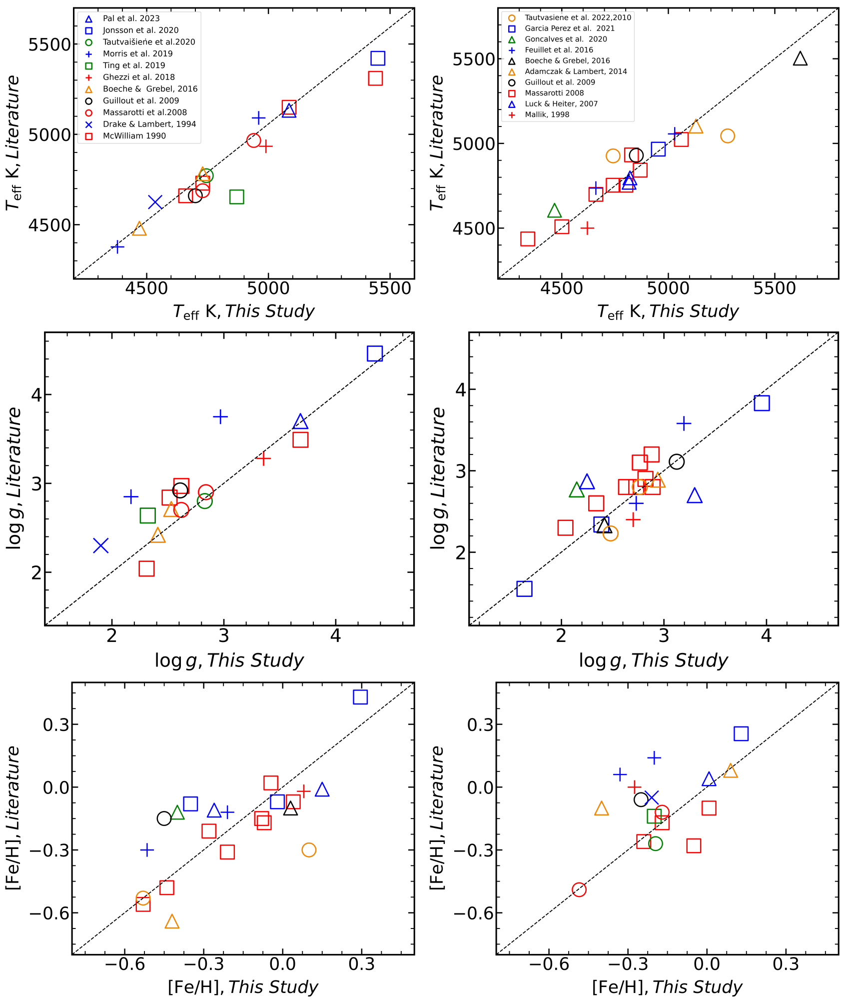

Figure 6: The main atmospheric parameters $T_{\rm eff}$, $\log g$, and [Fe/H], derived for the first subsample (the left column) and the second subsample (the right column) of RS CVn stars compared with studies listed in the section of Results.

with masses from 0.86 to 3.63 $M_\odot$. These values indicate a heterogeneous population dominated by giants at distinct evolutionary stages. Evolutionary states were determined from the $\log g$–$T_{\rm eff}$ diagram using PARSEC tracks (Bressan et al. 2012), taking into account the measured carbon and nitrogen abundances. For stars with $M < 2.2, M_\odot$, the RGB luminosity bump, where extra mixing occurs, manifests as a characteristic zigzag pattern. In contrast, more massive stars do not experience extra mixing during their first ascent of the RGB but instead undergo the second dredge-up later, during the asymptotic giant branch (AGB) phase, unless rotation-induced transport becomes efficient (Charbonnel & Lagarde 2010).

We validated our atmospheric parameters against literature (Fig. 6), including spectroscopic studies by (Tautvaišienė et al. 2022; García Pérez et al. 2021; Gonçalves et al. 2020; Ting et al. 2019; Feuillet et al. 2016; Boeche & Grebel 2016; Adamczak & Lambert 2014; Tautvaišienė et al. 2010a; Guillout et al. 2009; Massarotti et al. 2008; Luck & Heiter 2007; Mallik 1998) and targeted comparisons for individual stars *b01 Cyg, *ksi Leo, *62 Ser, *eps Leo (McWilliam 1990); *29 Dra (Tautvaišienė et al. 2020); *11 LMi (Jönsson et al. 2020); BD+15 3367 and HD 221639 (Morris et al. 2019); V* V403 Aur (Ting et al. 2019); V* BF Psc (Ghezzi et al. 2018); *mu. Leo and HD 145742 (Boeche & Grebel 2016); and V* CL Cam (Guillout et al. 2009); as well as photometric determinations for *b01 Cyg (Pal et al. 2023), *39 Cet and *ksi Leo (Massarotti et al. 2008), and *37 Com (Drake & Lambert 1994). Effective temperatures and surface gravities generally agree well; metallicities show larger dispersion, with discrepancies up to ± 0.3 dex.

The main atmospheric parameters of the first subsample of RS CVn stars are provided in Table B1, the main atmospheric parameters of the second subsample of RS CVn stars are provided in Table B2. And Table B3 has Mass, ^{12}C/^{13}C, C/N, NLTE Li abundances, and the evolutionary stage of the RS CVn stars in the first and second subsamples. Full Machine–readable catalogs Table A1 contains all the derived parameters for the first subsample. Table A2 contains the derived parameters for the second subsample. Table B3 contains lithium abundances for both first and second subsamples.

3.2 Attribution of stars to the evolutionary stages

The evolutionary stages of the RS CVn stars were established by combining spectroscopic parameters, stellar masses, and theoretical evolutionary tracks. Each star was placed in the $\log g$–$T_{\rm eff}$ diagram and compared with PARSEC

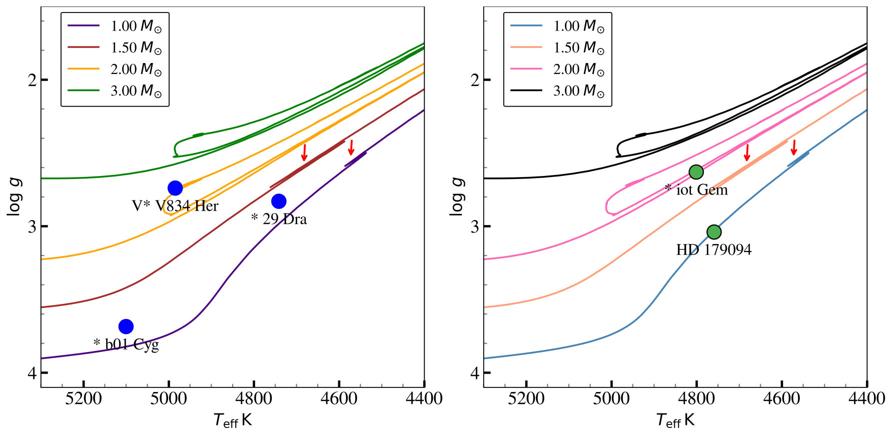

Figure 7: The log g versus $T_{\rm eff}$ diagrams showing *29 Dra (1.1 $M_\odot$), *b01 Cyg (1.2 $M_\odot$), V* V834 Her (2.2 $M_\odot$), *iot Gem (1.37 $M_\odot$), and HD 179094 (1.03 $M_\odot$) locations below the RGB luminosity bump marked by the red arrows on the PARSEC evolutionary tracks taken from Bressan et al. (2012) for the Solar metallicity.

isochrones of the appropriate metallicity (Bressan et al. 2012), which allowed a clear separation between subgiants, red giant branch (RGB) stars, and core helium-burning clump stars.

A crucial reference point in this analysis is the RGB luminosity bump, where the hydrogen burning shell meets the chemical discontinuity left by the first dredge-up, causing a temporary dip in stellar luminosity. On the $\log g$–$T_{\rm eff}$ diagram, the bump appears as a characteristic zigzag feature. For a $1\,M_\odot$ solar-metallicity model, it occurs near $\log g \sim 2.55$ and $T_{\rm eff} \sim 4550$ K.

Stars located below the bump (BB) are still ascending the lower RGB before the onset of extra mixing, while those above the bump (AB) have advanced further and may already display modified surface abundances.

The two illustrative cases are shown in Fig. 7. In addition, stars were attributed to the subgiant (SG) stage if they had not yet undergone the first dredge-up, or to the red clump (RC) if they were identified as core helium-burning giants. The assignments were further supported by the measured C/N and ^{12}C/^{13}C ratios, which are sensitive tracers of dredge-up and extra mixing processes. The dependence on the Galactic thin and thick discs was also determined as described in Subsection 2.8.

In the first subsample of 20 stars, 15 stars were assigned to the BB stage, five to the AB stage, one star *11 LMi to the SG stage, and one star *37 Com to the RC stage. One additional object HD 191588 was identified as a thick-disc member. In the second subsample of 32 stars, four stars were classified as SG, 18 as BB, eight as AB, and two as RC. *eta Boo was attributed to the thick-disc members.

Thus, across both samples, the stars were consistently attributed to main evolutionary categories: BB, AB, SG, SGTH (subgiant of thick disc), and RC, based on their placement in the $\log g$–$T_{\rm eff}$ diagram relative to PARSEC tracks and supported by chemical abundance analysis.

3.3 CNO abundances and carbon isotopic ratio

The carbon-isotope ratio $^{12}C/^{13}C$ ratio and carbon–to–nitrogen abundance ratio (C/N) are among the most informative diagnostics of interior mixing and therefore of stellar evolution. In RS CVn atmospheres, departures of these ratios from canonical expectations provide a clean window into the operation and timing of transport processes.

Early high–resolution work on RS CVn star λ And (Tautvaišienė et al. 2010b; Drake et al. 2011) and *29 Dra (Barisevičius et al. 2010) suggested that extra mixing can already act in low-mass, highly active giants *below* the red-giant-branch (RGB) luminosity bump. By contrast, comparably evolved but less active RS CVn stars did not show such a signature (Barisevičius et al. 2011; Tautvaišienė et al. 2011).

Structurally, the RGB bump appears when the H-burning shell reaches the μ–discontinuity left by the deepest extent of the first dredge–up (1DUP). The associated local decrease in mean molecular weight produces a temporary luminosity dip that gives rise to the bump in the luminosity function.

Throughout this phase, "extra mixing" is expected to set in and persist at least to the RGB tip. Thermohaline instability is a prime candidate driver (e.g. Charbonnel & Zahn 2007; Lagarde et al. 2019); in stars with $M \gtrsim 2.2 M_{\odot}$, such thermohaline-induced transport is not predicted on the RGB (cf. Lagarde et al. 2019), and the next major envelope–core exchange (the second dredge–up) occurs on the AGB unless rotation–induced mixing intervenes (Charbonnel & Lagarde 2010). During RGB extra mixing, as during 1DUP, ^{13}C and ^{14}N are transported outward while ^{12}C diffuses inward, further lowering both $^{12}C/^{13}C$ and C/N; of these, $^{12}C/^{13}C$ is the more sensitive probe (e.g. Charbonnel & Lagarde 2010; Lagarde et al. 2017).

In the first subsample of 20 stars, 15 lie BB and five AB. One BB object (*11 LMi) is a subgiant (BB SG), and one (HD 191588) belongs to the thick disc (BB Thick). Among the AB stars, *37 Com is likely in core He burning (see Aurière et al. 2015; Tsvetkova et al. 2014) and is labelled AB Clump. Table B3 summarises masses, ^{12}C/^{13}C, C/N, and evolutionary tags. Figures 8 and 9 compare our measurements with solar–metallicity models for FDU and thermohaline (TH) mixing (Lagarde et al. 2017), and with models including both thermohaline and rotation–induced transport (TH+ROT) (Charbonnel et al. 2017).

In the ^{12}C/^{13}C – mass plane (Fig. 8), AB objects (red circles) and the clump star with the lowest isotope ratio (red triangle) cluster near the TH and TH+ROT predictions, as expected for post–bump mixing. The C/N ratios show weaker leverage on transport; nonetheless, our stars follow the ranges anticipated by 1DUP and TH models for their evolutionary stages. The subgiant (blue plus) displays the largest C/N, as anticipated prior to 1DUP. Three objects *b01 Cyg, *29 Dra, and V* V834 Her exhibit unusually low ^{12}C/^{13}C but unremarkable C/N.

Most below–bump (BB) stars (blue circles) exhibit ^{12}C/^{13}C ratios consistent with 1DUP predictions. However, *29 Dra and *b01 Cyg display notably lower isotopic ratios (^{12}C/^{13}C $\approx$ 15), approaching thermohaline (TH) mixing predictions for $\sim 1.2 M_{\odot}$ models, despite their positions below the luminosity bump. The case of V* V834 Her is particularly intriguing: although it is more massive ($\sim 2.2 M_{\odot}$), TH+ROT models predict a post-bump lower limit near $\sim$ 17, yet this star resides below the bump and already exhibits a ratio of $\sim$ 12. While very rapid main sequence rotation ($\sim$ 250 km s^{-1}) has been proposed to initiate early extra mixing (Charbonnel & Lagarde 2010), such an origin appears improbable for V* V834 Her. Two additional objects, *62 Ser and *ksi Leo, show mildly reduced values (^{12}C/^{13}C $\approx$ 22); given current mass uncertainties, their measurements remain marginally compatible with 1DUP expectations.

In cases where isotopic ratios could not be determined, the C/N ratio was examined as an alternative indicator of extra mixing. However, no significant depletions were identified, given that typical C/N uncertainties can reach up to $\pm$0.4. This outcome highlights the superior diagnostic sensitivity of ^{12}C/^{13}C compared to C/N for tracing early or weak mixing processes.

Taken together, the low ^{12}C/^{13}C values in some *pre–bump* objects imply that extra mixing, classically tied to the bump, can commence earlier in low mass, chromospherically active giants. The pattern points to a multi-parameter control (mass, magnetic activity, rotation) on the onset and efficiency of transport in RS CVn stars and motivates a refinement of classical timelines.

This interpretation is consistent with Charbonnel et al. (2017), who linked

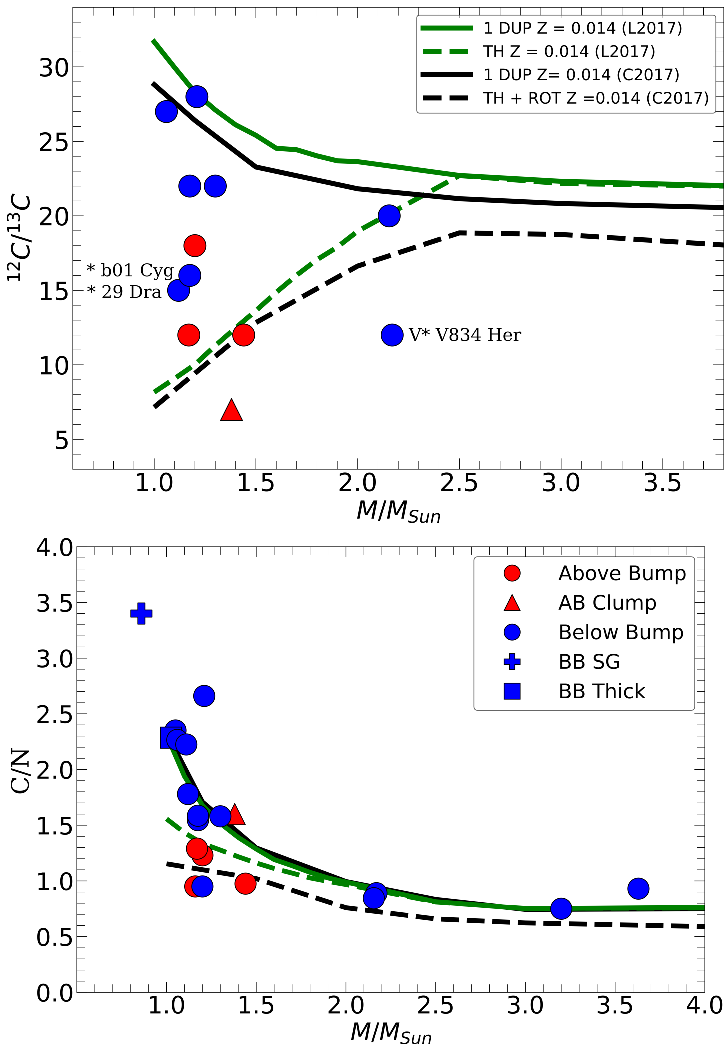

Figure 8: Ratios of $^{12}C/^{13}C$ and C/N of the investigated first subsample stars compared with theoretical models. The solid green line represents the $^{12}C/^{13}C$ and C/N ratios predicted by the model for stars at the first dredge-up (1 DUP), and the dashed green line represents the minimal values in the model with thermohaline-induced extra mixing (TH), both taken from Lagarde et al. (2017). The solid black line represents the $^{12}C/^{13}C$ and C/N ratios predicted by the model for stars at the first dredge-up (1 DUP) and the dashed black line represents the minimal values in the model with thermohaline- and rotation-induced extra mixing (TH+ROT), both taken from Charbonnel et al. (2017). Symbols are the same as in Fig. 5.

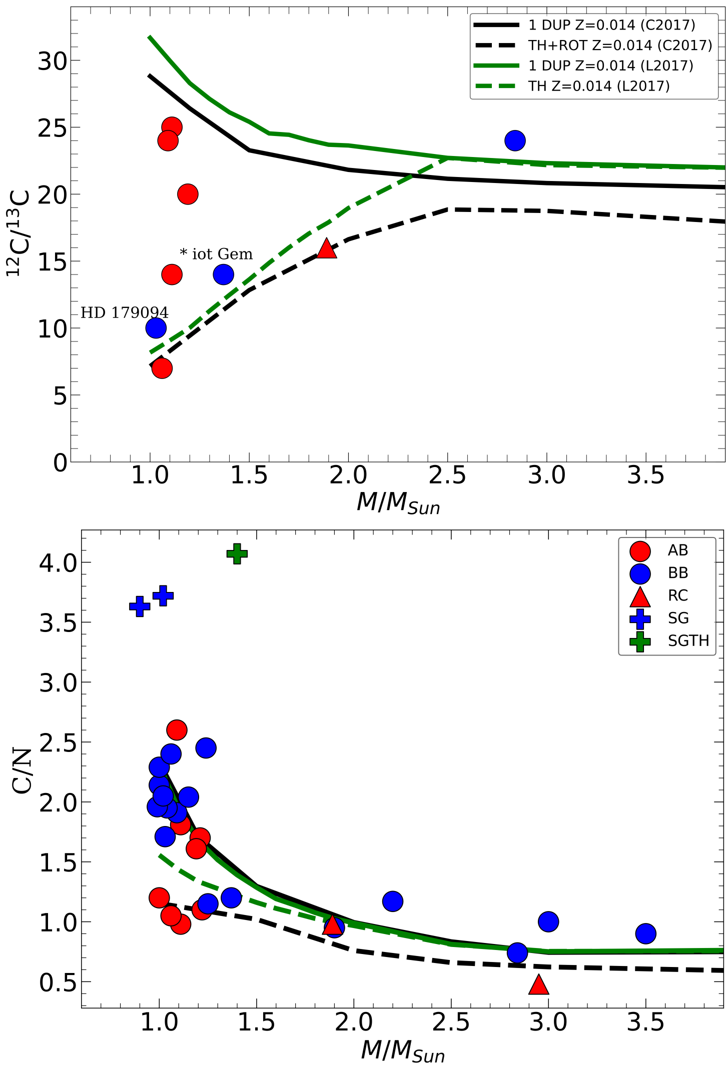

Figure 9: Comparison of $^{12}C/^{13}C$ and C/N ratios for the second subsample stars with theoretical predictions. The solid lines include the 1DUP, the dashed lines represent the models with thermohaline- and rotation-induced mixing. The black lines are for Charbonnel et al. (2017) model, the green lines are for Lagarde et al. (2017). The circles are for the red giant branch stars, the plus signs mark subgiant stars, and the triangles are for the red clump stars. The blue colour of symbols mean that a star is at the evolutionary stage below the RGB luminosity bump, and the red color is for stars at the evolutionary stage above the RGB luminosity bump. The green colour marks the stars of the thick disc.

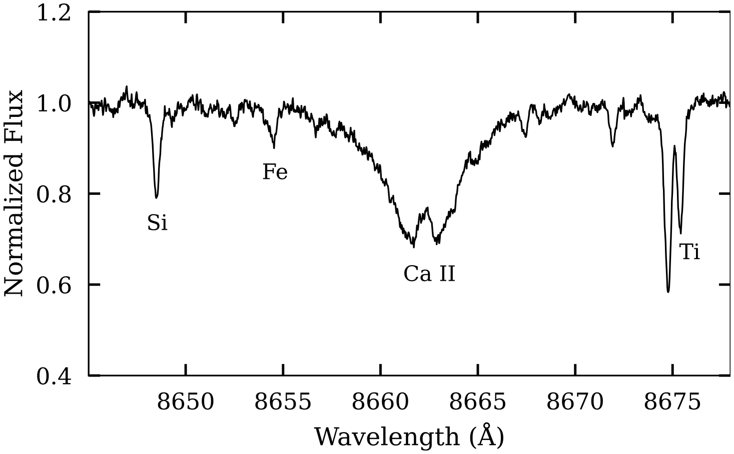

Figure 10: Example of emission in the core of Ca II line at 8662 Å in the spectrum of *29 Dra.

magnetic "strips" in the HR (mapped by spectropolarimetry) to epochs when dynamos may be efficient in convective envelopes: during 1DUP on the lower RGB and again during core He burning/early AGB. Our RS CVn subsample, having passed 1DUP, provides observational support that magnetic effects can modulate surface C and N at these important stages.

The magnetic activity of stars is often visible in the cores of the Ca II H&K doublet, but it is outside the spectral coverage of the VUES spectrograph, which covers 4000–8800 Å). Following Mallik (1997), we examined the Ca II infrared triplet (8498, 8542, 8662 Å); and we found emission features in some stars. An example is present for *29 Dra at 8662 Å in Fig. 10.

Figure 9 further presents the results of the second subsample of RS CVn stars and highlights an outlier among post–bump stars: V* OP And has a high C/N (2.60) and only mildly depleted $^{12}C/^{13}C$ (24), yet is Li-rich both here and in earlier studies (Balachandran et al. 2000; Gonçalves et al. 2020). Canonical Li production via TH or TH+ROT mixing (Cameron–Fowler mechanism; Cameron & Fowler 1971) is unlikely to be applicable as it should simultaneously lower C/N and $^{12}C/^{13}C$. Mass transfer from a companion appears unlikely given the lack of binarity evidence. Alternatives such as planet engulfment could be probed by searching for isotopic Li signatures; the origin of the Li excess in V* OP And remains open to investigation.

In the second subsample of RS CVn stars, we identify two additional below–bump stars *iot Gem and HD 179094 with low $^{12}C/^{13}C$ (~ 14 and ~ 10, respectively), consistent with thermohaline mixing despite their pre–bump positions. Ca II triplet emission is present in HD 179094.

Thus, roughly $\sim 10\%$ of the RS CVn stars studied in our sample show evidence for extra mixing starting before the bump, adding to *29 Dra, *b01 Cyg, V* V834 Her, and λ And (Tautvaišienė et al. 2010a; Drake et al. 2011; see also Barisevičius et al. 2010 for *29 Dra). The subgiants in our sample have the high C/N ratios, consistent with their pre–FDU status (Grevesse et al. 2007; Asplund et al. 2009).

3.4 Lithium abundances in RS CVn stars

Lithium abundances respond more strongly to stellar evolutionary processes than those of carbon or nitrogen. Low and intermediate-mass giants, with their extended convective envelopes, are therefore especially informative for tracing the evolution of lithium. Numerous observational and theoretical investigations have addressed this topic. Recent large spectroscopic surveys have measured lithium across extensive stellar samples, including GALAH (Deepak et al. 2020; Wang et al. 2024), *Gaia*-ESO (Magrini et al. 2021; Franciosini et al. 2022), and LAMOST (Zhou et al. 2022; Ding et al. 2024).

Interest in RS CVn stars peaked about three decades ago, when several groups explored whether lithium abundance is related to stellar magnetic activity (Pallavicini et al. 1990, 1992; Fekel & Balachandran 1993; Liu et al. 1993; Randich et al. 1993, 1994). A summary of work from that period is provided by Pallavicini (1994). With present-day access to large RGB samples for comparison, the ability to determine lithium in NLTE, and substantially improved theoretical models of lithium evolution, a more comprehensive analysis is now feasible.

Lagarde et al. (2012) presented a grid of stellar evolutionary models spanning four metallicities ($Z = 0.0001, 0.002, 0.004, 0.014$) over $0.85 - 6.0\ M_{\odot}$. Models were computed either with standard prescriptions or with both thermohaline convection and rotation-induced mixing acting together. The initial rotation on the ZAMS was set to 45 percent of the critical value, i.e., $V_{\rm ini}/V_{\rm crit} = 0.45$, consistent with the mean of observed velocity distributions for low and intermediate mass stars in young open clusters. This choice corresponds to the mean main sequence velocities of 90–137 km per second. In Fig.11, we present NLTE lithium abundances versus surface gravity ($\log g$) for the subsample (Table B4), alongside the Lagarde et al. (2012) models at three metallicities ($Z = 0.014$, 0.004, and 0.002). Stars are grouped by mass, and where appropriate, multiple metallicity tracks are shown.

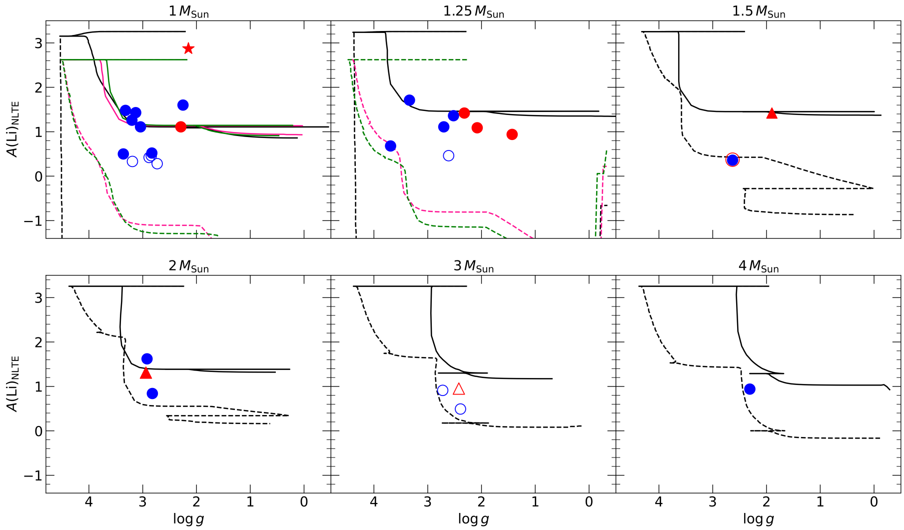

Figure 11: NLTE Li abundance as a function of $\log g$ for stars with different masses. The lines represent the models for stars evolving from the subgiant branch to the RGB tip; the solid lines include the 1DUP, the dashed lines represent the models with thermohaline- and rotation-induced mixing from Lagarde et al. (2012). The black lines are for $Z = 0.014$, the pink lines are for $Z = 0.004$, and the green lines are for $Z = 0.002$. The meaning of symbols is same as in Fig. 9. The unfilled symbols represent the upper lithium abundance limits. The Li-rich star is marked with the red star symbol.

Approximately half of the low mass stars with measured lithium lie near the predicted post–FDU plateau. The remainder including objects in which extra mixing appears to commence earlier exhibit depleted lithium. Among intermediate mass stars, Li abundances are lowered by rotation-induced mixing. In 18 stars, the lithium features were too weak for reliable abundance determinations.

Because Lagarde et al. (2012) did not provide models with thermohaline mixing alone, we also compared our measurements with the Charbonnel & Lagarde (2010) models, which explore thermohaline instability and rotation-induced mixing for $1-4\,M_{\odot}$ at the solar metallicity (Fig. 13). This comparison indicates that extra mixing in low-mass stars does not exceed that expected from pure thermohaline mixing, while it supports the conclusion that the additional lithium depletion in intermediate-mass stars is driven by rotation-induced mixing.

We also compared the Li abundances of our subsample with the data from Magrini et al. (2021) (Fig.12). We selected that study because as in our work, the giants are grouped by evolutionary phase (lower RGB, upper RGB, red clump). Since Magrini et al. (2021) reported the LTE abundances, we compare them with the LTE Li abundances derived here. The comparison shows that RS CVn stars follow the overall evolutionary decline of Li driven by 1DUP and subsequent extra mixing, and that among lower RGB stars some RS CVn objects exhibit Li depletion attributable to extra mixing or rotation depending on mass.

Several RS CVn subgiants also display reduced Li, with values between 2.24 and 0.74 dex; however, these fall within the same region occupied by normal subgiants with comparable atmospheric parameters (see, e.g., Fig.15 of Franciosini et al. 2022).

Finally, in Fig.14 we compare Li abundances with carbon isotopic ratios to assess any relationship. The subset with both A(Li) and ^{12}C/^{13}C is small. The dashed line indicates a weak, statistically insignificant positive trend for first-ascent giants (Pearson correlation PCC $= 0.48$, $p = 0.16$). The plot, however, highlights the red clump star *37 Com, which combines a low ^{12}C/^{13}C=7 with a relatively high A(Li)=1.42, consistent with possible Li enhancement near the RGB tip or during the helium flash – a scenario discussed extensively in recent literature (Schwab 2020; Mori et al. 2021; Mallick et al. 2025; Li et al. 2025, and references therein).

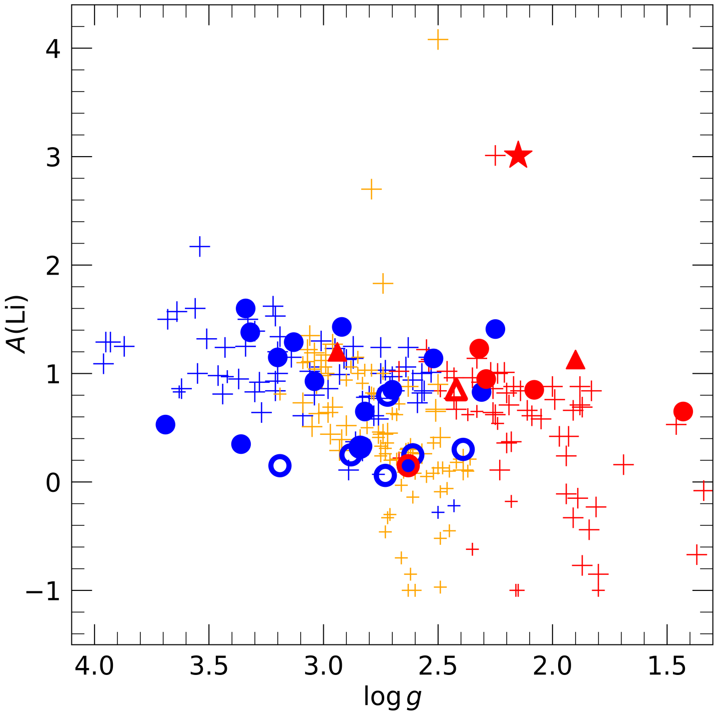

Figure 12: Comparison of LTE lithium abundances as a function of log g with results from Magrini et al. (2021). The meaning of symbols for results of this work are the same as in Fig. 11. The plus signs indicate the LTE lithium abundances from Magrini et al. (2021). The smaller plus signs indicate the upper limits. The blue colour marks the lower RGB stars, the red colour is for the upper RGB stars, and the yellow colour represents clump stars.

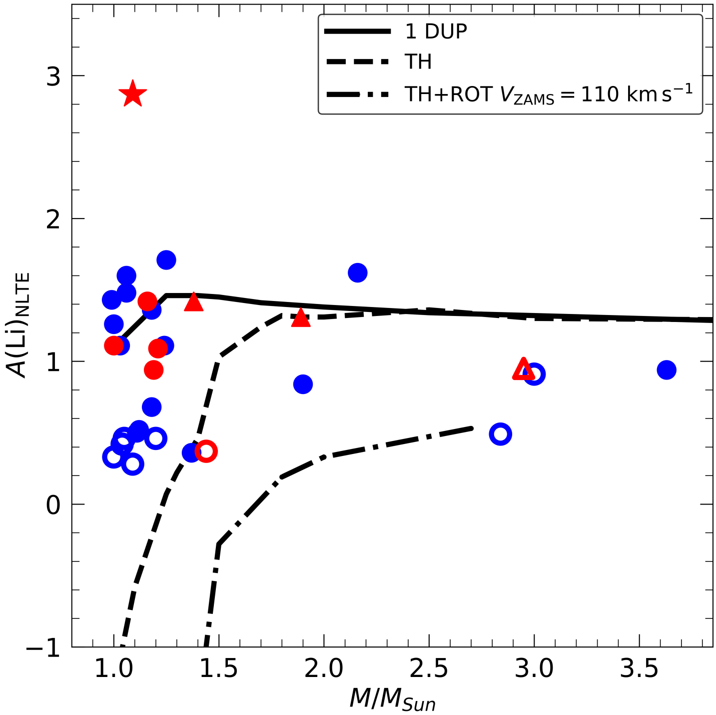

Figure 13: NLTE lithium abundance plotted against mass. The meaning of symbols for results of this work are the same as in Fig. 11. Unfilled symbols denote upper limits. The theoretical models were taken from Charbonnel & Lagarde (2010), where they were computed for solar metallicity stars. The solid black line represents the lithium abundance predicted at the first dredge-up (1 DUP), the dashed line is for just thermohaline-induced mixing (TH), and the dotted dashed line represents the minimal values in the model with thermohaline- and rotation-induced extra mixing (TH+ROT) with the rotation on ZAMS equal to about 110 km s^{-1}.

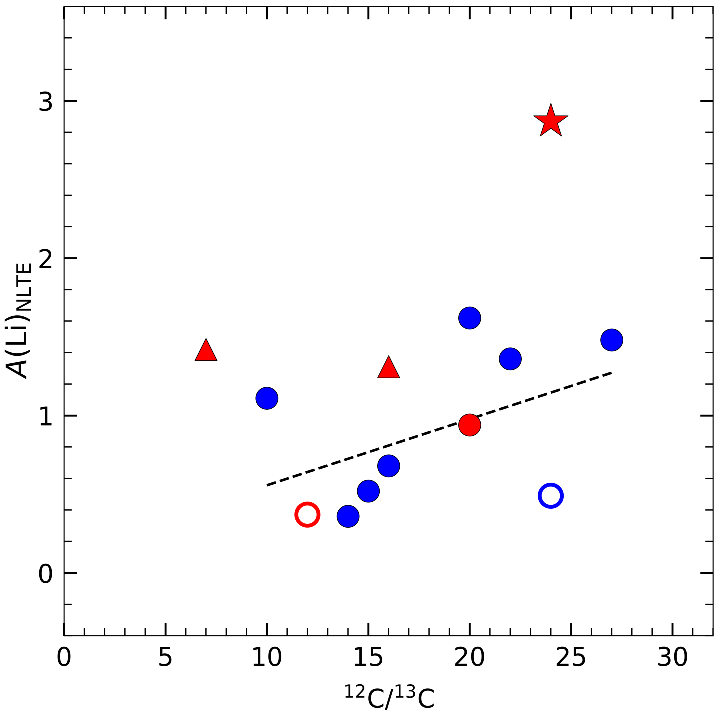

Figure 14: NLTE Li abundance as a function of $^{12}C/^{13}C$. The meaning of symbols is the same as in Fig. 11. The dashed line represents a linear statistically insignificant fit with PCC = 0.48 to the first-ascent giants.

3.5 Abundances of other chemical elements in RS CVn stars

In addition to C, N, O, and Li, abundances of several other chemical elements were determined for the investigated RS CVn stars. For the first subsample we derived abundances of C(C_2), N(CN), [O I], Mg I, Si I, Ca I, Sc I, Sc II, Ti I, Ti II, Cr I, Cr II, Fe I, Fe II, Co I, and Ni I. For the second subsample, we derived abundances of C(C_2), N(CN), [O I], Mg I and Li.

Figure 15 shows the element-to-iron abundance ratios [El/Fe] as a function of [Fe/H] for the first and second subsamples. For comparison, the figure includes results of RGB thin-disc stars analysed by Tautvaišienė et al. (2022) using the same telescope and methodology. The comparison of element-to-iron ratios, [El/Fe], with respect to [Fe/H] revealed that the RS CVn stars follow the same Galactic chemical evolution trends as predicted by Pagel & Tautvaisiene (1995). Chemically active RS CVn stars closely follow the behaviour of inactive RGB stars and the Galactic model in terms of O and Mg abundances. Carbon tends to be slightly more depleted, whereas a uniform nitrogen enhancement is not obvious over the sampled metallicity range. Thin–disc subgiants show somewhat higher C and lower N (pre–1DUP), and the thick–disc subgiant exhibits the expected elevation in C and α–elements. The thick-disc star in the sample shows enhanced light-element abundances, as expected, and also a higher carbon content relative to stars below the RGB luminosity bump, which generally display sub-solar [C/Fe] values. Nitrogen is consistently enhanced in most stars, except in the subgiant, where the composition remains unchanged because the 1DUP and extra mixing have not yet taken place.

Figure 16 displays the [El/Fe] ratios as a function of [Fe/H], shown alongside the predicted Galactic evolution trends from Pagel & Tautvaisiene (1995) for the first subsample. Figure 17 illustrates a comparable spread in [El/Fe] for the analysed elements, observed in stars situated both below and above the RGB luminosity bump. The subgiant of slightly super-solar metallicity exhibits nearly solar [El/Fe] values, including carbon and nitrogen, reflecting its early evolutionary stage before deep convective mixing. Its elemental composition likely represents the initial chemical conditions of the gas cloud from which it formed. Other stars, in contrast, show a broader scatter in [El/Fe], particularly for the mixing-sensitive elements carbon and nitrogen. This dispersion reflects the varying degrees of internal mixing influenced by stellar mass, metallicity, and evolutionary status. The red clump star exhibits [El/Fe] patterns similar to giants above the bump, while the thick-disc star shows the expected overall enhancement compared to thin-disc counterparts.

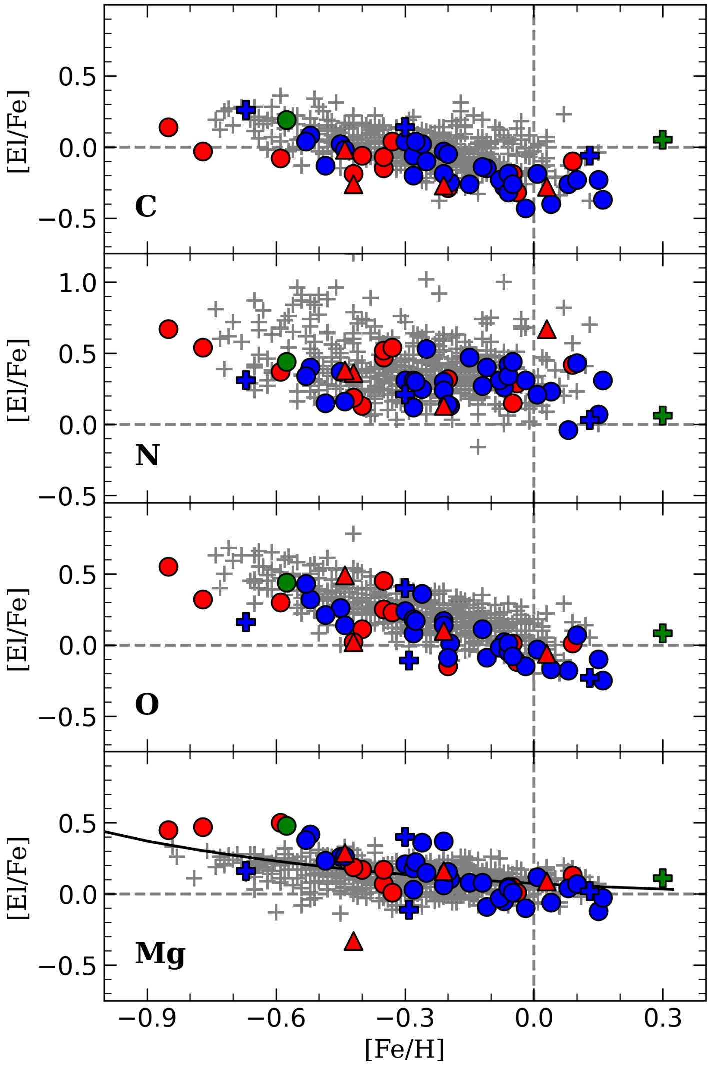

Figure 15: Element-to-iron abundance ratios determined in the first and second subsamples are plotted as a function of [Fe/H]. The solid line represents the Galactic chemical evolution model for the thin disc by Pagel & Tautvaisiene (1995). [El/Fe] abundances of the thin-disc RGB stars determined by Tautvaišienė et al. (2022) are plotted for comparison by the grey plus signs.

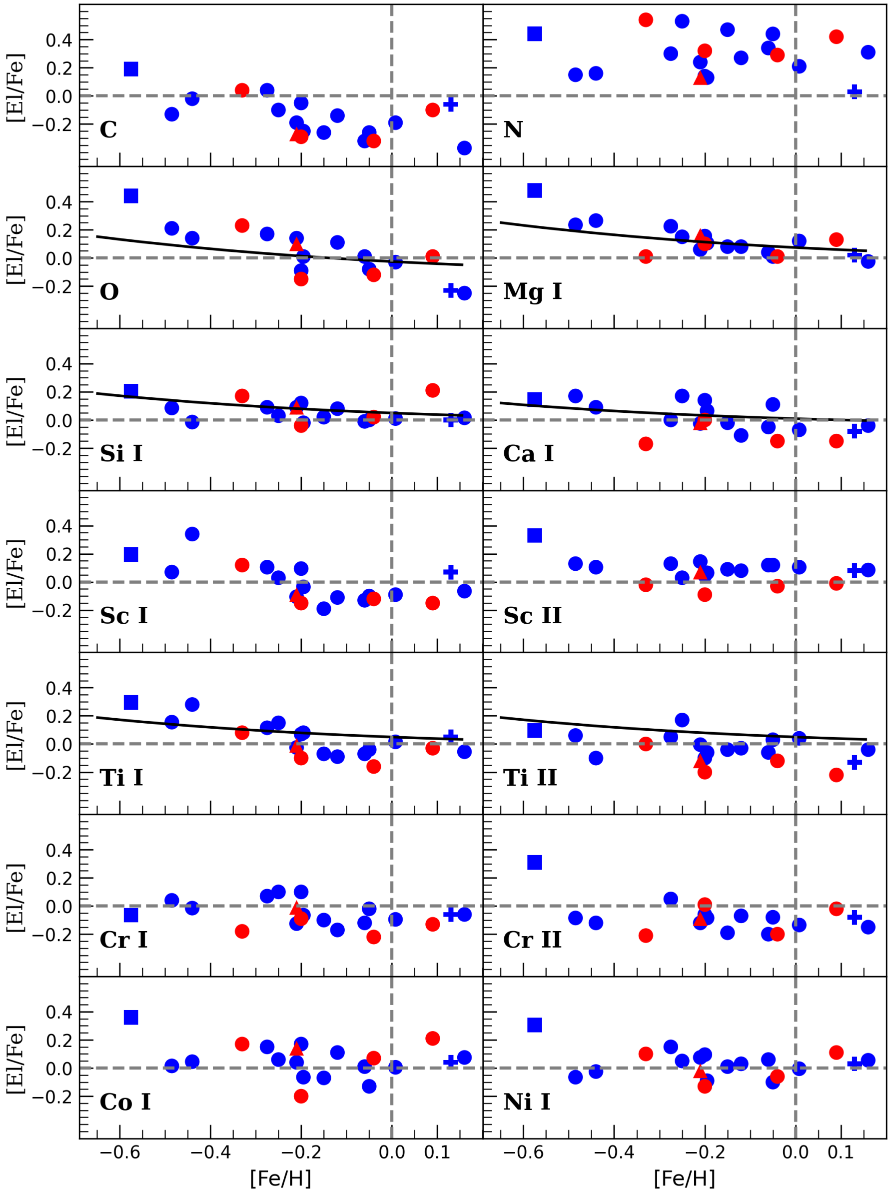

Figure 16: Ratios [El/Fe] as a function of [Fe/H]. The solid lines represent the trends of Galactic chemical evolution modeled by Pagel & Tautvaisiene (1995). The meaning of the symbols is the same as in Fig. 5.

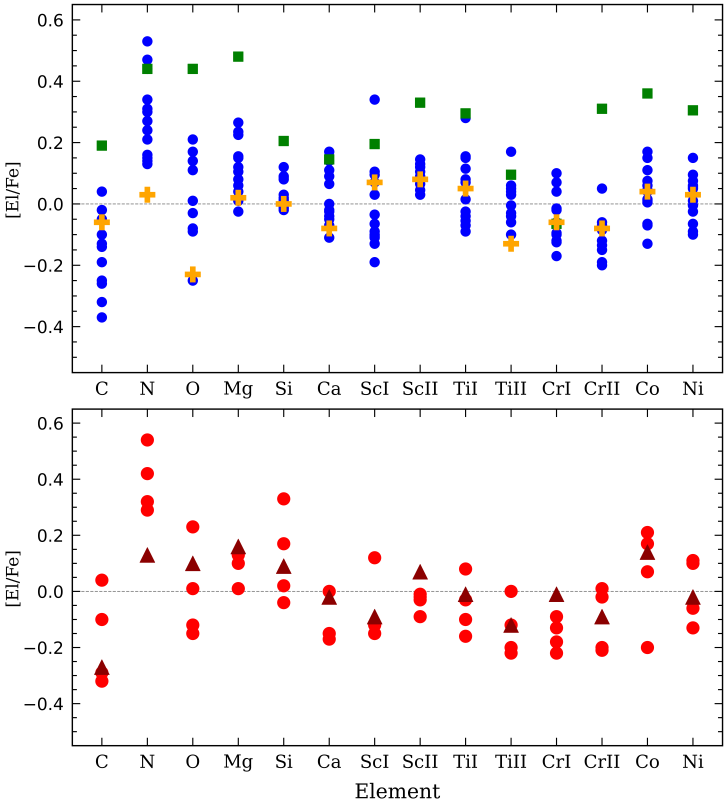

Figure 17: Ratio values of [El/Fe] for different elements in the first subsample stars located below the RGB luminosity bump in the upper panel and above the bump in the lower panel. For clarity, the thick disc star is shown as the green square, the subgiant star as the orange plus sign, and the clump star as the brown triangle.

In general, these results indicate that RS CVn stars do not deviate from the global Galactic abundance trends for α and iron-peak elements. The main differences are observed only in the mixing-sensitive elements, which are directly influenced by evolutionary processes and magnetic activity.

4 CNO abundances and carbon isotope ratios in eruptive stars

Of the 71 stars of the *Kepler* sample, 12 are eruptive stars in the core He–burning phase of evolution. Table 2 contains the main atmospheric parameters and masses, and Table 3 displays information about C, N, O, and ^{12}C/^{13}C for the investigated eruptive stars. Fig. 18 shows a comparison of $^{12}\mathrm{C}/^{13}\mathrm{C}$ and C/N ratios with normal stars and with the models by Lagarde et al. (2012) and Lagarde et al. (2017). Even though the eruptive variables are stars that undergo brightness variations driven by chromospheric and coronal flares, shell events, and episodic mass outflows, they exhibit C, N, and O abundances and $^{12}\mathrm{C}/^{13}\mathrm{C}$ ratios that are statistically indistinguishable from other core He–burning giants.

Although theoretical work, for example by Sackmann et al. (1974), predicted that very energetic flashes or strong mass-loss episodes could alter surface composition (for example, by enhancing ^{14}N and reducing ^{12}C), the measured C/N and $^{12}\mathrm{C}/^{13}\mathrm{C}$ values for the 12 eruptive objects in our dataset lie within the ranges of inactive stars of our sample. This implies that the internal mixing and dilution processes in these giants dominate over any chemical perturbations caused by eruptive activity. The consistency of their abundances with those of normal He–burning stars further supports the robustness of standard mixing models, indicating that transient surface phenomena such as flares or shell ejections do not significantly impact the long-term chemical evolution of the stellar envelope. Eruptive activity does not measurably affect the surface CNO or ^{12}C/^{13}C ratios of these stars.

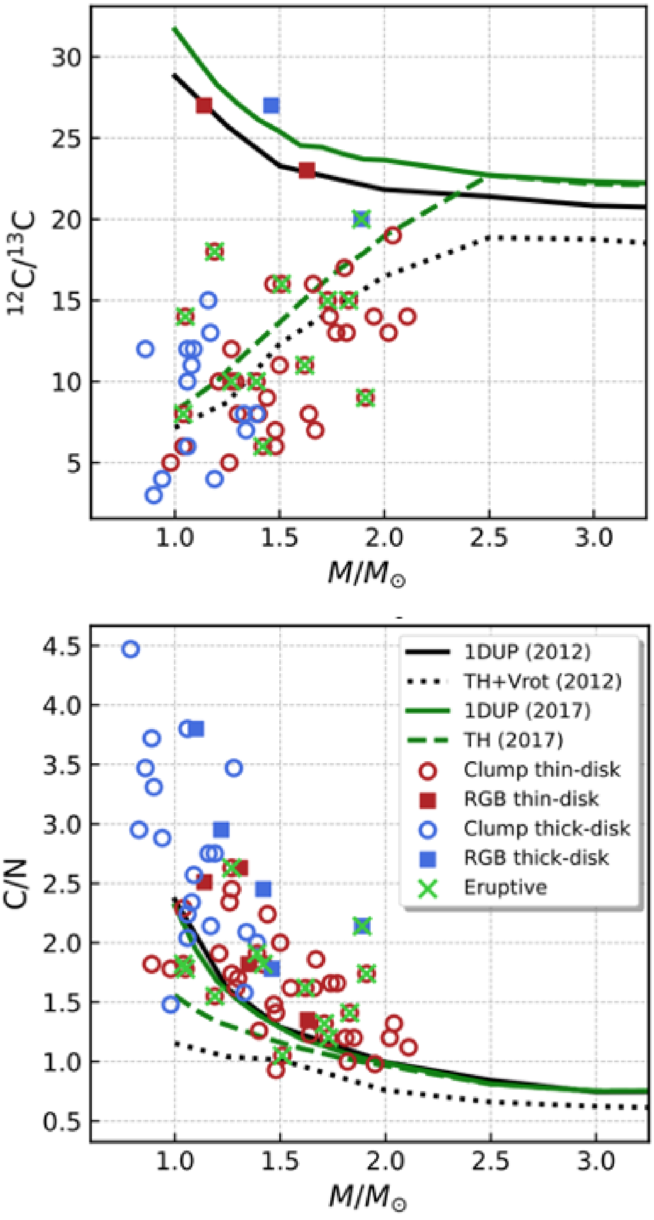

Figure 18: Comparison of $^{12}C/^{13}C$ and C/N ratios for the eruptive stars with theoretical models. The solid curves correspond to first dredge-up (1DUP) predictions, while the dashed curves represent models including thermohaline- and rotation-induced mixing. The black curves denote the models of Lagarde et al. (2012), and the green curves those of Lagarde et al. (2017). The red hollow circles represent the Clump thin disc stars, the red squares represent the RGB thin-disc stars, the blue hollow circles represent the Clump thick- stars disc, the blue squares represent the RGB thick-disc stars, the green crosses mark the eruptive stars.

Table 2: Main atmospheric parameters and mass of the eruptive stars.

Star	$T_{\rm eff}$	$e_{T_{\rm eff}}$	$\log g$	$e_{\log g}$	[Fe/H]	e[Fe/H]	$M/M_{\odot}$
KIC2696955	4727	61	2.93	0.19	0.02	0.11	1.64
KIC3730953	4908	50	2.61	0.23	−0.21	0.12	1.65
KIC3854605	4506	78	2.47	0.21	0.10	0.12	1.39
KIC4571402	4902	51	2.46	0.26	−0.26	0.12	1.34
KIC4575645	4540	65	2.48	0.20	0.09	0.11	1.32
KIC4755467	4834	48	2.49	0.22	−0.18	0.11	1.28
KIC6838707	4672	61	2.41	0.23	−0.11	0.13	1.13
KIC7374855	4674	56	2.42	0.19	0.01	0.10	2.18
KIC7820638	4800	53	2.59	0.18	−0.19	0.09	1.67
KIC9652494	4779	56	2.54	0.24	−0.11	0.13	1.50
KIC11188067	4552	59	2.48	0.19	0.03	0.11	1.39
KIC11819760	4748	51	2.37	0.22	−0.19	0.11	1.21

Table 3: C, N, O abundances and ^{12}C/^{13}C ratios of eruptive stars.

Star	A(C)	$e_{A(C)}$	A(N)	$e_{A(N)}$	A(O)	$e_{A(O)}$	^{12}C/^{13}C	$e_{(^{12}C/^{13}C)}$
KIC2696955	8.42	0.05	8.09	0.05	8.76	0.05	20	2
KIC3730953	8.06	0.02	7.82	0.03	8.66	0.05	9	3
KIC3854605	8.35	0.02	8.33	0.07	8.79	0.05	16	2
KIC4571402	7.89	0.01	7.64	0.02	8.53	0.05	14	3
KIC4575645	8.33	0.01	8.14	0.06	8.81	0.05	18	3
KIC4755467	8.07	0.01	7.81	0.03	8.64	0.05	6	2
KIC6838707	8.19	0.01	7.93	0.06	8.71	0.05	8	2
KIC7374855	8.20	0.01	8.12	0.06	8.69	0.05	15	4
KIC7820638	8.18	0.01	8.03	0.06	8.74	0.05	15	2
KIC9652494	8.09	0.05	7.88	0.04	8.67	0.05	11	1
KIC11188067	8.34	0.02	8.06	0.06	8.84	0.01	10	2
KIC11819760	8.07	0.02	7.65	0.04	8.63	–	10	2

5 Summary and Conclusions

In this thesis work, we present an investigation of chromospherically active RS CVn type and eruptive stars. The targeted stars were observed at high spectral resolution using the 1.65 m telescope at the Moletai Astronomical Observatory and the VUES spectrograph as well as the 2.65 m Nordic Optical Telescope and FIES spectrograph. We derived their atmospheric parameters and elemental abundances, including lithium, ^{12}C, ^{13}C, N, O, and up to 8 other chemical elements.

The main conclusions are as follows:

- **Early Extra-Mixing in RS CVn Giants:** Several RS CVn giants, namely *iot Gem, HD 179094, *29 Dra, *b01 Cyg, and V* V834 Her, exhibit reduced ^{12}C/^{13}C ratios while still being in the evolutionary stage below the red giant branch (RGB) luminosity bump. This suggests that extra-mixing processes in active RS CVn stars may commence earlier than in inactive red giants.
- **Anomalous Lithium Enrichment:** The Li-rich giant V* OP And displays relatively high C/N and ^{12}C/^{13}C ratios, posing questions regarding the origin of its enhanced lithium abundance.
- **Lithium Evolution and Mixing Mechanisms:** Among the low-mass giants for which lithium abundances were determined, approximately half conform to predictions from the first dredge-up (1DUP). The remainder, including those with evidence for early extra-mixing, show Li abundances depleted by thermohaline mixing. In contrast, intermediate-mass stars exhibit Li depletion likely caused by rotation-induced mixing.
- **Comparison with Normal Giants:** The RS CVn stars follow the overall decline of lithium with evolution driven by 1DUP and extra-mixing. Among the RS CVn stars, which are at the lower part of RGB there are stars with lithium depletion caused by extra-mixing or rotation, depending on their mass.
- **Eruptive Stars:** In eruptive core He-burning stars, despite the presence of intense flares, shell events, and episodic mass outflows, the CNO abundances and ^{12}C/^{13}C ratios are indistinguishable from ordinary core He-burning stars. This indicates that eruptive activity does not significantly modify their surface chemical composition.

6 Acknowledgements

I would like to sincerely thank my supervisor, Dr. Gražina Tautvaišienė, for her exceptional guidance, constructive feedback, and continuous encouragement throughout my PhD studies. Her expertise and mentorship have been instrumental in shaping the direction and quality of this work. I am thankful to Europlanet for organising the Moletai Summer School 2021, where I first met my supervisor. That encounter changed my life for the better and marked the beginning of immense personal and professional growth.

I am also deeply thankful to my colleagues Ashu, Markus, Bruno, Carlos, Edita, Šarūnas, Renata, Arnas, Vilius and Yuriy. A special thanks goes to Ashu, my "big brother," for being my strength, Markus for motivation and to Bruno for his sense of humour. I am grateful to Dr. Camilla Juul Hansen, with whom I had the pleasure of working closely and who also supervised me during the 2022 NEON Observing School in France and the ChETEC-INFRA Observational School (ChINOS) 2023 in Prague.

I would like to express my deepest gratitude to my parents and my younger brother for giving me a loving and blessed childhood and for their unwavering support throughout my life. I am thankful to the vibrant city of Mumbai, which taught me perseverance and the spirit of hustling, and to my home country, India, for instilling in me resilience, gratitude, warmth, and the colorful richness that continue to shape who I am. I am also, deeply grateful to Lithuania, which has been my home in recent years and has taught me endurance, strength, and self-discovery.

I am thankful to all women who have had to fight unseen and unspoken battles for their basic rights, especially to all women of colour who have had to prove themselves far more than others. Not everyone begins from a place of privilege or equality, yet so many women continue to challenge stereotypes, make countless sacrifices, and still rise.

I would also like to thank all the incredible friends I have met throughout my life. To my best friends of 25 years: Afrin and Nikhat, I love you more than you will ever know. To my teachers, school and college friends, and to my students and colleagues, thank you for shaping me into who I am. A heartfelt thank you to Kernius for the calmness and support. To all my wonderful non-academic friends in Lithuania and around the world, thank you for making me laugh, for giving me new perspectives. Finally, I would like to thank Dr. Taylor Swift whose music gave me strength, energy, and joy throughout my life.

7 Santrauka (Summary in Lithuanian)

Problemos išdėstymas ir tyrimo temos aktualumas

RS Canum Venaticorum (RS CVn) žvaigždės yra glaudžios dvinarės sistemos, pasižyminčios stipria chromosferine veikla, potvyniniu užsirakinimu ir greitu sukimusi. Šios sąlygos sukelia didelių žvaigždžių dėmių susidarymą, sproginėjimus ir padidintą emisiją Ca II H ir K linijose, todėl jos yra puikios magnetizmo, sukimosi ir vidinio maišymosi sąveikos tyrimams. Žvaigždžių evoliucijos teorija prognozuoja aiškius paviršiaus cheminės sudėties pokyčius, kai žvaigždės evoliucionuoja raudonųjų milžinų sekoje (RGB). Per pirmąjį medžiagos maišymosi epizodą (1DUP) konvekcinis apvalkalas perkelia susintetintą medžiagą į paviršių, sumažindamas $^{12}C/^{13}C$ ir C/N santykius, o ličio, jautraus sunaikinimui elementui palyginti žemoje temperatūroje, gausa taip pat sumažėja. Vėliau papildomi maišymo procesai (pvz., termohalininis arba sukimosi sukeltas maišymas) dar labiau pakeičia maišymuisi jautrių elementų gausas ties taip vadinamu milžinių sekos šviesio zigzagu. Teoriniuose modeliuose šie papildomi maišymo įvykiai tampa veiksmingi tik ties RGB šviesio zigzagu arba virš jo. Tačiau RS CVn žvaigždžių stebėjimai dažnai atskleidžia nukrypimus nuo šių teorinių prognozių. Kai kurios RS CVn milžinės rodo neįprastai didelę ličio gausą, palyginti su panašaus tipo neaktyviomis lauko žvaigždėmis, o kitos rodo paankstintą anglies izotopų santykio sumažėjimą žemiau RGB zigzago. Tokie rezultatai rodo, kad magnetinė veikla gali slopinti arba pagreitinti medžiagos maišymąsi. Tačiau ankstesni tyrimai dažnai buvo grindžiami mažais imtimis arba ribota chemine diagnostika, trūko vienalaikių ličio, CNO gausų ir izotopų santykių matavimų. Dėl to magnetinės veiklos vaidmuo žvaigždžių maišymosi procesuose liko neaiškus ir neatsakytas. Šio darbo tyrimai, apimantys daugiau nei 50 RS CVn žvaigždžių skirtinguose evoliucijos etapuose, įskaitant išsamius Li, C, N, O gausos ir izotopų santykių nustatymus, tiesiogiai užpildo šią spragą. Mes tiriam, ar magnetinė veikla iš esmės keičia cheminę evoliuciją RS CVn žvaigždėse. Šis tyrimas yra svarbus žvaigždžių ir galaktikų astrofizikai, nes parodo, kad papildomas maišymasis gali prasidėti anksčiau nei prognozuojama magnetiškai aktyviose žvaigždėse. Rezultatai suteikia duomenis žvaigždžių evoliucijos tyrimams ir dabartiniams modeliams, kurie apima termohalinio ir sukimosi sukeltus maišymo procesus.

Ličio gausa yra vienas jautriausių indikatorių apie vidinį maišymąsi žvaigždėse. RS CVn sistemų, kuriose yra ličio gausos sumažėjimas arba anomalus padidėjimas, aptikimas yra pagrindinis įrodymas, leidžiantis įvertinti, ar Li gausa kyla iš užslopinto maišymosi, naujos gamybos per Cameron–Fowler mechanizmą, ar išorinių akrecijos reiškinių, pvz., planetų įkritimo. Svarbus šio tyrimo aspektas yra nustatyti, ar RS CVn žvaigždės skiriasi nuo tipinių raudonųjų milžinų cheminės sudėties kitimo tendencijų.

Tyrimas taip pat apima dvylikos sproginėjančių žvaigždžių, kurioms būdinga smarki atmosferos veikla, pvz., blyksniai ir masės išsiveržimai. Jų buvimas imtyje suteikia galimybę ištirti ar epizodinis milžinų kintamumas sukelia nukrypimus nuo prognozuojamų CNO gausų ir 12C/13C santykių, helį centre deginančiose žvaigždėse.

Apibendrinant, šiame darbe tiriama, kaip magnetinis aktyvumas įtakoja vidinį medžiagos maišymąsi ir cheminę evoliuciją žvaigždėse. Tyrimo rezultatai pateikia naujus stebėjimų duomenis, kurie reikalingi paaiškinant žvaigždžių evoliucijos procesus. Kartu šie rezultatai sustiprina teorinių modelių ir stebėji mų ryšį, ir praturtina mūsų supratimą apie žvaigždžių ir galaktikų evoliuciją.

Pagrindiniai tikslai ir uždaviniai

Pagrindinis šio darbo tikslas – ištirti žvaigždžių magnetinio aktyvumo įtaką vidiniam cheminių elementų maišymui ir paviršiaus gausoms chromosferiškai aktyviose RS CVn ir sproginėjančiose žvaigždėse. Naudojant išsamią spektroskopinę diagnostiką ir palyginimą su teoriniais modeliais, tyrime nagrinėjamas maišymosi požymių pasireiškimas RS CVn žvaigždėse, kurių evoliucija nėra pasiekusi RGB sekos šviesio zigzagą, vertinamas magnetinių procesų poveikis stebimoms ličio, anglies, azoto ir kitų cheminių elementų gausoms. Siekiant įgyvendinti šio darbo tikslus, buvo atlikta aiškiai apibrėžtų užduočių seka, kiekviena iš jų rėmėsi ankstesniu žingsniu, siekiant sukurti nuoseklų pagrindą, leidžiantį suprasti magnetinio aktyvumo vaidmenį cheminėje RS CVn ir sproginėjančių žvaigždžių evoliucijoje.

Pirmasis etapas apėmė reprezentatyvių žvaigždžių, esančių skirtinguose evoliucijos etapuose, parinkimą. Toliau buvo atliktos šios užduotys: aukštos kokybės spektrų stebėjimas ir žvaigždžių atmosferos parametrų (efektinės temperatūros, paviršiaus gravitacijos, mikroturbulencijos greičio ir metalingumo), taip pat kitų pagrindinių parametrų, tokių kaip amžius, masė, evoliucijos stadija, priskyrimas Galaktikos plonajam ar storajam diskui ir t.t. nustatymas. Galutinė užduotis apėmė išsamią iki 13 cheminių elementų gausos analizę ir stebėjimo rezultatų palyginimą su teoriniais žvaigždžių evoliucijos modeliais ir Galaktikos cheminės evoliucijos tendencijomis.

Mokslinis naujumas

Šio tyrimo mokslinis naujumas yra išsamus spektroskopinis tyrimas RS CVn žvaigždžių, magnetiškai aktyvių dvinarių, kurių cheminė sudėtis anksčiau buvo nepakankamai ištirta. Nors ankstesni darbai pateikė dalinius įrodymus, kad aktyvumas gali turėti įtakos cheminių elementų gausoms, dauguma jų buvo apriboti nedidelėmis žvaigždžių imtimis, trūko anglies gausos matavimų arba buvo orientuoti į atskirus elementus, pavyzdžiui, tik į litį. Šis tyrimas daug išsamesnis, nes apima ličio, anglies, azoto ir deguonies gausų įvertinimą bei anglies izotopų santykių nustatymą daugiau nei 50 RS CVn žvaigždžių, apimančių platų evoliucijos etapų intervalą. Surinkus stebėjimų duomenis numatytam RS CVn žvaigždžių rinkiniui, tyrimas leidžia sistemingai lyginti rezultatus su įprastomis milžinėmis ir teoriniais žvaigždžių evoliucijos modeliais.

Svarbus naujas šio tyrimo aspektas yra įrodymas, kad papildomi maišymosi procesai magnetiškai aktyviose žvaigždėse gali prasidėti anksčiau nei panašios masės ir evoliucijos stadijos neaktyviose žvaigždėse. Ypač kelios RS CVn žvaigždės, esančios žemiau raudonųjų milžinų sekos šviesio zigzago, pasižymi sumažėjusiu anglies izotopų gausos santykiu ir sumažėjusia ličio gausa, o klasikiniai modeliai tai numato tik po raudonųjų milžinų sekos šviesio zigzago. Tai suteikia įrodymų, kad magnetinis aktyvumas keičia maišymosi pradžios laiką. Taip pat nauja yra ličio turtingos RS CVn milžinės identifikavimas ir charakterizavimas, kuris meta iššūkį esamoms ličio gausos padidėjimo hipotezėms bei kelia klausimus dėl planetų įtraukimo, dvinarių žvaigždžių sąveikos ar vidinės nukleosintezės vaidmens.

Ginamieji teiginiai

Šios hipotezės ir teiginiai yra ginami atlikto disertacinio darbo pagrindu:

- Chromosferiškai aktyviose RS CVn milžinėse papildomi maišymosi procesai prasideda anksčiau nei įprastose, neaktyviose milžinėse. Tai galima pastebėti sumažėjusiu anglies izotopų gausos santykiu žvaigždėse, esančiose evoliucijos stadijoje žemiau raudonųjų milžinių sekos šviesio zigzago.

- Li turtingų RS CVn žvaigždžių, tokių kaip V* OP And, egzistavimas rodo, kad apart pirmosios drumsties ir kitų sumodeliuotų papildomo maišymosi machanizmų, egzistuoja ir kitos priežąstys, atsakingos už ličio gausos padidėjimą magnetiškai aktyviose žvaigždėse.

- Ličio gausos elgsena RS CVn žvaigždėse priklauso nuo žvaigždės masės: mažos masės žvaigždėse po pirmosios drumsties seka termohalinis maišymasis, o vidutinės masės žvaigždėse ličio sumažėjimą pagrinde sąlygoja sukimosi sukeltas maišymasis.
- RS CVn žvaigždės atitinka bendrą ličio mažėjimo evoliucinę tendenciją, stebimą normaliose milžinėse, tačiau nukrypimai ankstyvesniuose evoliucijos etapuose patvirtina, kad magnetinis aktyvumas gali reikšmingai pakeisti kanoninius žvaigždžių cheminės evoliucijos kelius.
- Sproginėjančiose helį centre deginančiose žvaigždėse, nepaisant smarkių žybsnių, apvalkalo reiškinių ir epizodinių masės išsiveržimų, CNO gausos ir 12C/13C santykis lieka panašūs į neaktyvių tos pačios evoliucijos stadijos žvaigždžių. Tai rodo, kad žymiai tokia veikla žvaigždžių paviršiaus cheminės sudėties nekeičia.

Autorės įnašas

Pagrindinė šio darbo dalis, pagrįsta Molėtų astronomijos observatorijoje gautais duomenimis, buvo atlikta Lietuvoje bendradarbiaujant su Astrospektroskopijos ir egzoplanetų grupės kolegomis bei naudojant Vilniaus universiteto infrastruktūrą. Duomenų rinkimą ir apdorojimą atliko komanda. Autorės asmeninis indėlis apima tyrimo objektų atranką, pasirinktų objektų stebėjimą, spektrinių linijų ekvivalentinių pločių matavimus ir pagrindinių žvaigždžių atmosferos parametrų nustatymą, įvairių cheminių elementų gausos nustatymą, amžių, masės, orbitų ir kinematikos nustatymą. Be to, autorė buvo atsakinga už duomenų apdorojimą, statistinę analizę, tyrimą, konceptualizavimą, kritinį mokslinį vertinimą, rezultatų vizualizavimą, mokslinių straipsnių ir disertacijos rengimą, vadovaujant disertacijos vadovui.

Įvadas

Įvade pateikiama RS CVn žvaigždžių ir jų charakteristinių savybių apžvalga, aprašomi maišymosi procesai žvaigždžių atmosferose, ličio kaip žvaigždžių evoliucijos žymens vaidmuo žvaigždžių evoliucijoje ir sproginėjančių žvaigždžių charakteristikos.

1.1 poskyryje RS CVn žvaigždės pristatomos kaip magnetiškai aktyvios žvaigždės, kurių greitas sukimasis sukelia stiprią chromosferos emisiją, sudaro sąlygas didelių dėmių žvaigždžių paviršiuje formavimuisi ir sužadina žybsnius įvairiuose bangų ilgių diapazonuose (Berdyugina 2005, Zhilyaev ir kt. 2024, Strassmeier ir kt. 2000). Jų cheminė sudėtis yra ypač įdomi, nes lengvųjų elementų gausos ir izotopų santykiai rodo, kaip magnetiniai laukai keičia vidinio medžiagos maišymosi procesus, lyginant su įprastomis milžinėmis.

1.2 poskyryje apibendrinama žvaigždžių maišymosi požymių klasifikacija ir už juos atsakingi fizikiniai procesai. Jame aprašoma, kaip klasikiniai ir neklasikiniai pernašos mechanizmai, tokie kaip pirmoji drumstis, sukimasis, termohalininis nestabilumas, gravitacinės bangos ir magnetiniai efektai, keičia CNO gausas ir izotopų santykius žvaigždžių evoliucijos metu (Day ir kt. 1973, Gratton ir kt. 2000, Denissenkov ir kt. 2006, Busso ir kt. 2007).

1.3 poskyryje apibendrinama ličio kilmė, gausos jautrumas atmosferos pokyčiams ir diagnostinė svarba žvaigždžių evoliucijoje, pabrėžiant, kaip standartiniai ir nestandartiniai maišymosi procesai sumažina arba pakeičia jo gausą (Randich ir kt. 1993, 1994). Jame akcentuojami įvairūs mechanizmai, siūlomi ličio anomalijoms milžinėse paaiškinti (Cameron ir Fowler 1971; Adamów ir kt. 2012), ir pažymima, kad RS CVn žvaigždės dažnai pasižymi netikėtai dideliu arba kintamu Li kiekiu, kuris gali būti susijęs su magnetiniu aktyvumu, slopinamu maišymusi arba epizodiniu praturtinimu. Taigi, ličio tyrimas padeda suprasti, kaip sukimasis ir magnetizmas veikia vidinę pernašą šiose aktyviose žvaigždėse.

1.4 poskyryje sproginėjančios žvaigždės pristatomos kaip objektai, kurių netolygūs ryškio pokyčiai atsiranda dėl chromosferos ir vainiko aktyvumo, įskaitant žybsnius, masės praradimą ir epizodinius apvalkalo išmetimus (Good 2003). Šie įvykiai, kuriuos lemia magnetiniai procesai, sukelia stiprų kintamumą daugelyje bangos ilgių ir kartais sustiprėjusių žvaigždžių vėjų požymius. Remiantis teorija, stiprūs sprogimai gali pakeisti paviršiaus gausas, tačiau šiuo metu yra mažai empirinių įrodymų apie ilgalaikius CNO pokyčius, todėl yra labai svarbu vykdyti tęstinius sproginėjančių žvaigždžių stebėjimus.

Tyrimo metodika

2 skyriuje pateikiama tyrimo metodika, įskaitant objektų atranką, stebėjimus, diferencinę analizę spektrinių linijų ekvalentinių pločių ir sintetinių spektrų metodu, atmosferos parametrų nustatymą, elementų gausos ir anglies izotopų santykių nustatymą, nelokalios termodinaminės pusiausvyros (NLTE) poveikio įskaitymą, žvaigždžių masės įvertinimus, kinematinių parametrų ir paklaidų vertinimą.

2.1 poskyryje aprašomas didelės, reprezentatyvios 52 RS CVn žvaigždžių, pasirinktų dėl stipraus chromosferos aktyvumo, ryškumo ir tinkamumo aukštos skiriamosios gebos spektroskopijai, imties sudarymas. Objektai buvo paimti iš pagrindinių katalogų, siekiant užtikrinti platų masių, spektrinių tipų ir aktyvumo lygių diapazoną, įtraukiant žvaigdes, kurių spektre matomos tik vienos komponentės linijos. Sproginėjančios žvaigždės buvo pasirinktos iš Keplerio kosminio teleskopo stebėjimų lauko.

2.2 poskyryje aprašoma diferencinės gausų analizės metodologija. Buvo naudojama dviguba strategija: gerai izoliuotoms atominėms linijoms buvo taikytas ekvivalentinių pločių metodas, o molekulinėms ir izotopų linijoms – spektrų sintezė. Automatizuoti ekvivalentinių linijų pločių matavimo įrankiai ir kruopščiai atrinktų linijų sąrašai užtikrino tikslumą, o spektrinė sintezė leido patikimai modeliuoti molekulines ir izotopų linijas, tokias kaip C_2, CN, [O I], $^{12}C/^{13}C$ bei šiek tiek blenduotas Li linijas.

2.3 poskyryje apibendrinami spektroskopiniai stebėjimai, atlikti 2021-2024 m., naudojant 1,65 m MAO teleskopą ir VUES spektrografą (Jurgenson ir kt., 2016), dviem etapais buvo stebėtos 52 RS CVn žvaigždės. Stebėjimai buvo vykdomi dviem skiriamosiomis skiriamosiomis gebomis, reikalingomis pagrindinių gausų analizei įvairaus ryškio žvaigždėms. Duomenys buvo apdoroti naudojant specialų programinį paketą ir interaktyviai normalizuoti. Taip pat buvo gauti didelės skiriamosios gebos spektrai su Šiaurės optiniu teleskopu ir FIES spektrografu sproginėjančioms žvaigždėms, pateikiantys nuosekliai apdorotus, didelio signalo ir triukšmo santykio duomenis, tinkamus tiksliai CNO ir anglies izotopų analizei mažesnio ryškio žvaigždėms Keplerio stebėjimų lauke.

2.4 poskyryje aprašomas žvaigždžių atmosferų parametrų nustatymas naudojant klasikinę diferencialinę spektrų analizės techniką, pagrįstą Fe I/Fe II linijų ekvivalentiniais pločiais. Efektinės temperatūros, mikroturbulencijos greičiai, gravitacijos pagreičio žvaigždės paviršiuje parametrai ir metalingumai buvo nustatyti iteraciniu būdu su `MOOG` programiniu paketu naudojant kruopščiai atrinktų geležies linijų sąrašą ir `MARCS` (Gustafsson et al. 2008) atmosferų modelius, užtikrinant suderintus parametrus visoms RS CVn žvaigždėms. Sproginėjančioms žvaigždėms spektroskopinės temperatūros buvo derinamos su asteroseisminiais gravitacijos pagreičio parametrais, siekiant padidinti žvaigždžių atmosferos parametrų nustatymo tikslumą.

2.5 poskyryje aprašyta, kaip buvo nustatytos cheminių elementų gausos ir anglies izotopų santykiai naudojant detalią spektrų sintezę su `TURBOSPECTRUM` programiniu paketu. Anglies, azoto ir deguonies gausos buvo gautos iš C_2, CN ir [O I] linijų, taikant iteracinę molekulinės pusiausvyros procedūrą, o ^{12}C/^{13}C santykiai nustatyti iš ^{13}CN molekulinių juostų. Ličio gausos buvo nustatytos iš Li I 6707.8 Å dubleto su NLTE korekcijomis, o magnis pasitarnavo kaip deguonies pakaitalas ten, kur atmosferinės linijos buvo užsiklojusios ant [O I] linijos. Kitų elementų gausos buvo gautos iš ekvivalentinių pločių matavimų naudojant `DAOSPEC` ir `MOOG` programinius paketus.

2.6 poskyryje apibendrinama NLTE efektų įtaka, pabrėžiant, kad ličio gausos tyrimų atveju reikia atlikti NLTE korekcijas, kurios buvo atliktos naudojant `INSPECT` programinį paketą (Lind ir kt. 2009) ir reikšmingai pakoregavo nustatytas gausas tiek ličio stokojančioms, tiek ličiu praturtintoms žvaigždėms. Anglis ir deguonis buvo analizuojami naudojant linijas, kurioms LTE prielaidas taikyti iš esmės pakanka, kaip ir CN pagrindu apskaičiuotoms azoto gausoms ir ^{12}C/^{13}C santykiams. Taigi, litis yra pagrindinis elementas, kurio gausų rezultatams šiose aktyviose RS CVn žvaigždėse NLTE pataisos turi reikšmingą įtaką.

2.7 poskyryje aprašomas žvaigždžių masių nustatymas naudojant Bajeso analitinį metodą su `UniDAM` programiniu paketu, kuris apjungia spektroskopinius parametrus ir infraraudonųjų spindulių fotometriją su `PARSEC` izochronomis, kad būtų gauti kiekvienos RS CVn žvaigždės parametrų duomenys. Šis metodas leidžia gauti patikimus masės įverčius ir evoliucines klasifikacijas, suteikiančias esminį kontekstą stebimų gausų interpretavimui. Sproginėjančių žvaigždžių masės buvo nepriklausomai įvertintos naudojant `SPInS` MCMC sistemą, parodant, kad atsižvelgus į seisminius kriterijus, gaunami žymiai tikslesni rezultatai; taigi, kur įmanoma, buvo naudojamos seisminės `PARAM` masės, o žvaigždėms, neturinčioms asteroseisminių duomenų, buvo naudojamas `SPInS`.

2.8 poskyryje apibendrinamos tirtų žvaigždžių imties kinematinės charakteristikos, kur Galaktikos erdviniai greičiai buvo gauti naudojant `galpy` programinį paketą kartu su `Gaia` DR3 astrometrija, Bajeso atstumo įverčiais ir darbe išmatuotais radialiniais greičiais. Plonojo ir storojo diskų populiacijoms atskirti buvo naudojama Toomre diagrama ir klasikinės greičio ribos, o vėliau nustatymai buvo patikslinti naudojant [α/Fe]–[Fe/H] gausų tendencijas. Ši kombinuota chemokinematinė analizė identifikavo HD 191588 ir η Boo žvaigždes kaip storojo disko nares, o visos kitos RS CVn žvaigždės priklauso plonajam diskui.

2.9 poskyryje aprašomas paklaidų įvertinimas, atskiriant sistematinius efektus, kurių įtaka sumažinama atliekant diferencinę analizę, nuo atsitiktinių paklaidų, atsirandančių dėl ištisinio spektro padėties įvertinimo bei atskirų linijų analizės. Atmosferos parametrų T_{eff}, $\log g$, v_{t} ir [Fe/H] paklaidos buvo kiekybiškai įvertintos, gaunant tipines paklaidas atitinkamai $\sim$ 50–80 K, 0.1–0.2 dex, 0.1 km s^{-1} ir ±0.05 dex. Gausų paklaidos buvo įvertintos pagal verčių, nustatytų iš keletos linijų, išsibarstymą, o turint tik vieną liniją, pavyzdžiui, [O I] ir ^{12}C/^{13}C atveju – naudojant signalo triukšmo santykio ir ištisinio spektro padėti-es vertinimą. Buvo ištirtas molekulinės pusiausvyros jautrumas tarp C, N ir O, o masės ir amžiaus paklaidos buvo paimtos iš su `UniDAM` programiniu papetu gautų duomenų. Apskritai ši procedūra užtikrina patikimus ir nuoseklius paklaidų įverčius visiems išmatuotiems dydžiams.

RS CVn žvaigždžių tyrimo rezultatai

3 skyriuje pateikiami RS CVn žvaigždžių analizės rezultatai ir jų aptarimas, apimantis žvaigždžių parametrus, CNO gausas, anglies izotopų santykius, ličio ir kitų tirtų elementų gausas bei elementų maišymosi procesus.

3.1 poskyryje aptariami atmosferos parametrai. Pirmosios RS CVn žvaigždžių imties parametrai pasiskirsto šiuose intervaluose: $T_{\mathrm{eff}} = 4380 – 5450$ K, $\log g = 1.9 – 4.35$, $[\mathrm{Fe/H}] = -0.60 – +0.17$ ir $v_t = 0.72 – 1.83$ km s^{-1}. Antrosios imties rėžiai yra: $T_{\mathrm{eff}} = 4120 – 6220$ K, $\log g = 1.4 – 4.3$ ir $[\mathrm{Fe/H}] = -0.85 – +0.34$. Amžiaus diapazonas apima 224 mln. m. – 11.7 mlrd. m., o masės – 0.86 – 3.63 $M_{\odot}$. Gauti parametrai gerai atitinka literatūroje pateiktas vertes, išskyrus nedidelius metalingumo nuokrypius.

3.2 poskyryje apibendrinama RS CVn žvaigždžių evoliucijos etapų klasifikacija. Žvaigždės buvo suskirstytos į kategorijas – milžinės iki šviesio zigzago (BB), milžinės, perkopusios šviesio zigzagą (AB), submilžinės (SG), storojo disko submilžinės ($\mathrm{SG_{TH}}$) ir raudonosios sankaupos milžinės (RC) – remiantis jų pozicijomis T_{eff}–$\log g$ diagramoje kartu su `PARSEC` isochronomis (Bressan et al. 2012) ir papildomai pagrindžiant žvaigždžių masių, C/N santykių ir ^{12}C/^{13}C verčių analize. RGB šviesio zigzagas veikia kaip pagrindinis atskaitos taškas, skiriantis žemiau esančias milžinių sekos žvaigždes (BB) nuo šviesio zigzagą perkopusių (AB) objektų.

3.3 poskyryje apibendrinami rezultatai, parodantys, kad ^{12}C/^{13}C ir C/N leidžia patikimai nustatyti papildomą maišymąsi RS CVn žvaigždėse. 19 ir 20 pav. dauguma žemiau šviesio zigzago esančių objektų atitinka standartines 1DUP prognozes, tačiau apie 10% pasižymi netikėtai mažu ^{12}C/^{13}C, o tai rodo, kad aktyviose, mažos masės milžinėse papildomas maišymasis gali prasidėti prieš RGB šviesio zigzagą. Žvaigždžių, perkopusių šviesio zigzagą, vertės atitinka termohalinį arba TH+sukimosi sukelto maišymosi modelius, o submilžinės išlaiko aukštą C/N, kaip ir galima tikėtis. Šie rezultatai rodo, kad masė,

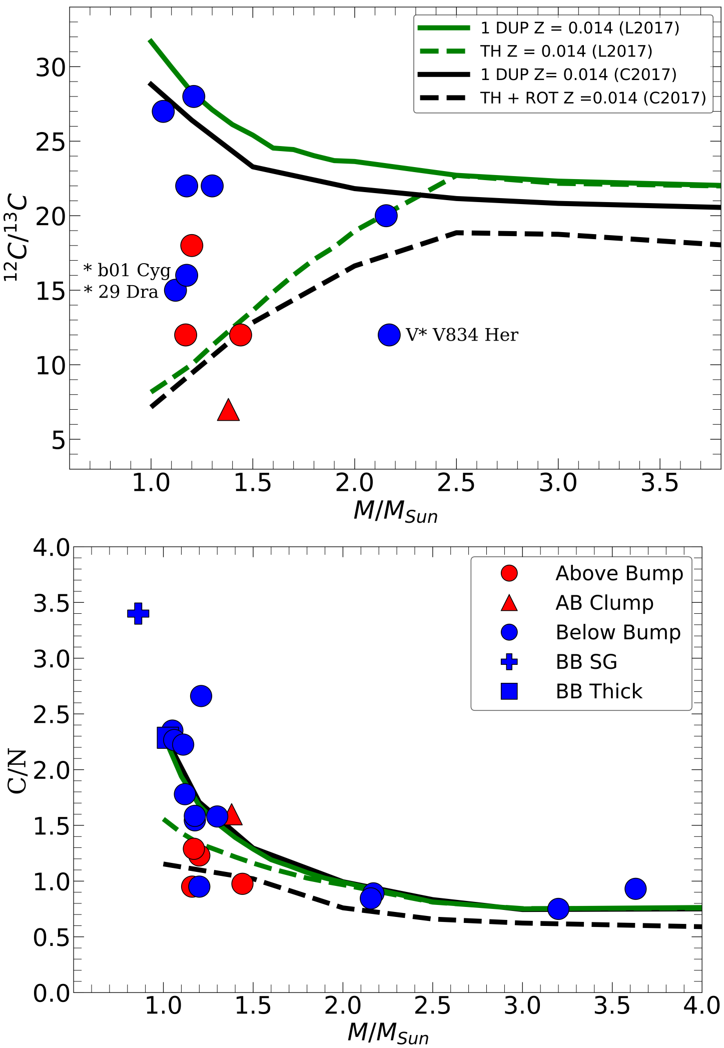

Figure 19: ^{12}C/^{13}C ir C/N santykių palyginimas pirmajai RS CVn žvaigždžių imčiai su teoriniais modeliais. Ištisinės linijos rodo 1DUP modelius, punktyrinės linijos atitinka modelius su termohaliniu ir sukimosi sukeltu maišymusi. Juodos linijos yra Charbonnel et al. (2017) modeliai, žalios linijos yra iš Lagarde et al. (2017) darbo. Apskritimai žymi raudonųjų milžinų sekos žvaigždes, pliuso ženklai žymi submilžines žvaigždes, o trikampiai – helį centre deginančias žvaigždes. Mėlyna simbolių spalva reiškia, kad žvaigždė yra evoliucijos stadijoje žemiau RGB šviesio zigzago, o raudona spalva žymi žvaigždes, esančias evoliucijos stadijoje po RGB šviesio zigzago. Žalia spalva žymi žvaigždes, esančias storame Galaktikos diske.

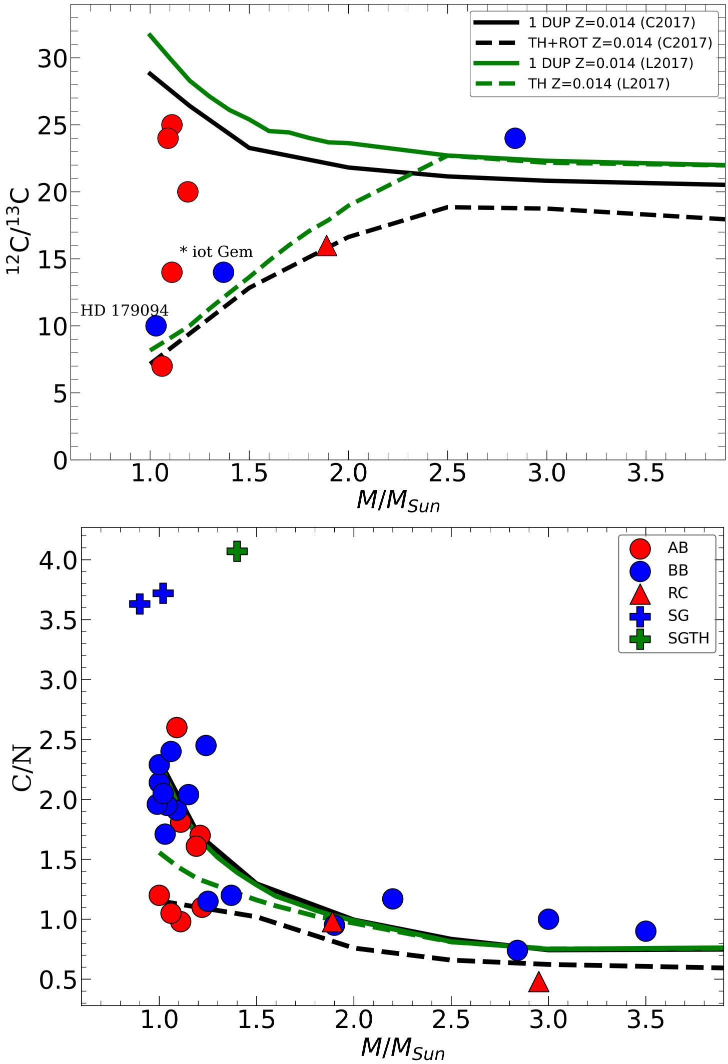

Figure 20: $^{12}C/^{13}C$ ir C/N santykių palyginimas antrajai RS CVn žvaigždžių imčiai su teoriniais modeliais. Ištisinės linijos rodo 1DUP modelius, punktyrinės linijos atitinka modelius su termohaliniu ir sukimosi sukeltu maišymusi. Juodos linijos yra Charbonnel et al. (2017) modeliai, žalios linijos yra iš Lagarde et al. (2017) darbo. Apskritimai žymi raudonųjų milžinų sekos žvaigždes, pliuso ženklai žymi submilžines žvaigždes, o trikampiai – helį centre deginančias žvaigždes. Mėlyna simbolių spalva reiškia, kad žvaigždė yra evoliucijos stadijoje žemiau RGB šviesio zigzago, o raudona spalva žymi žvaigždes, esančias evoliucijos stadijoje po RGB šviesio zigzago. Žalia spalva žymi žvaigždes, esančias storame Galaktikos diske.

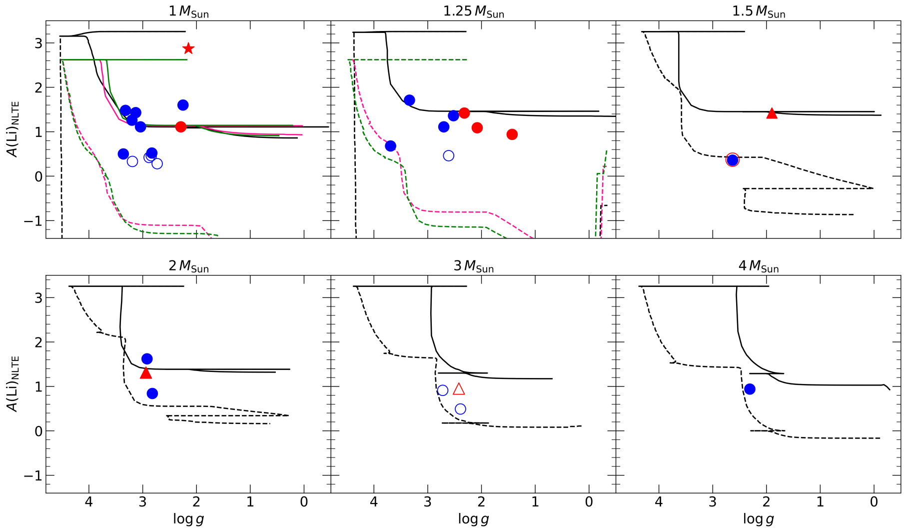

Figure 21: NLTE Li gausos kaip $\log g$ funkcija žvaigždėms su skirtingomis masėmis. Linijos atitinka modelius žvaigždėms, besivystančioms nuo submilžinių į RGB viršūnę; ištisinės linijos apima 1DUP, punktyrinės linijos atitinka modelius su termohaliniu ir sukimosi sukeltu maišymu iš Lagarde ir kt. (2012). Juodos linijos yra Z=0,014, rožinės linijos yra Z=0,004, o žalios linijos yra Z=0,002. Simbolių reikšmės yra tokios pačios kaip ir 19 pav. Tušti simboliai žymi viršutines ličio gausos ribas. Li turtinga žvaigždė pažymėta raudonu žvaigždės simboliu.

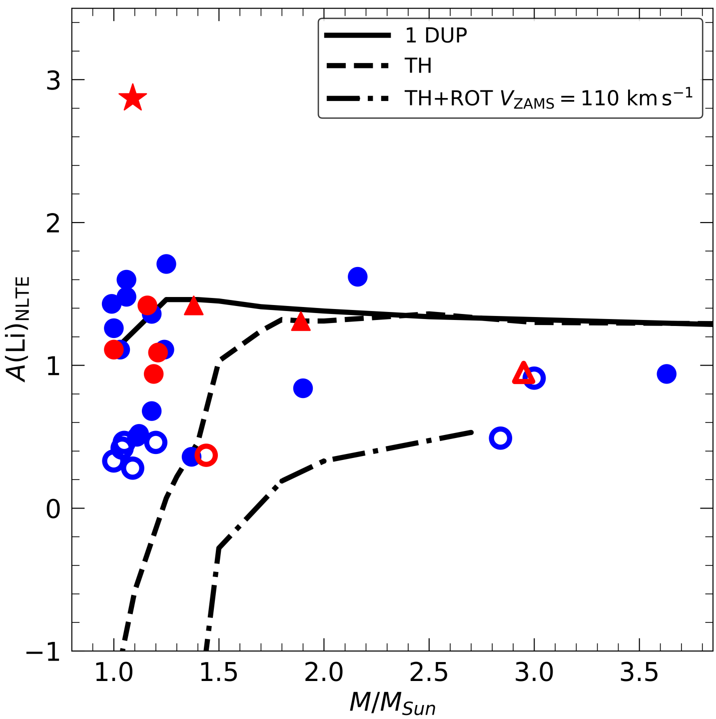

Figure 22: NLTE ličio gausos priklausomybė nuo masės. Šio darbo rezultatų simbolių reikšmės yra tokios pačios kaip ir 21 pav. Tušti simboliai žymi gausų viršutines ribas. Teoriniai modeliai buvo paimti iš Charbonnel ir Lagarde (2010), kur jie buvo apskaičiuoti Saulės metalingumo žvaigždėms. Ištisinė juoda linija žymi ličio gausą, numatytą pirmojosios drumsties (1 DUP), punktyrinė linija – tik termohalinio sukelto maišymosi atveju (TH), o punktyrinė taškinė linija – minimalias modelio vertes su termohalino ir rotacijos sukeltu papildomu maišymusi (TH+ROT), kai žvaigždės sukimasis pagrindinėje sekoje yra lygus maždaug 110 km/s.

sukimasis ir magnetinis aktyvumas daro įtaką maišymo pradžiai ir efektyvumui ir kelios žvaigždės (pavyzdžiui, *29 Dra, *b01 Cyg, V* V834 Her, V* OP And, *iot Gem, HD 179094) tai patvirtina.

3.4 poskyryje analizuojama ličio elgsena RS CVn žvaigždėse lygint su evoliuciniais modeliais. 21 paveiksle parodyta, kad beveik pusėje mažos masės milžinų NLTE Li matavimai yra netoli numatomos plokštumos po pirmosios drumsties, o likusiose - papildomas sumažėjimas, susijęs su ankstyvu papildomu maišymusi. Vidutinės masės žvaigždėse stebimas Li sumažėjimas, atitinkantis sukimosi sukeltą pernašą. Palyginimai su termohalininiais ir sukimosi modeliais 22 paveiksle patvirtina, kad RS CVn žvaigždės iš esmės atitinka kanoninį Li sumažėjimą, tačiau yra keletas objektų su neįprastai sumažėjusia arba padidėjusia gausa. Įpatingas objektas yra raudonosios sankaupos žvaigždė *37 Com, kurios didelė Li gausa ir mažas $^{12}C/^{13}C$ santykis gali signalizuoti apie Li gamybą netoli RGB viršūnės arba helio užsidegimo metu.

3.5 poskyryje aptariama kitų cheminių elementų gausa RS CVn žvaigždėse. Žvaigždės atitinka standartines Galaktikos cheminės evoliucijos tendencijas α ir geležies piko elementams, kurios atitinka Galaktikos cheminės evoliucijos modelio (Pagel & Tautvaisiene 1995) prognozes. Kai kurie nukrypimai atsiranda labiausiai maišymui jautriems elementams: anglies kiekis yra šiek tiek mažesnis, o azoto kiekis padidėjęs, priklausomai nuo evoliucijos etapo. Submilžinės išlaiko artimą Saulei sudėtį, o storojo disko žvaigždė rodo įprastinį α-elementų gausos padidėjimą.

Sproginėjančių žvaigždžių tyrimo rezultatai

4 skyriuje pateikiami ir aptariami sproginėjančių žvaigždžių tyrimo rezultatai, apimantys CNO gausas, anglies izotopų santykius ir elementų maišymosi procesus. Parodyta, kad 12 šiame darbe tirtų sproginėjančių *Kepler* branduolyje He degančių žvaigždžių pasižymi C, N ir O gausomis ir $^{12}C/^{13}C$ santykiais, gerai atitinkančiais normalių branduolyje He degančių žvaigždžių rodiklius. Nepaisant stipraus chromosferos aktyvumo, žybsnių ir epizodinių masės išmetimo įvykių, jų cheminė sudėtis atitinka standartines maišymosi prognozes ir nerodo pastebimų žybsnių sukeltų pokyčių.

Išvados

Pagrindinės išvados yra tokios:

- **Ankstyvas papildomas maišymasis RS CVn milžinėse:** Keletas RS C-Vn milžinų, būtent *iot Gem, HD 179094, *29 Dra, *b01 Cyg ir V* V834 Her, pasižymi sumažėjusiu $^{12}C/^{13}C$ santykiu, nors savo evoliucijoje dar nėra pasiekusios raudonųjų milžinų sekos (RGB) šviesio zigzago. Tai rodo, kad papildomas maišymasis aktyviose RS CVn žvaigždėse gali prasidėti anksčiau nei neaktyviose raudonosiose milžinėse.

- **Anomalus ličio gausos padidėjimas**: Li turtinga milžinė V* OP And rodo palyginti aukštus C/N ir $^{12}C/^{13}C$ santykius, o tai kelia klausimų dėl jos padidėjusio ličio kiekio kilmės.

- **Ličio evoliucija ir maišymosi mechanizmai**: Tarp mažos masės milžinių, kurių ličio gausa buvo nustatyta, maždaug pusė atitinka pirmosios drumsties (1DUP) prognozes. Likusi dalis, įskaitant tas, kurios turi ankstyvo papildomo maišymosi požymių, rodo ir Li gausos sumažėjimą dėl termohalinio maišymosi. Tuo tarpu, vidutinės masės žvaigždės rodo Li sumažėjimą, greičiausiai sukeltą sukimosi sukelto maišymosi.

- **Palyginimas su įprastomis milžinėmis**: RS CVn žvaigždės seka bendrą ličio kiekio mažėjimą, kurį lemia pirmoji drumstis ir papildomas maišymasis, o tarp RS CVn žvaigždžių, esančių apatinėje RGB dalyje, yra žvaigždžių, kuriose ličio išeikvojimą sukelia papildomas maišymasis arba sukimasis, priklausomai nuo jų masės.

- **Sproginėjančios žvaigždės**: Sproginėjančiose helį centre deginančiose žvaigždėse, nepaisant intensyvių blyksnių, paviršiaus reiškinių ir epizodinių masės išsiveržimų, CNO gausos ir $^{12}C/^{13}C$ santykiai nesiskiria nuo kitų He centre deginančių žvaigždžių. Tai rodo, kad dėl sproginėjimų jų paviršiaus cheminė sudėtis žymiai nepasikeičia.

8 CV

Barkha Bale

Work experience

2023–Current	Junior Researcher, Institute of Theoretical Physics and Astronomy, Vilnius University.
2023–Current	Project Specialist: • Chemical elements as a clock for stellar age determination. Funded by the Research Council of Lithuania. • The history of C, N, O. DAINA3- Research grant of the Polish National Science Center and the Research Council of Lithuania.
2023	Teaching assistant for Numerical Method course, Light engineering, Bachelor studies, Faculty of Physics, Vilnius university.
2022	English Teacher at Anglų kalbu studija, Lithuania.
2019–2021	Physics and Mathematics Teacher, Arya Vidya Mandir, Mumbai, India.
2012–2019	Physics, Mathematics, Biology, Chemistry Teacher at various institutes and coaching centres in Mumbai, India.

Publications

1. **Bale B.**, Tautvaišienė G., Minkevičiūtė R., Drazdauskas A., Mikolaitis Š., Stonkutė E., Ambrosch M., *Chromospherically active stars: Lithium and CNO abundances in northern RS CVn stars*, Astronomy & Astrophysics, Vol. 703, A128, 2025.

2. **Bale B.**, Tautvaišienė G., Minkevičiūtė R., Drazdauskas A., Mikolaitis Š., Stonkutė E., Ambrosch M., *Chromospherically active stars: Chemical composition of photospheres in 20 RS CVn stars*, Astronomy & Astrophysics, Vol. 696, A23, 2025.

3. Lagarde N., Minkevičiūtė R., Drazdauskas A., Tautvaišienė G., Charbonnel C., Reylé C., Miglio A., Kushwahaa T., **Bale B.**, $^{12}C/^{13}C$ *of*

Kepler giant stars: The missing piece of the mixing puzzle, Astronomy & Astrophysics, Vol. 684, A70, 2024.

Education

2021–2025	Ph.D. Student in Astronomy and Astrophysics, Vilnius University. Advisor: Dr. Gražina Tautvaišienė. Research: Chemical composition of magnetically active RS CVn stars.
2017–2019	B.Ed. (Science, Math, Action Research), HJCE, Mumbai, India.
2015–2017	M.Sc. (Physics), The Institute of Science, Mumbai, India. Specialisation: Electronics, microcontrollers, Programming: C++, C and python.
2012–2015	B.Sc. (Physics), Patkar-Varde College, Mumbai, India. Specialisation: Electronics.

Presentations at International Conferences

1. European Astronomical Society Annual Meeting, 23–27 June 2025, Cork, Ireland. Poster presentation: "Chemical composition of photospheres in 20 RS CVn stars."

2. Open Readings, 23–26 April 2024, Vilnius, Lithuania. Oral presentation: "Mixing process in the atmosphere of magnetically active RS CVn giants."

3. European Astronomical Society Annual Meeting, 10–14 July 2023, Kraków, Poland. Poster presentation: "Mixing process in the atmospheres of RS CVn giants."

4. Cambridge Workshop on Cool Stars, Stellar Systems and the Sun, 4–9 July 2022, Toulouse, France. Remote participation. Poster presentation: "CNO abundances in magnetically active RS CVn giants."

Presentations at National Conferences

1. 46th Lithuanian National Physics Conference (LNFK'46), 8–10 October 2025, Vilnius, Lithuania. Oral presentation: "Lithium and CNO abundances in chromospherically active RS CVn stars."

2. 45th Lithuanian National Physics Conference (LNFK'45), 25–27 October 2023, Vilnius, Lithuania. Poster presentation: "Mixing process in the atmosphere of RS CVn giants."

Scientific and Public Talks

- "Overcoming Obstacles", **TEDx Talk**, Vilnius International School, Vilnius, Lithuania, May 2022.
- "The End of the Universe", Neveronių Gimnazija, Kaunas, Lithuania, 2025.
- Talks at Mokslo Festivalis, Erdvėlaivis Žemė, Lithuania: "Biomarkers & Biosignatures in the Search for Extraterrestrial Life", September 2024; "The End of the Universe", July 2023; "The Seen and the Unseen Universe", September 2022.
- "Methodologies of Teaching Physics", Invited Talk, HJCE, Mumbai, India, 2018, 2019.

Summer Schools, Workshops, and Internships

1. 1st ChETEC-INFRA Observational School (ChINOS), Ondřejov Observatory, 3 nights remotely on Nordic Optical Telescope, Czech Republic, July 2023.
2. Pro-Am Workshop, IAU, IIT Bombay, Mumbai, December 2023.
3. Europlanet Summer School: Space missions, ground-based observations and science communication, Lithuania, August 2023.
4. Milkyway Gaia Better Inclusion, Better Science, Building Impact in MW-GAIA, Lithuania, July 2023.
5. NEON Observing School, Observatoire de Haute-Provence, France, October 2022.
6. Europlanet Telescope Network Science Workshop, Lithuania, February 2022.
7. Large-Volume Spectroscopic Analyses of AGN and Star-Forming Galaxies in the Era of JWST, March 2022.

8. Sagan Exoplanet Summer Hybrid Workshop: Exoplanet Science in the Gaia Era, July 2022.
9. Asteroid Photometry, Molėtai Observatory, August 2021.
10. Sagan Summer Workshop on “Circumstellar Disks and Young Planets”, July 2021.
11. Internship: 6 weeks internship at SSERD, India. Worked on a project titled *Light Curves and Rotational Period of Natural Satellites*, 2021.
12. National Symposium on Recent Developments in Astrophysics & Astronomy, India, July 2021.

LOC

Milky Way Gaia: Better Inclusion, Better Science, Building Impact in MW-GAIA, Vilnius, July 2023.

Awards

1. Best Master’s project: “Soil moisture sensor using microcontroller”, 2017.
2. Sci-fi story writing competition, Second position, The Institute of Science, 2017.
3. Preliminary discovery of five asteroids, International Astronomical Search Collaboration, 2020–2021.
4. Best Student of the Year, MVM School, Mumbai, 2010.

Languages

1. English: Native, Lithuanian: A1–A2, German: A1–A2.
2. Fluent languages: Hindi, Marathi, Arabic, Urdu, Punjabi, Gujarati.

Competitive Exams Cleared

1. PhD Entrance Test (PET) at the University of Mumbai, 2020.
2. Teacher Eligibility Test (TET), National exam, 2018, India.

3. Graduate Aptitude Test in Engineering (GATE), for Research & Industry, 2016, India.

Certifications

1. 25+ certifications in areas including teaching methodologies, leadership development, inclusive education, gamification in teaching, educational content creation and writing, and data analytics.

2. Data-Driven Astronomy, University of Sydney, Coursera, June 2021.

3. Data-Driven Astronomy, Positron Foundation, India, August 2021.

4. Course in Astronomy and Astrophysics, May 2021.

5. Quantum Mechanics for Scientists and Engineers, Stanford University (Remote), 2018.

References

Adamczak, J. & Lambert, D. L. 2014, Carbon and Oxygen Abundances across the Hertzsprung Gap, Astrophys. J., 791, 58

Adamów, M., Niedzielski, A., Villaver, E., Nowak, G., & Wolszczan, A. 2012, BD+48 740—Li Overabundant Giant Star with a Planet: A Case of Recent Engulfment?, Astrophys. J. Lett., 754, L15

Asplund, M. 2005, New Light on Stellar Abundance Analyses: Departures from LTE and Homogeneity, Annu. Rev. Astron. Astrophys., 43, 481

Asplund, M., Grevesse, N., Sauval, A. J., & Scott, P. 2009, The Chemical Composition of the Sun, Annu. Rev. Astron. Astrophys., 47, 481

Aurière, M., Konstantinova-Antova, R., Charbonnel, C., et al. 2015, The magnetic fields at the surface of active single G-K giants, Astron. Astrophys., 574, A90

Bailer-Jones, C. A. L., Rybizki, J., Fouesneau, M., Demleitner, M., & Andrae, R. 2021, Estimating Distances from Parallaxes. V. Geometric and Photogeometric Distances to 1.47 Billion Stars in Gaia Early Data Release 3, Astron. J., 161, 147

Balachandran, S. C., Fekel, F. C., Henry, G. W., & Uitenbroek, H. 2000, Two K Giants with Supermeteoritic Lithium Abundances: HDE 233517 and HD 9746, Astrophys. J., 542, 978

Baliunas, S. L. & Dupree, A. K. 1982, Ultraviolet and optical spectrum studies of lambda Andromedae : evidence for atmospheric inhomogeneities., Astrophys. J., 252, 668

Barisevičius, G., Tautvaišienė, G., Berdyugina, S., Chorniy, Y., & Ilyin, I. 2010, Chemical Composition of the RS CVn-type Star 29 Draconis, Baltic Astronomy, 19, 157

Barisevičius, G., Tautvaišienė, G., Berdyugina, S., Chorniy, Y., & Ilyin, I. 2011, Chemical Composition of the RS CVn-type Star 33 Piscium, Baltic Astronomy, 20, 53

Berdyugina, S. V. 2005, Starspots: A Key to the Stellar Dynamo, Living Reviews in Solar Physics, 2, 8

Berdyugina, S. V., Ilyin, I., & Tuominen, I. 1999, The long-period RS Canum Venaticorum binary IM Pegasi. I. Orbital and stellar parameters, Astron. Astrophys., 347, 932

Berdyugina, S. V., Jankov, S., Ilyin, I., Tuominen, I., & Fekel, F. C. 1998, The active RS Canum Venaticorum binary II Pegasi. I. Stellar and orbital parameters, Astron. Astrophys., 334, 863

Boeche, C. & Grebel, E. K. 2016, SP_Ace: a new code to derive stellar parameters and elemental abundances, Astron. Astrophys., 587, A2

Boothroyd, A. I. & Sackmann, I. J. 1999, The CNO Isotopes: Deep Circulation in Red Giants and First and Second Dredge-up, Astrophys. J., 510, 232

Bovy, J. 2015, galpy: A python Library for Galactic Dynamics, Astrophys. J. Suppl. Ser., 216, 29

Bressan, A., Marigo, P., Girardi, L., et al. 2012, PARSEC: stellar tracks and isochrones with the PAdova and TRieste Stellar Evolution Code, Mon. Not. R. Astron. Soc., 427, 127

Buccino, A. P. & Mauas, P. J. D. 2009, Long-term chromospheric activity of non-eclipsing RS CVn-type stars, Astron. Astrophys., 495, 287

Busso, M., Wasserburg, G. J., Nollett, K. M., & Calandra, A. 2007, Can Extra Mixing in RGB and AGB Stars Be Attributed to Magnetic Mechanisms?, Astrophys. J., 671, 802

Cameron, A. G. W. & Fowler, W. A. 1971, Lithium and the s-PROCESS in Red-Giant Stars, Astrophys. J., 164, 111

Cantiello, M. & Langer, N. 2010, Thermohaline mixing in evolved low-mass stars, Astron. Astrophys., 521, A9

Cao, D. & Gu, S. 2025, Further Investigation on Chromospheric Activity Patterns of the RS Canum Venaticorum Star V711 Tauri, Astron. J., 169, 198

Cao, D., Gu, S., Wolter, U., et al. 2023, Prominence detection and chromosphere feature on the prototype RS CVn of active binary systems, Mon. Not. R. Astron. Soc., 523, 4146

Casey, A. R., Ho, A. Y. Q., Ness, M., et al. 2019, Tidal Interactions between Binary Stars Can Drive Lithium Production in Low-mass Red Giants, Astrophys. J., 880, 125

Chanamé, J., Pinsonneault, M., & Terndrup, D. M. 2005, Abundance Anomalies and Rotational Evolution of Low-Mass Red Giants: A Maximal Mixing Approach, Astrophys. J., 631, 540

Charbonnel, C. 1994, Clues for non-standard mixing on the red giant branch from 12C/13C and 12C/14N ratios in evolved stars., Astron. Astrophys., 282, 811

Charbonnel, C., Brown, J. A., & Wallerstein, G. 1998, Mixing processes during the evolution of red giants with moderate metal deficiencies: the role of molecular-weight barriers, Astron. Astrophys., 332, 204

Charbonnel, C., Decressin, T., Lagarde, N., et al. 2017, The magnetic strip(s) in the advanced phases of stellar evolution. Theoretical convective turnover timescale and Rossby number for low- and intermediate-mass stars up to the AGB at various metallicities, Astron. Astrophys., 605, A102

Charbonnel, C. & Lagarde, N. 2010, Thermohaline instability and rotation-induced mixing. I. Low- and intermediate-mass solar metallicity stars up to the end of the AGB, Astron. Astrophys., 522, A10

Charbonnel, C., Lagarde, N., Jasniewicz, G., et al. 2020, Lithium in red giant stars: Constraining non-standard mixing with large surveys in the Gaia era, Astron. Astrophys., 633, A34

Charbonnel, C. & Zahn, J. P. 2007, Inhibition of thermohaline mixing by a magnetic field in Ap star descendants: implications for the Galactic evolution of ^{3}He, Astron. Astrophys., 476, L29

Creevey, O. L., Thévenin, F., Basu, S., et al. 2013, A large sample of calibration stars for Gaia: log g from Kepler and CoRoT fields, Mon. Not. R. Astron. Soc., 431, 2419

Cutri, R. M., Wright, E. L., Conrow, T., et al. 2021, VizieR Online Data Catalog: AllWISE Data Release (Cutri+ 2013), VizieR On-line Data Catalog: II/328. Originally published in: IPAC/Caltech (2013)

Cyburt, R. H., Fields, B. D., & Olive, K. A. 2008, An update on the big bang nucleosynthesis prediction for ^{7}Li: the problem worsens, J. Cosmol. Astropart. Phys., 2008, 012

Day, R. W., Lambert, D. L., & Sneden, C. 1973, The ^{12}C/^{13}C ratio in stellar atmospheres. I. Alpha Serpentis and Alpha Bootis., Astrophys. J., 185, 213

Deepak, Lambert, D. L., & Reddy, B. E. 2020, Abundance analyses of Li-enriched and normal giants in the GALAH survey, Mon. Not. R. Astron. Soc., 494, 1348

Denissenkov, P. A., Chaboyer, B., & Li, K. 2006, From Canonical to Enhanced Extra Mixing in Low-Mass Red Giants: Tidally Locked Binaries, Astrophys. J., 641, 1087

Denissenkov, P. A. & Herwig, F. 2004, Enhanced Extra Mixing in Low-Mass Red Giants: Lithium Production and Thermal Stability, Astrophys. J., 612, 1081

Denissenkov, P. A., Pinsonneault, M., & MacGregor, K. B. 2009, Magneto-Thermohaline Mixing in Red Giants, Astrophys. J., 696, 1823

Denissenkov, P. A. & Tout, C. A. 2000, On a physical mechanism for extra mixing in globular cluster red giants, Mon. Not. R. Astron. Soc., 316, 395

Ding, M.-Y., Shi, J.-R., Yan, H.-l., et al. 2024, Lithium Abundances from the LAMOST Medium-resolution Survey Data Release 9, Astrophys. J. Suppl. Ser., 271, 58

Drake, J. J., Ball, B., Eldridge, J. J., Ness, J. U., & Stancliffe, R. J. 2011, Close to the Dredge: Precise X-Ray C and N Abundances in λ Andromeda and Its Precocious Red Giant Branch Mixing Problem, Astron. J., 142, 144

Drake, J. J. & Lambert, D. L. 1994, Sodium in Weak G-Band Giants, Astrophys. J., 435, 797

Eaton, J. A., Henry, G. W., & Fekel, F. C. 1996, Random Spots on Chromospherically Active Stars, Astrophys. J., 462, 888

Eggenberger, P., Maeder, A., & Meynet, G. 2005, Stellar evolution with rotation and magnetic fields. IV. The solar rotation profile, Astron. Astrophys., 440, L9

Eggleton, P. P., Dearborn, D. S. P., & Lattanzio, J. C. 2006, Deep Mixing of ^{3}He: Reconciling Big Bang and Stellar Nucleosynthesis, Science, 314, 1580

Eggleton, P. P., Dearborn, D. S. P., & Lattanzio, J. C. 2008, Compulsory Deep Mixing of ^{3}He and CNO Isotopes in the Envelopes of Low-Mass Red Giants, Astrophys. J., 677, 581

Eker, Z., Ak, N. F., Bilir, S., et al. 2008, A catalogue of chromospherically active binary stars (third edition), Mon. Not. R. Astron. Soc., 389, 1722

Fekel, F. C. & Balachandran, S. 1993, Lithium and Rapid Rotation in Chromospherically Active Single Giants, Astrophys. J., 403, 708

Fekel, F. C., Moffett, T. J., & Henry, G. W. 1986, A Survey of Chromospherically Active Stars, Astrophys. J. Suppl. Ser., 60, 551

Feuillet, D. K., Bovy, J., Holtzman, J., et al. 2016, Determining Ages of APOGEE Giants with Known Distances, Astrophys. J., 817, 40

Franciosini, E., Randich, S., de Laverny, P., et al. 2022, The Gaia-ESO Survey: Lithium measurements and new curves of growth, Astron. Astrophys., 668, A49

Gaia Collaboration, Brown, A. G. A., Vallenari, A., et al. 2021, Gaia Early Data Release 3. Summary of the contents and survey properties, Astron. Astrophys., 649, A1

Gao, Q., Shi, J.-R., Yan, H.-L., et al. 2019, Lithium-rich Giants in LAMOST Survey. I. The Catalog, Astrophys. J. Suppl. Ser., 245, 33

García Pérez, A. E., Sánchez-Blázquez, P., Vazdekis, A., et al. 2021, An extension of the MILES library with derived T_{eff}, log g, [Fe/H], and [α/Fe], Mon. Not. R. Astron. Soc., 505, 4496

Ghezzi, L., Montet, B. T., & Johnson, J. A. 2018, Retired A Stars Revisited: An Updated Giant Planet Occurrence Rate as a Function of Stellar Metallicity and Mass, Astrophys. J., 860, 109

Gilmore, G. & Reid, N. 1983, New light on faint stars - III. Galactic structure towards the South Pole and the Galactic thick disc., Mon. Not. R. Astron. Soc., 202, 1025

Gilroy, K. K. 1989, Carbon Isotope Ratios and Lithium Abundances in Open Cluster Giants, Astrophys. J., 347, 835

Gilroy, K. K. & Brown, J. A. 1991, Carbon Isotope Ratios along the Giant Branch of M67, Astrophys. J., 371, 578

Gonçalves, B. F. O., da Costa, J. S., de Almeida, L., Castro, M., & do Nascimento, Jr., J. D. 2020, Li-rich giant stars under scrutiny: binarity, magnetic activity, and the evolutionary status after Gaia DR2, Mon. Not. R. Astron. Soc., 498, 2295

Good, G. A. 2003, Observing Variable Stars

Gratton, R. G., Sneden, C., Carretta, E., & Bragaglia, A. 2000, Mixing along the red giant branch in metal-poor field stars, Astron. Astrophys., 354, 169

Grevesse, N., Asplund, M., & Sauval, A. J. 2007, The Solar Chemical Composition, Space Sci. Rev., 130, 105

Guandalini, R., Palmerini, S., Busso, M., & Uttenthaler, S. 2009, Extra-Mixing in Luminous Cool Red Giants: Hints from Evolved Stars With and Without Li, Publ. Astron. Soc. Aust., 26, 168

Guillout, P., Klutsch, A., Frasca, A., et al. 2009, A spectroscopic survey of the youngest field stars in the solar neighbourhood. I. The optically bright sample, Astron. Astrophys., 504, 829

Gustafsson, B., Edvardsson, B., Eriksson, K., et al. 2008, A grid of MARCS model atmospheres for late-type stars. I. Methods and general properties, Astron. Astrophys., 486, 951

Gustafsson, B., Karlsson, T., Olsson, E., Edvardsson, B., & Ryde, N. 1999, The origin of carbon, investigated by spectral analysis of solar-type stars in the Galactic Disk, Astron. Astrophys., 342, 426

Hall, D. S. 1976, in Astrophysics and Space Science Library, Vol. 60, IAU Colloq. 29: Multiple Periodic Variable Stars, ed. W. S. Fitch, 287

Heiter, U., Lind, K., Asplund, M., et al. 2015, Atomic and molecular data for optical stellar spectroscopy, , 90, 054010

Herbig, G. H. 1965, Lithium Abundances in F5-G8 Dwarfs., Astrophys. J., 141, 588

Iben, Jr., I. 1968, Low-Mass Red Giants, Astrophys. J., 154, 581

Iben, Icko, J. 1965, Stellar Evolution. II. The Evolution of a 3 M_{sun} Star from the Main Sequence Through Core Helium Burning., Astrophys. J., 142, 1447

Israelian, G., Santos, N. C., Mayor, M., & Rebolo, R. 2004, Lithium in stars with exoplanets, Astron. Astrophys., 414, 601

Izzo, L., Della Valle, M., Mason, E., et al. 2015, Early Optical Spectra of Nova V1369 Cen Show the Presence of Lithium, Astrophys. J. Lett., 808, L14

Jönsson, H., Holtzman, J. A., Allende Prieto, C., et al. 2020, APOGEE Data and Spectral Analysis from SDSS Data Release 16: Seven Years of Observations Including First Results from APOGEE-South, Astron. J., 160, 120

Jurgenson, C., Fischer, D., McCracken, T., et al. 2016, Design and Construction of VUES: The Vilnius University Echelle Spectrograph, Journal of Astronomical Instrumentation, 5, 1650003

Katz, D., Favata, F., Aigrain, S., & Micela, G. 2003, The photospheric abundances of active binaries. I. Detailed analysis of HD 113816 (IS Vir) and HD 119285 (V851 Cen), Astron. Astrophys., 397, 747

Keller, G. & Limber, D. N. 1951, A Photoelectric Study of the Eclipsing Stars RS Canum Venaticorum and YY Sagittarii., Astrophys. J., 113, 637

King, J. R., Deliyannis, C. P., Hiltgen, D. D., et al. 1997, Lithium Abundances in the Solar Twins 16 CYG A and B and the Solar Analog alpha CEN A, Calibration of the 6707 Angstrom Li Region Linelist, and Implications, Astron. J., 113, 1871

Kowalski, A. F. 2024, Stellar flares, Living Reviews in Solar Physics, 21, 1

Kumar, Y. B., Reddy, B. E., Campbell, S. W., et al. 2020, Discovery of ubiquitous lithium production in low-mass stars, Nature Astronomy, 4, 1059

Lagarde, N., Decressin, T., Charbonnel, C., et al. 2012, Thermohaline instability and rotation-induced mixing. III. Grid of stellar models and asymptotic asteroseismic quantities from the pre-main sequence up to the AGB for low- and intermediate-mass stars of various metallicities, Astron. Astrophys., 543, A108

Lagarde, N., Reylé, C., Robin, A. C., et al. 2019, The Gaia-ESO Survey: impact of extra mixing on C and N abundances of giant stars, Astron. Astrophys., 621, A24

Lagarde, N., Robin, A. C., Reylé, C., & Nasello, G. 2017, Population synthesis to constrain Galactic and stellar physics. I. Determining age and mass of thin-disc red-giant stars, Astron. Astrophys., 601, A27

Lambert, D. L. & Ries, L. M. 1977, Carbon, nitrogen, and oxygen abundances in 11 G and K giants., Astrophys. J., 217, 508

Lambert, D. L. & Ries, L. M. 1981, Carbon, nitrogen, and oxygen abundances in G and K giants., Astrophys. J., 248, 228

Lamers, H. J. G. L. M., Korevaar, P., & Cassatella, A. 1985, The ejection of shells in the stellar wind of the hypergiant P Cygni (B1Ia+)., Astron. Astrophys., 149, 29

Lebreton, Y. & Reese, D. R. 2020, SPInS, a pipeline for massive stellar parameter inference. A public Python tool to age-date, weigh, size up stars, and more, Astron. Astrophys., 642, A88

Li, X.-F., Shi, J.-R., Li, Y., Yan, H.-L., & Zhang, J.-H. 2025, Meridional Circulation. I. A Formation Channel for Lithium-rich and Super-lithium-rich Red Clump Stars, Astrophys. J. Lett., 982, L4

Lind, K., Asplund, M., & Barklem, P. S. 2009, Departures from LTE for neutral Li in late-type stars, Astron. Astrophys., 503, 541

Liu, X.-f., Zhao, G., Tan, H.-s., & Lu, F.-j. 1993, Lithium abundance and activity for 57 RS CVn systems, Chinese Astron. Astrophys., 17, 51

Luck, R. E. & Heiter, U. 2007, Giants in the Local Region, Astron. J., 133, 2464

Lyubimkov, L. S. 2016, Lithium in Stellar Atmospheres: Observations and Theory, Astrophysics, 59, 411

Magrini, L., Smiljanic, R., Franciosini, E., et al. 2021, Gaia-ESO survey: Lithium abundances in open cluster Red Clump stars, Astron. Astrophys., 655, A23

Mallick, A., Singh, R., & Reddy, B. E. 2023, Lithium Abundances in Giants as a Function of Stellar Mass: Evidence for He Flash as the Source of Li Enhancement in Low-mass Giants, Astrophys. J. Lett., 944, L5

Mallick, A., Sneden, C., Reddy, B. E., & Afşar, M. 2025, High Lithium Abundance Connection with the Chromospheric Helium in Red Giants: Spectroscopic and Asteroseismic Analyses, Astrophys. J., 980, 265

Mallik, S. V. 1997, The CA II triplet lines as diagnostics of luminosity, metallicity and chromospheric activity in cool stars, Astron. Astrophys. Suppl., 124, 359

Mallik, S. V. 1998, Chromospheric activity in cool stars and the lithium abundance, Astron. Astrophys., 338, 623

Massarotti, A., Latham, D. W., Stefanik, R. P., & Fogel, J. 2008, Rotational and Radial Velocities for a Sample of 761 HIPPARCOS Giants and the Role of Binarity, Astron. J., 135, 209

McWilliam, A. 1990, High-Resolution Spectroscopic Survey of 671 GK Giants. I. Stellar Atmosphere Parameters and Abundances, Astrophys. J. Suppl. Ser., 74, 1075

Mikolaitis, Š., Tautvaišienė, G., Gratton, R., Bragaglia, A., & Carretta, E. 2011a, Chemical composition of evolved stars in the open cluster IC 4651, Mon. Not. R. Astron. Soc., 413, 2199

Mikolaitis, Š., Tautvaišienė, G., Gratton, R., Bragaglia, A., & Carretta, E. 2011b, Chemical composition of evolved stars in the open cluster NGC 2506, Mon. Not. R. Astron. Soc., 416, 1092

Mikolaitis, Š., Tautvaišienė, G., Gratton, R., Bragaglia, A., & Carretta, E. 2012, C, N, O abundances and carbon isotope ratios in evolved stars of the open clusters Collinder 261 and NGC 6253, Astron. Astrophys., 541, A137

Mints, A. & Hekker, S. 2017, A Unified tool to estimate Distances, Ages, and Masses (UniDAM) from spectrophotometric data, Astron. Astrophys., 604, A108

Mints, A. & Hekker, S. 2018, Isochrone fitting in the Gaia era, Astron. Astrophys., 618, A54

Molaro, P., Izzo, L., Mason, E., Bonifacio, P., & Della Valle, M. 2016, Highly enriched ^{7}Be in the ejecta of Nova Sagittarii 2015 No. 2 (V5668 Sgr) and the Galactic ^{7}Li origin, Mon. Not. R. Astron. Soc., 463, L117

Montesinos, B., Gimenez, A., & Fernandez-Figueroa, M. J. 1988, General properties of RS CVn systems., Mon. Not. R. Astron. Soc., 232, 361

Morel, T., Micela, G., Favata, F., & Katz, D. 2004, The photospheric abundances of active binaries. III. Abundance peculiarities at high activity levels, Astron. Astrophys., 426, 1007

Morel, T., Micela, G., Favata, F., Katz, D., & Pillitteri, I. 2003, The photospheric abundances of active binaries. II. Atmospheric parameters and abundance patterns for 6 single-lined RS CVn systems, Astron. Astrophys., 412, 495

Morel, T. & Miglio, A. 2012, Assessing the accuracy of the surface gravity determination in late-type stars with solar-like pulsators, Mon. Not. R. Astron. Soc., 419, L34

Mori, K., Kusakabe, M., Balantekin, A. B., Kajino, T., & Famiano, M. A. 2021, Enhancement of lithium in red clump stars by the additional energy loss induced by new physics, Mon. Not. R. Astron. Soc., 503, 2746

Morris, B. M., Curtis, J. L., Sakari, C., Hawley, S. L., & Agol, E. 2019, Stellar Properties of Active G and K Stars: Exploring the Connection between Starspots and Chromospheric Activity, Astron. J., 158, 101

Mosser, B., Goupil, M. J., Belkacem, K., et al. 2012, Spin down of the core rotation in red giants, Astron. Astrophys., 548, A10

Mucciarelli, A., Monaco, L., Bonifacio, P., et al. 2022, Discovery of a thin lithium plateau among metal-poor red giant branch stars, Astron. Astrophys., 661, A153

Nordhaus, J., Busso, M., Wasserburg, G. J., Blackman, E. G., & Palmerini, S. 2008, Magnetic Mixing in Red Giant and Asymptotic Giant Branch Stars, Astrophys. J. Lett., 684, L29

Norris, J. E., Yong, D., Frebel, A., & Ryan, S. G. 2023, A critique of the Spite Plateau and the astration of primordial lithium, Mon. Not. R. Astron. Soc., 522, 1358

Olive, K. A. & Schramm, D. N. 1992, Astrophysical ^{7}Li as a product of Big Bang nucleosynthesis and galactic cosmic-ray spallation, Nature, 360, 439

Pace, G. 2013, Chromospheric activity as age indicator. An L-shaped chromospheric-activity versus age diagram, Astron. Astrophys., 551, L8

Pagel, B. E. J. 1974, CN strengths in M67 and NGC 188., Mon. Not. R. Astron. Soc., 167, 413

Pagel, B. E. J. & Tautvaisiene, G. 1995, Chemical evolution of primary elements in the Galactic disc: an analytical model, Mon. Not. R. Astron. Soc., 276, 505

Pakhomov, Y. V., Chugai, N. N., Bondar', N. I., Gorynya, N. A., & Semenko, E. A. 2015, Evolutionary status of the active star PZ Mon, Mon. Not. R. Astron. Soc., 446, 56

Pal, T., Khan, I., Worthey, G., Gregg, M. D., & Silva, D. R. 2023, HST Low-resolution Stellar Library, Astrophys. J. Suppl. Ser., 266, 41

Palacios, A., Talon, S., Charbonnel, C., & Forestini, M. 2003, Rotational mixing in low-mass stars. I Effect of the mu-gradients in main sequence and subgiant Pop I stars, Astron. Astrophys., 399, 603

Pallavicini, R. 1994, in Astronomical Society of the Pacific Conference Series, Vol. 64, Cool Stars, Stellar Systems, and the Sun, ed. J.-P. Caillault, 244

Pallavicini, R., Randich, S., Giampapa, M., & Cutispoto, G. 1990, Lithium in chromospherically active stars., The Messenger, 62, 51

Pallavicini, R., Randich, S., & Giampapa, M. S. 1992, Lithium in RS CVn binaries and related chromospherically active stars. I.Observational results., Astron. Astrophys., 253, 185

Palmerini, S., Busso, M., Maiorca, E., & Guandalini, R. 2009, Nucleosynthesis of Light-Element Isotopes in Evolved Stars Experiencing Extended Mixing, Publ. Astron. Soc. Aust., 26, 161

Pinsonneault, M. 1997, Mixing in Stars, Annu. Rev. Astron. Astrophys., 35, 557

Pitrou, C., Coc, A., Uzan, J.-P., & Vangioni, E. 2018, Precision big bang nucleosynthesis with improved Helium-4 predictions, Phys. Rep., 754, 1

Plez, B. 2012, Turbospectrum: Code for spectral synthesis, Astrophysics Source Code Library, record ascl:1205.004

Popper, D. M. & Ulrich, R. K. 1977, The evolutionary status of RS Canum Venaticorum binaries., Astrophys. J. Lett., 212, L131

Randich, S., Giampapa, M. S., & Pallavicini, R. 1992, in Astronomical Society of the Pacific Conference Series, Vol. 26, Cool Stars, Stellar Systems, and the Sun, ed. M. S. Giampapa & J. A. Bookbinder, 576

Randich, S., Giampapa, M. S., & Pallavicini, R. 1994, Lithium in RS Canum Venaticorum binaries and related chromospherically active stars. III. Northern RS CVn systems., Astron. Astrophys., 283, 893

Randich, S., Gratton, R., & Pallavicini, R. 1993, Lithium in RS CVn binaries and related chromospherically active stars . II. Spectrum synthesis analysis., Astron. Astrophys., 273, 194

Randich, S. & Magrini, L. 2021, Light Elements in the Universe, Frontiers in Astronomy and Space Sciences, 8, 6

Recio-Blanco, A., de Laverny, P., Kordopatis, G., et al. 2014, The Gaia-ESO Survey: the Galactic thick to thin disc transition, Astron. Astrophys., 567, A5

Reeves, H., Fowler, W. A., & Hoyle, F. 1970, Galactic Cosmic Ray Origin of Li, Be and B in Stars, Nature, 226, 727

Rucinski, S. M., Krogulec, M., & Seaquist, E. R. 1993, A Search for Rapid Radio Flux Variations in two RS CVn Binary Systems, Astron. J., 105, 2308

Rukeya, R., Lü, G., Wang, Z., & Zhu, C. 2017, Novae Contribution to the Galactic Lithium Enhancement, Publ. Astron. Soc. Pac., 129, 074201

Sackmann, I. J. & Boothroyd, A. I. 1992, The Creation of Superrich Lithium Giants, Astrophys. J. Lett., 392, L71

Sackmann, I. J., Smith, R. L., & Despain, K. H. 1974, Carbon and eruptive stars: surface enrichment of lithium, carbon, nitrogen, and ^{13}C by deep mixing., Astrophys. J., 187, 555

Savanov, I. S. & Berdyugina, S. V. 1994, The chemical composition of the atmosphere of the active giant λ And, Astronomy Letters, 20, 227

Schmitt, J. H. M. M. & Stern, R. A. 1994, in Astronomical Society of the Pacific Conference Series, Vol. 64, Cool Stars, Stellar Systems, and the Sun, ed. J.-P. Caillault, 134

Schwab, J. 2020, A Helium-flash-induced Mixing Event Can Explain the Lithium Abundances of Red Clump Stars, Astrophys. J. Lett., 901, L18

Sciortino, S., Micela, C., Kashyap, V., Harnden, F. R., J., & Rosner, R. 1994, in Astronomical Society of the Pacific Conference Series, Vol. 64, Cool Stars, Stellar Systems, and the Sun, ed. J.-P. Caillault, 140

Skrutskie, M. F., Cutri, R. M., Stiening, R., et al. 2006, The Two Micron All Sky Survey (2MASS), Astron. J., 131, 1163

Smiljanic, R., Gauderon, R., North, P., et al. 2009, CNONa and $^{12}C/^{13}C$ in giant stars of 10 open clusters, Astron. Astrophys., 502, 267

Sneden, C. A. 1973, PhD thesis, University of Texas, Austin

Soderblom, D. R. 1984, in Cool Stars, Stellar Systems, and the Sun, ed. S. L. Baliunas & L. Hartmann, Vol. 193, 205

Spite, F. & Spite, M. 1982, Abundance of lithium in unevolved stars and old disk stars : Interpretation and consequences., Astron. Astrophys., 115, 357

Starrfield, S., Truran, J. W., Sparks, W. M., & Arnould, M. 1978, On ^{7}Li production in nova explosions., Astrophys. J., 222, 600

Stetson, P. B. & Pancino, E. 2008, DAOSPEC: An Automatic Code for Measuring Equivalent Widths in High-Resolution Stellar Spectra, Publ. Astron. Soc. Pac., 120, 1332

Stonkutė, E., Chorniy, Y., Tautvaišienė, G., et al. 2020, High-resolution Spectroscopic Study of Dwarf Stars in the Northern Sky: Lithium, Carbon, and Oxygen Abundances, Astron. J., 159, 90

Strassmeier, K., Washuettl, A., Granzer, T., Scheck, M., & Weber, M. 2000, The Vienna-KPNO search for Doppler-imaging candidate stars. I. A catalog of stellar-activity indicators for 1058 late-type Hipparcos stars, Astron. Astrophys. Suppl., 142, 275

Strassmeier, K. G. 1994, Chromospheric activity in G and K giants: the spectroscopic data base, Astron. Astrophys. Suppl., 103, 413

Strassmeier, K. G., Fekel, F. C., Bopp, B. W., Dempsey, R. C., & Henry, G. W. 1990, Chromospheric CA II H and K and H alpha Emission in Single and Binary Stars of Spectra Types F6–M2, Astrophys. J. Suppl. Ser., 72, 191

Tautvaisiene, G., Kriukelis, S., & Bikmaev, I. 1992, Element abundances in the RS CVn-type star lambda Andromedae., Baltic Astronomy, 1, 450

Tautvaišienė, G., Barisevičius, G., Berdyugina, S., Chorniy, Y., & Ilyin, I. 2010a, Chemical Composition of the RS CVn-type Star Lambda Andromedae, Baltic Astronomy, 19, 95

Tautvaišienė, G., Barisevičius, G., Berdyugina, S., Ilyin, I., & Chorniy, Y. 2011, Chemical composition of AY Ceti: A flaring, spotted star with a white dwarf companion, Astronomische Nachrichten, 332, 925

Tautvaišienė, G., Drazdauskas, A., Mikolaitis, Š., et al. 2015, The Gaia-ESO Survey: CNO abundances in the open clusters Trumpler 20, NGC 4815, and NGC 6705, Astron. Astrophys., 573, A55

Tautvaišienė, G., Edvardsson, B., Puzeras, E., Barisevičius, G., & Ilyin, I. 2010b, C, N and O abundances in red clump stars of the Milky Way, Mon. Not. R. Astron. Soc., 409, 1213

Tautvaišienė, G., Edvardsson, B., Puzeras, E., & Ilyin, I. 2005, Chemical composition of evolved stars in the open cluster NGC 7789, Astron. Astrophys., 431, 933

Tautvaišienė, G., Edvardsson, B., Tuominen, I., & Ilyin, I. 2001, Chemical composition of red horizontal branch stars in the thick disk of the Galaxy, Astron. Astrophys., 380, 578

Tautvaišienė, G., Mikolaitis, Š., Drazdauskas, A., et al. 2020, Chemical Composition of Bright Stars in the Continuous Viewing Zone of the TESS Space Mission, Astrophys. J. Suppl. Ser., 248, 19

Tautvaišienė, G., Mikolaitis, Š., Drazdauskas, A., et al. 2022, Chemical Composition of Bright Stars in the Northern Hemisphere: Star-Planet Connection, Astrophys. J. Suppl. Ser., 259, 45

Telting, J. H., Avila, G., Buchhave, L., et al. 2014, FIES: The high-resolution Fiber-fed Echelle Spectrograph at the Nordic Optical Telescope, Astronomische Nachrichten, 335, 41

Testa, P., Saar, S. H., & Drake, J. J. 2015, Stellar activity and coronal heating: an overview of recent results, Philosophical Transactions of the Royal Society of London Series A, 373, 20140259

Ting, Y.-S., Conroy, C., Rix, H.-W., & Cargile, P. 2019, The Payne: Self-consistent ab initio Fitting of Stellar Spectra, Astrophys. J., 879, 69

Toet, S. E. B., Vedantham, H. K., Callingham, J. R., et al. 2021, Coherent radio emission from a population of RS Canum Venaticorum systems, Astron. Astrophys., 654, A21

Tomkin, J., Luck, R. E., & Lambert, D. L. 1976, The $^{12}C/^{13}C$ ratio in stellar atmospheres. VII. 38 giants and supergiants., Astrophys. J., 210, 694

Tsvetkova, S., Petit, P., Konstantinova-Antova, R., et al. 2014, in IAU Symposium, Vol. 302, Magnetic Fields throughout Stellar Evolution, ed. P. Petit, M. Jardine, & H. C. Spruit, 367–368

Veronig, A. M., Odert, P., Leitzinger, M., et al. 2021, Indications of stellar coronal mass ejections through coronal dimmings, Nature Astronomy, 5, 697

Vigroux, L. & Arnould, M. 1979, in Liege International Astrophysical Colloquia, Vol. 22, Liege International Astrophysical Colloquia, ed. A. Boury, N. Grevesse, & L. Remy-Battiau, 47–52

Villaver, E. & Livio, M. 2009, The Orbital Evolution of Gas Giant Planets Around Giant Stars, Astrophys. J. Lett., 705, L81

Škoda, P., Draper, P. W., Neves, M. C., Andrešič, D., & Jenness, T. 2014, Spectroscopic analysis in the virtual observatory environment with SPLAT-VO, Astronomy and Computing, 7, 108

Walter, F. M., Cash, W., Charles, P. A., & Bowyer, C. S. 1980, X-rays from RS CVn systems : a HEAO 1 survey and the development of a coronal model., Astrophys. J., 236, 212

Wang, E. X., Nordlander, T., Buder, S., et al. 2024, 3D NLTE Lithium abundances for late-type stars in GALAH DR3, Mon. Not. R. Astron. Soc., 528, 5394

White, N. E., Sanford, P. W., & Weiler, E. J. 1978, An X-ray outburst from the RS CVn binary HR1099, Nature, 274, 569

Xing, L.-F., Li, Y.-C., Chang, L., Wang, C.-J., & Bai, J.-M. 2021, Lithium abundance in a sample of active stars: High-resolution spectrograph observation with the 1.8 m telescope, Astron. Astrophys., 653, A28

Yoshii, Y. 1982, Density distribution of faint stars in the direction of the north galactic pole., Publ. Astron. Soc. Jpn, 34, 365

Zahn, J. P., Talon, S., & Matias, J. 1997, Angular momentum transport by internal waves in the solar interior., Astron. Astrophys., 322, 320

Zhilyaev, B., Andreev, M., & Verlyuk, I. 2024, Fast spectral variability of the RS CVn-type chromosphere-active star II Peg, Bulgarian Astronomical Journal, 40, 3

Zhou, Y., Wang, C., Yan, H., et al. 2022, Li-rich Giants in LAMOST Survey. III. The Statistical Analysis of Li-rich Giants, Astrophys. J., 931, 136

A Machine readable tables of results

Table A1: Contents of the machine-readable table available online at the CDS for the first subsample of RS CVn stars.

Col	Label	Units	Explanations
1	ID	–	Tycho-2 catalogue identification
2	Name	–	Stellar name
3	Res	–	Spectral resolution
4	$T_{\rm eff}$	K	Effective temperature
5	$e\_T_{\rm eff}$	K	Uncertainty in effective temperature
6	Log g	dex	Stellar surface gravity
7	e_Log g	dex	Uncertainty in stellar surface gravity
8	[Fe/H]	dex	Metallicity
9	e_Fe I	dex	Uncertainty in [Fe I/H]
10	n_Fe I	–	Number of Fe I lines
11	e_Fe II	dex	Uncertainty in [Fe II/H]
12	n_Fe II	–	Number of Fe lines
13	$V_{\rm t}$	km s^{-1}	Microturbulence velocity
14	e_Vt	km s^{-1}	Uncertainty in microturbulence velocity
15	[C/H]	dex	Carbon abundance
16	e_[C/H]	dex	Uncertainty in carbon abundance
17	n_C	–	Number of C_2 lines
18	[N/H]	dex	Nitrogen abundance
19	e_[N/H]	dex	Uncertainty in nitrogen abundance
20	n_N	–	Number of CN lines
21	[O/H]	dex	Oxygen abundance
22	e_[O/H]	dex	Uncertainty in oxygen abundance
23	n_O	–	Number of oxygen lines
24	[Mg/H]	dex	Magnesium abundance
25	e_[Mg/H]	dex	Uncertainty in magnesium abundance
26	n_Mg	–	Number of magnesium lines
27	[Si/H]	dex	Silicon abundance
28	e_[Si/H]	dex	Uncertainty in silicon abundance
29	n_Si	–	Number of silicon lines
30	[Ca/H]	dex	Calcium abundance
31	e_[Ca/H]	dex	Uncertainty in calcium abundance
32	n_Ca	–	Number of calcium lines
33	[Sc I/H]	dex	Scandium abundance from neutral lines
34	e_[Sc I/H]	dex	Uncertainty in [Sc I/H] abundance
35	n_Sc I	–	Number of Sc I lines
36	[Sc II/H]	dex	Scandium abundance from ionized lines
37	e_[Sc II/H]	dex	Uncertainty in [Sc II/H] abundance
38	n_Sc II	–	Number of Sc II lines
39	[Ti I/H]	dex	Titanium abundance from neutral lines
40	e_[Ti I/H]	dex	Uncertainty in [Ti I/H] abundance
41	n_Ti I	–	Number of Ti I lines
42	[Ti II/H]	dex	Titanium abundance from ionized lines
43	e_[Ti II/H]	dex	Uncertainty in [Ti II/H] abundance
44	n_Ti II	–	Number of Ti II lines
45	[Cr I/H]	dex	Chromium abundance from neutral lines
46	e_[Cr I/H]	dex	Uncertainty in [Cr I/H] abundance
47	n_Cr I	–	Number of Cr I lines
48	[Cr II/H]	dex	Chromium abundance from ionized lines
49	e_[Cr II/H]	dex	Uncertainty in [Cr II/H] abundance
50	n_Cr II	–	Number of Cr II lines
51	[Co/H]	dex	Cobalt abundance
52	e_[Co/H]	dex	Uncertainty in cobalt abundance
53	n_Co	–	Number of cobalt lines
54	[Ni/H]	dex	Nickel abundance
55	e_[Ni/H]	dex	Uncertainty in nickel abundance
56	n_Ni	–	Number of nickel lines
57	$^{12}C/^{13}C$	–	Carbon isotope ratio
58	$e\_^{12}C/^{13}C$	–	Uncertainty in carbon isotope ratio
59	C/N	–	Carbon-to-nitrogen abundance ratio
60	Mass	$M_{\odot}$	Stellar mass
61	e_Mass	$M_{\odot}$	Uncertainty of mass
62	Age	Gyr	Stellar age
63	e_Age	Gyr	Uncertainty of age
64	$R_{\rm mean}$	kpc	Mean galactocentric distance
65	$e\_R_{\rm mean}$	kpc	Uncertainty of mean galactocentric distance

Table A2: Determinations of stellar main parameters and C, N, O, and Mg abundances for the second subsample of RS CVn stars.

Col	Label	Units	Explanations
1	ID	–	Tycho-2 catalogue identification
2	Name	–	Stellar name
3	Res	–	Spectral resolution
4	$T_{\rm eff}$	K	Effective temperature
5	$e\_T_{\rm eff}$	K	Uncertainty in effective temperature
6	Log g	dex	Stellar surface gravity
7	e_Log g	dex	Uncertainty in stellar surface gravity
8	[Fe/H]	dex	Metallicity
9	e_Fe I	dex	Uncertainty in [Fe I/H]
10	n_Fe I	–	Number of Fe I lines
11	e_Fe II	dex	Uncertainty in [Fe II/H]
12	n_Fe II	–	Number of Fe lines
13	$V_{\rm t}$	km s^{-1}	Microturbulence velocity
14	e_Vt	km s^{-1}	Uncertainty in microturbulence velocity
15	[C/H]	dex	Carbon abundance
16	e_[C/H]	dex	Uncertainty in carbon abundance
17	n_C	–	Number of C_2 lines
18	[N/H]	dex	Nitrogen abundance
19	e_[N/H]	dex	Uncertainty in nitrogen abundance
20	n_N	–	Number of CN lines
21	[O/H]	dex	Oxygen abundance
22	e_[O/H]	dex	Uncertainty in oxygen abundance
23	n_O	–	Number of oxygen lines
24	[Mg/H]	dex	Magnesium abundance
25	e_[Mg/H]	dex	Uncertainty in magnesium abundance
26	n_Mg	–	Number of magnesium lines
27	^{12}C/^{13}C	–	Carbon isotope ratio
28	e_^{12}C/^{13}C	–	Uncertainty in carbon isotope ratio
29	C/N	–	Carbon-to-nitrogen abundance ratio
30	Mass	$M_{\odot}$	Stellar mass
31	e_Mass	$M_{\odot}$	Uncertainty of mass
32	Evol	–	Evolutionary stage (BB or AB – stars below or above the RGB luminosity bump, respectively. RC – Clump stars, SG – subgiant stars)
33	Emission	–	Yes – if emission is visible in the Ca II lines

B Parameters of stars

Table B1: Main atmospheric parameters of the first subsample of RS CVn stars

Star	T_{eff} K	$e_{T_{\mathrm{eff}}}$ K	$\log g$	$e_{\log g}$	[Fe/H]	$e_{\mathrm{Fe\,I}}$	$\mathrm{n}_{\mathrm{Fe\,I}}$	$e_{\mathrm{Fe\,II}}$	$\mathrm{n}_{\mathrm{Fe\,II}}$	V_{t} $\mathrm{km\,s^{-1}}$	$e_{V_{\mathrm{t}}}$ $\mathrm{km\,s^{-1}}$
*39 Cet	4940	32	2.81	0.13	−0.46	0.06	74	0.06	6	1.37	0.14
*39 Cet(†)	4920	41	2.87	0.19	−0.51	0.09	97	0.11	15	1.76	0.20
V* BF Psc	4990	68	3.37	0.21	−0.26	0.10	65	0.02	5	0.78	0.35
V* BF Psc(†)	4896	65	3.34	0.18	−0.29	0.09	61	0.10	10	0.72	0.34
*3 Cam	4705	55	2.27	0.19	−0.15	0.10	67	−0.15	7	1.29	0.19
V* CL Cam	4700	50	2.61	0.19	−0.25	0.11	72	−0.25	9	1.47	0.14
V* V403 Aur	4870	42	2.32	0.19	−0.20	0.09	68	0.10	5	1.47	0.18
*ksi Leo	4730	62	2.54	0.17	−0.12	0.09	65	0.06	6	1.41	0.20
*11 LMi	5450	32	4.35	0.08	0.13	0.03	52	0.05	6	1.17	0.13
*eps Leo	5440	36	2.31	0.15	−0.05	0.07	74	0.05	5	1.83	0.17
*mu. Leo	4470	75	2.41	0.14	0.09	0.08	55	0.04	7	1.72	0.23
*37 Com	4535	68	1.90	0.20	−0.21	0.11	66	0.13	10	1.80	0.2
HD 145742	4730	38	2.53	0.18	−0.04	0.09	75	0.07	5	1.20	0.22
HD 145742(†)	4790	40	2.73	0.14	0.01	0.08	71	0.08	5	1.20	0.16
*29 Dra	4745	40	2.87	0.18	−0.17	0.10	77	0.06	9	1.64	0.23
*29 Dra(†)	4738	62	2.79	0.18	−0.22	0.09	63	0.08	6	1.65	0.23
V* V834 Her	4985	47	2.74	0.17	−0.06	0.08	70	0.03	5	1.07	0.22
BD+15 3367	4380	68	2.17	0.22	−0.33	0.13	71	0.13	10	0.87	0.29
*62 Ser	4660	52	2.54	0.16	−0.19	0.09	72	0.07	5	1.09	0.20
*62 Ser(†)	4690	50	2.49	0.20	−0.23	0.11	112	0.10	16	1.23	0.18
*b01 Cyg	5085	37	3.67	0.12	0.02	0.06	73	0.04	6	0.74	0.25
*b01 Cyg(†)	5116	45	3.70	0.13	−0.01	0.06	65	0.04	6	0.77	0.24
HD 191588	4590	70	2.69	0.19	−0.55	0.10	52	0.09	6	1.49	0.25
HD 191588(†)	4547	65	2.56	0.17	−0.60	0.09	44	0.08	6	1.54	0.24
HD 200740	4920	50	2.87	0.16	0.17	0.08	70	0.07	7	1.10	0.23
HD 200740(†)	4966	55	2.96	0.08	0.15	0.09	69	0.08	7	1.22	0.21
V* KX Peg	5050	60	3.25	0.21	−0.46	0.09	62	0.08	7	1.08	0.25
V* KX Peg(†)	5072	60	3.38	0.19	−0.42	0.09	54	0.09	7	1.08	0.24
HD 221639	4960	45	3.08	0.19	−0.19	0.09	80	0.06	8	0.92	0.24
HD 221639†)	4965	40	2.86	0.16	−0.21	0.08	75	0.06	7	0.96	0.19

(†) Results obtained from observations with $R \sim 68\,000$. Other results were obtained with $R \sim 36\,000$.

Table B2: Main atmospheric parameters of the second subsample of RS CVn stars

Star	$T_{\rm eff}$ K	$eT_{\rm eff}$ K	$\log g$	$e_{\log g}$	[Fe/H]	$e_{\rm Fe\,I}$	$n_{\rm Fe\,I}$	$e_{\rm Fe\,II}$	$n_{\rm Fe\,II}$	$V_{\rm t}$ km s^{-1}	$eV_{\rm t}$ km s^{-1}
*33 Psc	4660	55	2.73	0.15	−0.21	0.06	64	0.03	6	1.00	0.21
HD 6497	4345	50	2.37	0.16	−0.07	0.10	72	0.08	5	1.12	0.22
HD 6497(†)	4335	45	2.31	0.14	−0.02	0.08	74	0.07	5	1.02	0.19
V* OP And(†)	4466	55	2.15	0.17	−0.40	0.10	71	0.05	6	1.77	0.18
V* V1149 Ori	4613	58	2.08	0.18	−0.42	0.10	65	0.06	7	1.52	0.18
*iot Gem	4801	50	2.63	0.15	−0.07	0.08	64	0.07	6	1.32	0.17
* sig Gem(†)	4620	85	2.70	0.07	0.08	0.08	27	0.09	7	1.64	0.26
* bet Gem	4868	45	2.82	0.15	0.04	0.08	72	0.04	7	1.33	0.17
* g Gem	4125	80	1.64	0.16	−0.35	0.10	58	0.03	5	1.49	0.18
HD 71028	4580	60	1.75	0.19	−0.77	0.10	60	0.10	6	1.31	0.20
V* FI Cnc	5175	55	3.34	0.25	−0.11	0.12	75	0.08	9	1.43	0.24
* 10 LMi	5061	50	2.89	0.16	−0.08	0.07	58	0.05	6	1.31	0.20
V* FG UMa	4697	48	2.29	0.18	−0.85	0.09	55	0.08	5	1.84	0.19
* tau Leo	4953	40	2.39	0.16	−0.02	0.08	75	0.09	7	1.59	0.15
* 93 Leo(†)	5130	45	2.94	0.16	−0.42	0.07	58	0.04	6	0.48	0.33
* c Vir	4500	48	2.04	0.11	−0.44	0.06	58	0.07	6	1.60	0.12
V* BM CVn	4816	85	3.20	0.07	0.15	0.08	35	0.07	5	1.89	0.28
V* IT Com	4705	70	3.19	0.18	−0.30	0.09	66	0.07	6	1.55	0.23
* 7 Boo	5367	50	2.82	0.22	−0.04	0.10	50	0.09	7	1.87	0.21
* 7 Boo(†)	5313	50	2.61	0.21	−0.07	0.09	57	0.08	6	1.83	0.20
* eta Boo	6220	60	3.95	0.21	0.34	0.08	71	0.07	9	1.59	0.23
* eta Boo(†)	6158	55	3.96	0.20	0.25	0.08	69	0.09	7	1.67	0.22
V* FR Boo	4355	70	2.29	0.17	−0.35	0.10	52	0.08	6	1.57	0.21
V* HK Boo(†)	4948	50	3.41	0.19	−0.67	0.09	61	0.08	6	1.16	0.23
HD 141690	6085	88	4.27	0.12	−0.29	0.09	42	0.06	5	1.99	0.60
HD 161832	4420	80	1.41	0.16	−0.59	0.08	35	0.08	5	1.77	0.16
HD 161832(†)	4430	65	1.44	0.16	−0.59	0.08	43	0.08	4	1.81	0.16
V* V835 Her(†)	5280	60	3.86	0.21	−0.30	0.10	60	0.10	5	1.57	0.30
HD 179094	4758	58	3.03	0.19	−0.25	0.10	58	0.08	7	1.70	0.24
HD 179094(†)	4760	62	3.05	0.19	−0.30	0.10	58	0.06	6	1.85	0.24
* f Aql(†)	4827	35	2.88	0.11	−0.28	0.05	72	0.09	7	0.84	0.14
V* V1971 Cyg	4885	55	3.15	0.18	−0.47	0.09	48	0.08	7	1.68	0.22
V* V1971 Cyg(†)	4815	72	3.10	0.19	−0.43	0.10	46	0.10	6	1.67	0.26
V* V2075 Cyg	5040	65	3.29	0.21	−0.52	0.10	48	0.10	6	1.86	0.28
V* V2075 Cyg(†)	5020	52	3.10	0.19	−0.51	0.09	49	0.10	4	1.87	0.24
V* IM Peg(†)	4820	59	2.25	0.19	−0.26	0.10	47	0.12	8	1.89	0.19
* lam And	4750	35	2.73	0.17	−0.50	0.09	80	0.08	7	1.14	0.18
* lam And(†)	4732	30	2.80	0.13	−0.56	0.07	81	0.09	7	1.25	0.13
* alf Sge	5610	55	2.48	0.09	0.03	0.08	64	0.05	6	1.78	0.22
* alf Sge(†)	5630	45	2.36	0.07	0.03	0.06	63	0.09	6	1.83	0.19
* eps UMi	5279	55	2.48	0.10	0.10	0.10	49	0.09	6	1.47	0.20

(†)Results obtained from observations with $R \sim 68\,000$. Other results were obtained with $R \sim 36\,000$.

Table B3: Mass, ^{12}C/^{13}C, C/N, NLTE Li abundances, LTE Li abundances and the evolutionary stage of the RS CVn stars in the first and second subsamples.

Name	Mass $M_{\odot}$	^{12}C/^{13}C	C/N	$A(\mathrm{Li})_{\mathrm{NLTE}}$	$A(\mathrm{Li})_{\mathrm{LTE}}$	Evol. stage
*39 Cet	1.10		2.19	0.49$^{(*)}$	0.35$^{(*)}$	BB
*39 Cet$^{(\dagger)}$)	1.00		2.51	0.43$^{(*)}$	0.29$^{(*)}$	BB
V* BF Psc	1.06		2.00			BB
V* BF Psc$^{(\dagger)}$)	1.16		2.45	0.50	0.35	BB
*3 Cam	3.20		0.75			BB
V* CL Cam	1.20		0.95	0.46$^{(*)}$	0.25$^{(*)}$	BB
V* V403 Aur	1.16		0.95	1.42	1.23	AB
*ksi Leo	1.30	22	1.58			BB
*11 LMi	0.86		3.40	0.74	0.65	SG
*eps Leo	3.63		0.93	0.94	0.83	BB
*mu. Leo	1.20	18	1.23			AB
*37 Com	1.38	7	1.60	1.42	1.13	RC
HD 145742	1.42	12	1.02	0.38$^{(*)}$	0.15$^{(*)}$	AB
HD 145742 $^{(\dagger)}$)	1.46	12	0.93	0.36$^{(*)}$	0.15$^{(*)}$	AB
*29 Dra	1.11	15	1.86	0.50	0.30	BB
*29 Dra$^{(\dagger)}$)	1.13		1.70	0.55	0.35	BB
V* V834 Her	2.17	12	0.89			BB
BD+15 3367	1.17	12	1.29			AB
*62 Ser	1.16	22	1.55	1.33	1.11	BB
*62 Ser$^{(\dagger)}$)	1.19	22	1.54	1.38	1.17	BB
*b01 Cyg	1.19		1.47	0.70	0.55	BB
*b01 Cyg$^{(\dagger)}$)	1.16	16	1.70	0.65	0.50	BB
HD 191588	1.02		2.23			BB$^{(\ddagger)}$
HD 191588$^{(\dagger)}$)	1.03		2.34			BB$^{(\ddagger)}$
HD 200740	2.17	20	0.78	1.60	1.41	BB
HD 200740$^{(\dagger)}$)	2.14		0.91	1.63	1.45	BB
V* KX Peg	1.06	27	2.24	1.46	1.35	BB
V* KX Peg$^{(\dagger)}$)	1.06		2.29	1.51	1.41	BB
HD 221639	1.11		2.51		BB	
HD 221639$^{(\dagger)}$)	1.31	28	2.81		BB	
*33 Psc	1.09	–	1.91	0.28$^{(*)}$	0.06$^{(*)}$	BB
HD 6497	1.11	24	1.58	–	–	AB
HD 6497$^{(\dagger)}$	1.11	26	2.04	–	–	AB
V* OP And$^{(\dagger)}$	1.09	24	2.60	2.87	3.01	AB
V* V1149 Ori	1.21	–	1.70	1.09	0.85	AB
*iot Gem	1.37	14	1.20	0.36	0.15	BB
*sig Gem$^{(\dagger)}$	1.24	–	2.45	1.11	0.85	BB

Table B4: Table B3 continued.

Name	Mass $M_\odot$	$^{12}C/^{13}C$	C/N	$A(\mathrm{Li})_{\mathrm{NLTE}}$	$A(\mathrm{Li})_{\mathrm{LTE}}$	Evol. stage
*bet Gem	1.90	–	0.95	0.84	0.65	BB
*g Gem	1.11	14	0.98	–	–	AB
HD 71028	1.22	–	1.10	–	–	AB
V* FI Cnc	1.25	–	1.15	1.71	1.60	BB
*10 LMi	2.20	–	1.17	–	–	BB
V* FG UMa	1.00	–	1.20	1.11	0.95	AB
*tau Leo	2.84	24	0.74	0.49(*)	0.30(*)	BB
*93 Leo(†)	1.89	16	0.98	1.31	1.20	RC
*c Vir	1.89	16	0.98	–	–	RC
V* BM CVn	1.15	–	2.04	–	–	BB
V* IT Com	1.00	–	2.14	0.33(*)	0.15(*)	BB
*7 Boo	3.00	–	0.93	0.96(*)	0.85(*)	BB
*7 Boo(†)	3.00	–	1.07	0.87(*)	0.75(*)	BB
*eta Boo	1.40	–	–	–	–	SG(‡)
*eta Boo(†)	1.40	–	4.07	–	–	SG(‡)
V* FR Boo	1.06	7	1.05	–	–	AB
V* HK Boo(†)	0.90	–	3.63	1.73	1.65	SG
HD 141690	1.15	–	–	2.24	2.25	SG
HD 161832	1.19	–	1.55	0.95	0.65	AB
HD 161832(†)	1.19	20	1.66	0.94	0.65	AB
V* V835 Her(†)	1.02	–	3.72	–	–	SG
HD 179094	1.03	10	1.60	1.10	0.90	BB
HD 179094(†)	1.03	10	1.82	1.12	0.95	BB
*f Aql(†)	1.04	–	1.95	0.42(*)	0.25(*)	BB
V* V1971 Cyg	0.99	–	1.91	1.36	1.23	BB
V* V1971 Cyg(†)	0.99	–	2.00	1.49	1.35	BB
V* V2075 Cyg	1.00	–	–	1.26	1.15	BB
V* V2075 Cyg(†)	1.00	–	2.29	1.27	1.15	BB
V* IM Peg(†)	1.06	–	2.40	1.60	1.41	BB
*lam And	1.02	–	2.00	–	–	BB
*lam And(†)	1.02	–	2.09	–	–	BB
*alf Sge	2.95	–	0.51	0.95(*)	0.85(*)	RC
*alf Sge(†)	2.95	–	0.44	0.95(*)	0.85(*)	RC
*eps UMi	3.50	–	0.90	–	–	BB

(†)Results obtained from observations with $R \sim 68\,000$. (*)Upper lithium abundance value. BB or AB – stars below or above the RGB luminosity bump, respectively. RC – Clump star. SG – subgiant star. (‡)The star is attributed to the thick disc of the Galaxy.

Vilniaus universiteto leidykla
Saulėtekio al. 9, III rūmai, LT-10222 Vilnius El. p. info@leidykla.vu.lt
www.leidykla.vu.lt
bookshop.vu.lt, journals.vu.lt
Tiražas 25 egz.